Impacts of earthworm bioturbation on elemental cycles in soils: An application of a geochemical mass balance to an earthworm invasion chronosequence in a sugar maple forest in Northern Minnesota.

A Thesis
SUBMITTED TO THE FACULTY OF
UNIVERSITY OF MINNESOTA
BY

Kathryn "Kit" Elizabeth Resner

IN PARTIAL FULFILLMENT OF THE REQUIREMENTS
FOR THE DEGREE OF
MASTER OF SCIENCE

Adviser Kyungsoo Yoo

June 2013

Acknowledgements

First and foremost I would like to express my sincere thanks to my adviser, Dr. Kyungsoo Yoo, for the opportunity to work with him on the earthworm invasion project. Kyungsoo has given me invaluable guidance throughout the research process. Kyungsoo has dedicated time beyond what I could have expected to help me become a better student and beginning scientist.

Thanks to my committee members, Dr. Stephen Sebestyen, Dr. Carrie Jennings, and Dr. Edward Nater, for providing with endless help and scientific discussion throughout the course of my graduate career. Their diverse perspectives, both scientifically and academically, have helped me to gain a much needed broader view, which will serve me well in the years to come. I cannot express how grateful and happy I am to have worked with such an incredible group of scientists.

I would like to extend thanks to my lab group, including Dr. Brent Dalzell, for his continuous help and lab assistance. I would especially like to thank Amy Lyttle, who has not only been a collaborator on the project, but a friend who has made this process much more manageable and fun. I would also like to thank a former lab member, Dr. Beth Weinman, who inspired me on a personal and academic level to keep improving my work. Beth has dedicated incredible amounts of time to scientific conversation with me and has contributed countless ideas and suggestions to my thesis work.

I would like to thank the Physical Research Laboratory in Ahmadabad India for the opportunity to visit and conduct research, and a very special thanks to Dr. Ashok

Singhvi for kindly welcoming me to his laboratory, and for sharing his expertise on optically stimulated luminescence dating.

Lastly, I would like to thank my family and loved ones, who have supported me throughout the graduate school process. I thank and dedicate my thesis, to Ken Paul, my grandfather and number one supporter.

Abstract

Earthworms are arguably the best known soil bioturbator, yet their impacts on soil biogeochemistry are difficult to quantify as a function of their roles in physically mixing soils. In glaciated regions of North America, northern hardwood forests have evolved without native earthworms since the last glacial retreat. However, earthworms have invaded northern hardwood forests owing to agricultural expansion, fishing, recreational, and logging activities. Earthworm consumption of the organic horizon in Minnesota hardwood forests has resulted in dramatically changing forest floor ecology and soil morphology, yet their impacts on soil biogeochemistry remain largely unknown. An earthworm invasion chronosequence near Leech Lake in Northern Minnesota provides an ideal outdoor laboratory to quantify the interactions between biogeochemical and physical processes associated with different earthworm species and biomasses. Across the earthworm invasion transect, the A horizon elemental chemistry profiles show that earthworms have vertically relocated minerals, which is consistent with ^{210}Pb activity profiles. While soil elemental depth profiles confirm increased mixing with earthworm invasion, the depth profiles cannot be solely explained by mixing. I used a geochemical mass balance model to examine soils' biogeochemical responses to invasive earthworms. Fractional and absolute mass losses/gains of biologically important elements such as Ca, P, K, Fe, and Si, relative to the parent material, are substantially altered by invasive earthworm species. The arrival of A-horizon-mixing, endogeic earthworms most dramatically reduces the level of the elemental enrichments in the A horizons. The declined elemental enrichments are likely derived from the consumption of particulate

organic matter by endogeic species, which leads to the mineralization and leaching of Ca, P, K. The dramatic losses of the enrichments also suggest that the newly mineralized nutrients are in excess of the nutrient demand from understory plants. Our results indicate the significant and potentially negative impacts of invasive earthworms on the soil nutrient cycling and consequently the sustainability of the hardwood forests in the Great Lakes Region.

Table of Contents

List of Tables

List of Figures

Chapter 1

Influence of non-native earthworms on soil inorganic biogeochemical cycles: an example from a northern hardwood sugar maple forest in Minnesota

"*It may be doubted whether there are many other animals which have played so important a part in the history of the world as these lowly organized creatures*"
-Charles Darwin 1881

Chapter Overview

The hardwood forests of the Great Lakes Region have evolved without the presence of native earthworms since the Last Glacial Maximum but are now facing the invasion of exotic earthworms due to fishing, logging, and recreational activities. Exotic earthworms are known to increase soil mixing and dramatically alter soil morphology. However, how such a physical disturbance interferes with soil biogeochemical processes remains largely unknown. I use a geochemical mass balance model to examine the biogeochemical responses to exotic earthworms along an earthworm invasion chronosequence in a northern Minnesota sugar maple forest. Fractional and absolute mass changes of biologically important elements such as Ca, P, K, Fe, and Si relative to the parent material were greatly altered by different invasive earthworm ecological groups. In less impacted soils with only litter-dwelling epigeic species, Si, Ca, P, and K are greatly enriched in the soil A horizons. The subsequent invasions of epi-endogeic and epi-anecic earthworms resulted in further fractional- and total-mass enrichments by incorporating leaf organic matter and leaching nutrients into shallow horizons. However, the arrival of endogeic earthworms dramatically reduced the level of elemental enrichments. The declined elemental enrichments were likely derived from the loss of particulate organic matter due to endogeic species, which lead to the mineralization of Ca, P, K. The dramatic loss of enrichment also suggested that the newly released nutrients into A horizons were in excess of the nutrient demand from understory plants. Our results demonstrate the significant and potentially negative impacts of invasive earthworms on soil nutrient cycling and subsequently the sustainability of hardwood forests in the Great Lakes Region.

1. Introduction

The pedosphere is a thin layer of the earth's terrestrial surface where geochemical, physical, and biological processes tightly interact. One of the results from these interconnected processes is the cycling of inorganic elements. The significance of elemental cycling has been appreciated in the context of chemical weathering and nutrient demands from terrestrial and aquatic ecosystems. Whether a study's impetus lies in understanding soil geochemistry, global biogeochemical cycles, or long-term climate change, it has been widely recognized that physical and chemical weathering processes work in concert to shape Earth's thin mantle of soil. More specifically, in the fields of geomorphology and geochemistry, it has been hypothesized and repeatedly confirmed that the physical incorporation of silicate minerals into the more biochemically reactive soil zone by erosion accelerates the chemical weathering of minerals. This concept has been fundamental to the well-known proposal that tectonics and climate changes are coupled, affecting the global climate system over the geological time scales (Raymo and Ruddiman 1992; Berner 1992; Riebe et al. 2003).

However, before invoking tectonic processes and erosion, we believe that there are ubiquitous physical disturbance mechanisms that strongly affect chemical weathering and cycling of inorganic nutrients. In soil mantled landscapes, physical incorporation of minerals from the underlying geologic materials into a chemically reactive soil zone is mediated by numerous agents that physically perturb soils. Particularly in temperate and tropical environments, bioturbation plays a critical role in vertically transporting soil minerals (Hole 1981, Johnson 2005). Soil bioturbators have complex relationships with the soils they inhabit, making it difficult to quantitatively distinguish their direct impact on physical processes and properties of soils and their indirect influences over soil biogeochemistry. For example, plant rooting may exude organic acids that alter minerals' geochemical environments (Kelly et al. 1998) and weaken the physical strength of bedrock by expanding their roots, and may mix soil horizons through tree throw events (Schaetzl et al. 1989). This is also true for wide spread soil macrofauna such as ants, termites, earthworms, and fossorial mammals, which cause physical disturbances in soils while burrowing for food and shelter (Hole et al. 1981; Schaetzl and Anderson 2005). While soil macrofauna contribute to elemental cycles in soils through the consumption of organic matter, their physical disturbances also change the pathways and timing that materials and resources are routed, thus perturbing elemental cycles.

Earthworms are arguably the best known, and in many cases, the most important among soil perturbing animals (Hendrix and Bohlen, 2002). They occur in every bioregion on the earth, excluding the coldest and driest habitats (Hendrix et al., 2008), and physically move large masses of soil (Lee 1985). The manner in which earthworm species mix soil is largely a function of their ecological group, each of which exhibits a unique burrowing habit associated with different mixing depths and feeding behaviors. Anecic species, such as the nightcrawler (*Lumbricus terrestris*), are deep soil burrowers and consume leaf litter; endogeic species mix within the A horizon and ingest organic matter and mineral material; and epigeic species only dwell in the litter layer feeding primarily on fungi and bacteria (Hale et al. 2004, Frelich et al. 2006, Hale et al. 2007, Hendrix et al. 2008).

Addressing the impacts of earthworm mixing on soil biogeochemistry in their natural environment is challenging because of their virtually ubiquitous presence.

Northern hardwood forests of the United States have been free of native earthworms since the last glaciation (Figure 1.1) (Bohlen 2004a, Hale et al. 2005a, Eisenhauer et al. 2006). However, over the last century, exotic European earthworms have progressively invaded previously earthworm-free forest ecosystems. Their migration has been influenced by the use of earthworms for fishing bait (Alban and Berry 1994, Gates 1982), expansion of agriculture, and logging activities. The formerly glaciated forested areas of Minnesota are currently undergoing invasion by exotic earthworms and can provide an ideal natural laboratory to study how, and to what degree bioturbation interferes with soil biogeochemical cycles.

In the United States' Great Lakes region, it has been shown that invasive earthworms dramatically alter soil physical properties. Exotic earthworms remove the leaf litter layer (O horizon) (Hale et al. 2006), which results in the loss of growth medium and a protective barrier for some native plants species (Frelich et al. 2006) and forest floor animals (Maerz et al. 2009, Loss and Blair 2011). Earthworm consumption and physical incorporation of the O horizon into the underlying mineral soil drastically alters soil morphology (Eisenhauer et al. 2007, Alban and Berry 1994). After earthworm invasion, A horizons are intensely mixed and thickened at the expense of the overlying O horizon and underlying E or B horizons. Altered E horizon morphology associated with earthworm invasion has also been observed (Alban and Berry 1994). The structure of A horizon materials is also transformed from single grain or fine granular to medium to large granules (Six et al. 2004). Contrary to the common perception of earthworms aerating and loosening soils, forest soils that have been mixed by invasive earthworms have higher bulk densities than earthworm-free soils (Hale et al. 2005).

In addition to the physical perturbation of soils, earthworms alter P and N cycles (Hale et al. 2005b, Bohlen et al. 2004b, Suarez et al. 2004). Hale et al. (2005b) found that soils from a Minnesota northern hardwood forest had lower phosphate, ammonium, and nitrate availabilities where earthworm biomass was high, compared to soil plots with low earthworm biomass. Bohlen and others (2004c) found mixed results between their study sites in New York, but suggested that N leaching might have been facilitated by earthworm invasion at one of their two study sites under a sugar maple dominated forest. At the same site, Suarez et al., (2004) reported that *Lumbricus rubellus,* an epi-endogeic species, may have aided in leaching P by altering soil exchangeable pools while deep burrowing anecic species *L. terrestris* may have contributed to increased soil total P by incorporating subsoil materials into the shallow soil zone.

In a recent dendrochronological study, Larson et al. (2010) were able to detect negative responses in the annular growth of tree rings associated with the stages of earthworm invasion in a hardwood forest in northern Minnesota, illustrating the importance of carefully constraining earthworms' species-specific effects on the soil nutrient pools in predicting and scaling up the forest's responses to earthworm invasion.

Building on these previous studies, my objective was to quantity interactions between soil physical mixing and elemental cycles along an active earthworm invasion front. Unlike previous studies that focused on P and N, this study examines a suite of major soil elements. By conducting the study on a well-studied earthworm invasion chronosequence in a deciduous forest in northern Minnesota (Hale et al. 2005a, Hale et al. 2005b, Hale et al. 2006), I further explored the feedbacks between soil physical mixing, elemental cycles, and exotic earthworms species composition. I apply a geochemical mass balance approach (Brimhall et al. 1987, Merritts 1992, Riebe et al., 2003, Oh & Ritcher 2005) to quantify the redistribution and gains/losses of major elements *via* physical mixing and biogeochemical processes in response to invasive earthworms. To my knowledge, this is the first application of geochemical mass balance to study the biogeochemical impacts of soil bioturbators. The outcomes of this study allows us to understand the degree to which invasive earthworms affect the biological retention of key nutrient elements (P, Ca, and K) and the most abundant soil cations (Si, Fe, and Al).

2. Methods

2.1 Field site and sampling

The Ottertail earthworm invasion transect is located near Leech Lake in north central Minnesota (Figure 1.2). The 190 meter transect was established in 1998 to study the effect of earthworm invasion on understory plant communities (Hale et al. 2006). The transect includes heavily invaded soils next to a recreational road and extends 190 meters into the forest where few to no earthworms are found. The composition of overstory tree species is highly homogeneous along the transect. Sugar maples, *Acer sacharuum*, dominate the tree composition with interspersed birch (*Betula papyrifera, Betula alleghaniensis*) and basswood (*Tilia americana)* (Hale et al. 2005a). Understory plant communities are heterogeneous across the transect because of varied degree of earthworm invasion (Hale et al. 2006). The area is largely flat, but the presence of topography is still significant enough to create seasonal vernal pools. Otherwise, the timing and degree of earthworm invasion appear to be the dominant factors responsible for the variation in surficial soil properties along the transect.

The soil at the site is mapped as the Warba soil series which is classified as a fine-loamy, mixed, superactive, frigid Haplic Glossudalf. The Warba series is described to have A, E, Bt, and C horizons, where the C horizon is a calcareous glacial till formed during the late Wisconsinan glaciation (NRCS 2006). The E horizon has higher silt content than the underlying Bt and C horizons and appears to homogeneously blanket the landscape. The chemistry of the silty material is highly consistent across the transect, and has a fine silty texture that is distinguishable from the underlying clay rich B horizons. Our observation of soil morphology, in conjunction with the homogenous chemistry of the loess materials across the transect, suggests that the silty material is aeolian derived and will be refered to as the loess parent material for the overlying A horizons.

In 2006, two end member soil pits along an earthworm invasion chronosequence established by Hale et al. (2005a, 2005b) were excavated: one is close to the fishing road (hereafter 0 meter) and the opposite end of the transect 190 meters from the first soil pit (Figure 1.2). In 2009, additional soil pits were dug at distances of 0, 50, 100, 150, 160, and 190 meters along the transect. Soils were sampled by 2.5 cm depth increment for the A horizons (approximately 0-10 cm), 5cm increments for the loess layer (approximately 10-40 cm) and 10 cm increments thereafter. At each soil pit, leaf litter thickness was measured and collected from a 0.09x0.09m^2 quadrat for determining litter biomass and foliar elemental composition. Nineteen plots were established across the transect for fine scaled monitoring of earthworm populations. Plots were designated every ten meters with plot 1 next to soil pit at 0 meter and plot 19 next to the soil pit at 190 meter (Figure 1.3).

Earthworms were sampled at each plot in 2009, 2010, and 2011 using a liquid mustard extraction (Hale 2004).

2.2 Mass Balance Calculations

My primary objective is to quantify the elemental gains or losses via biogeochemical processes from the physically mixed A horizon soils, as invasive earthworms physically affect the material exchanges between the A horizon and the overlying litter layer and underlying loess material. Focusing on major inorganic elements, I accomplished this goal by normalizing the elemental fluxes relative to the element, Zr, that is physically incorporated into the A horizon from the underlying loess materials but is conservative to the combined process of dissolution, leaching, and biological uptake. Our focus on the A horizon is based on the observations that it is the zone of: (1) most intense earthworm bioturbation, and (2) highly concentrated biological nutrient cycling.

The geochemical mass balance model has been commonly used for assessing the elemental losses and gains in soils (Brimhall et al. 1987, Merritts 1992, Riebe et al. 2003, Oh & Ritcher 2005). This paper, however, is the first application of this mass balance approach to understand the role of bioturbation on biogeochemical processes. Fractional mass depletion (negative values) or enrichment (positive values), tau (τ), of an individual element from an A horizon (w) relative to the underlying loess parent material (p) can be quantified as:

(1a) $\tau_j = \left(\frac{C_{j,w}C_{i,p}}{C_{j,p}C_{i,w}}\right) - 1,$

where c is the mass concentration [kg kg^{-1}] of the element of interest (*j*) and index element (*i*). Additionally, total fractional mass change, τ , of the soil is calculated as:

(1b) $\tau_{total} = \frac{C_{i,p}}{C_{i,w}}$ -1.

For both τ_j and τ_{total}, negative values represent mass losses from the A horizons via dissolution, leaching, and biological uptake, and positive values represent mass gains. In the case where A horizon materials are physically moved from the loess without undergoing biogeochemical change, the τ values of these elements will be zero.

The absolute mass losses (positive) or gains (negative), δ, of a given element (*j*) and their sum (total) from an A horizon can be calculated as:

(2a) $\delta_j = \left(C_{j,w} - C_{j,w}\frac{C_{i,w}}{C_{i,p}}\right)\rho_w \Delta h_w,$

and

(2b) $\delta_{total} = \left(\frac{C_{i,w}}{C_{i,p}}\right)\rho_w \Delta h_w$,

where ρ_w is the soil bulk density (g/cm^3) and Δh is the thickness (cm) of A horizon. We found that earthworm invasion significantly increases the bulk densities of A horizon materials and thus used average A horizon bulk densities of 0.61 g cm^{-3} for the most invaded pits (0 and 50 meter) and 0.43 g cm^{-3} for less invaded soils (at 190, 160, 150, and 100 meter), respectively.

Lastly, volumetric strain of the A horizon relative to the volume of its parent material is calculated as:

$$(3)\ \ \varepsilon_{i,w} = \frac{V_{w-}V_p}{V_p} = \left(\frac{\rho_p C_{i,p}}{\rho_w C_{i,w}}\right) - 1,$$

where V_w is the volume (m^3) of the A horizon and V_p is the volume (g/m^3) of its parent material. The strain, when greater than 0, represents volumetric dilation, while its value is negative when volumetric collapse has occurred.

We assume that Zr is conservative during leaching and dissolution processes. By comparing enrichment levels of other potentially insoluble elements (as in Kurtz et al. 2002) we confirmed that Zr is the least mobile among the elements measured. In our mass balance calculations, we use the loess material as the A horizons' parent material. The loess parent material has remarkably homogenous elemental chemistry and XRD spectra across the transect. In calculating fractional and absolute elemental mass losses (Eq. 1a and 2a), we measured elemental concentrations of samples after removing carbon by loss of ignition. However, for the total fractional and absolute mass losses (Eq. 1b and 2b) and volumetric changes (Eq.3) that require the consideration of organic matter present in the soils we used the elemental concentrations of unheated samples without normalizing against the loss of ignition.

2.3 Laboratory analysis

Total elemental chemistry

To constrain elemental chemistry, soil samples (n=102) were treated with a lithium borate fusion and analyzed by Inductively Coupled Plasma–Mass Spectrometry (ICP-MS) at Australian Laboratory Services (ALS) Chemex. The coarse fractions

(>2mm), which contribute only <5% to the sample masses were ignored. The coarse and fine fractions of the soil were initially separated by wet sieving (2mm).

pH

Soil samples (n=52) were measured for pH with a Fisher Scientific Accumet Basic AB15 pH meter using a 1:1 mixture of 20 g soil sample with 20 mL DI water.

Exchangeable Chemistry

Exchangeable cations (Na, P, K, and Ca) were determined for a subset of soil samples (n=29). Three grams of fine fraction (<2mm) air dried soil were mixed with 30 mL solution of 1*M* NH_4OAc at pH 7 and then shaken for 20 minutes prior to centrifuging (Thomas 1982). Cation concentrations of extracts were determined using inductively coupled plasma atomic emission spectroscopy (ICP-AES) at the University of Minnesota Research Analytical Lab.

Quantitative XRD

We conducted quantitative XRD analysis on samples (n=34) selected from three soil pits (0, 100, and 190 meter) that represent three stages of earthworm invasion: all three major functional groups of epigeic, endogeic, and anecic species are present (0 meter); endogeic species are present on top of epigeic species (100 meter), and only epigeic species are present (190 meter). Soil samples were sent for quantitative mineralogical analysis at the United States Geological Survey (USGS) in Boulder, Colorado. XRD data were normalized to 100% inorganic mass after the removal of organic matter.

3. Results

3.1 Contextual data: soil morphology, texture, bulk density, pH, and mineralogy.

Based on our earthworm sampling along the transect from 2009 to 2011, the leading edge of invasion proceeds at the rate of 5 m yr^{-1} away from the recreation road. Earthworm consumption of the leaf litter in combination with mixing soils results in thickening A horizons at the expense of O and the underlying loess layer. In contrast to clear horizon boundaries between the A horizons and the loess layer in the pre-invasion soils, the boundaries become diffuse or irregular after the arrival of endogeic species (Figure 1.4). In soils prior to the arrival of endogeic species, A horizons have silty textures, whereas the soils with endogeic earthworms have sandier A horizon textures (Table 1). Soils with the presence of both endogeic and anecic species have less clay in the A horizons, which is consistent with quantitative XRD data (Table 2).

A common view of the impacts of earthworms on the soil includes their ability to decrease bulk density by creating macropores. However, pre-invasion soils have lower bulk densities compared to highly earthworm invaded soils (Table 3). Low bulk densities in pre-invasion soils may be due to undigested organic matter. The average A horizon bulk density for the least invaded soil (190,160, 150, 100 meter) is 0.43± 0.05 g/cm^3, whereas the average A horizon bulk density for invaded soils (0, 50 meters) is 0.61±0.02 g/cm^3.

Soil pH values do not show a clear invasion trend across the invasion transect, but endogeic and anecic earthworms homogenize soil pH depth profiles (Table 3).

Soil mineralogy is mainly of quartz and feldspars. Within the feldspars, potassium feldspar is the most prevalent. While earthworm mixing may alter mineralogical profiles in the upper 0-10 cm (i.e. A horizons) (Figure 1.5), mineralogical profiles in the loess material and B horizons are exceedingly homogeneous across the studied transect. Therefore, the observed systematic variations in the elemental compositions of A horizons along the transect (described below) are not inherited from parent material heterogeneity. XRD spectra confirm the presence of calcite and dolomite in the glacial till (>80 cm). The absence of calcite and dolomite throughout the A horizon and loess material (Table 2) indicates that mixing by earthworms is constrained above the B horizons. While making detailed soil profile descriptions (Table 3), we observed that earthworm burrows are limited in the A horizons and only rarely observed in the loess layer, which agrees with the XRD and bulk density results.

3.2 Earthworm biomass and species composition along the gradient

Ecological composition

Results from 2009 earthworm sampling and identification show initial colonization by epigeic species, followed by endogeic species, and lastly anecic species (Figure 1.6), which agree with the earlier observations made by Hale et al. (2005a). Plots at 190-160 meter have few to no earthworms present. Plots from 190 to 120 meter have litter dwelling epigeic earthworms but no adult A horizon mixers, although epi-endogeic and juvenile epi-anecic species were present in small biomasses. Epi-anecic species are juvenile earthworms within the same genus but are unidentifiable to the species level because of immaturity, and epi-endogeic earthworms represent the species (e.g. *L. rubellus*) that mixes in both the litter and in the mineral A horizon soils. The mid-section of the transect (100-70 meter) is populated with endogeic A horizon mixers as well as interspersed epigeic and epi-anecic earthworms. Plots from 60 meter to 0 meter are heavily populated with deep burrowing anecic species, in addition to endogeic and epigeic species.

Earthworm biomass

Plots at distances 190, 160, and 150 meters, hereafter ***the frontal group***, have low biomasses comprised of epi-endogeic, epi-anecic (juvenile), epigeic or no earthworms. The soil at 100 meter marks the forefront of adult endogeic earthworms that vigorously mix the A horizon. Earthworm biomass is generally highest at distances 0, 50, 100 meters, hereafter ***the rear group***, (Figure 1.6). The greater earthworm biomasses in the rear group are largely derived by anecic individuals who have large body masses.

3.3 Mineralogical Compositions

Depth profiles of mineralogical compositions in A horizons are substantially altered by earthworm invasion (Figure 1.5). Mineralogy of the loess material is virtually identical to the underlying B and C horizons with the exception of calcite that occurs only in the lower B or C horizons. This indicates that the loess layer is likely made of locally reworked aeolian material, and its calcite component has since been dissolved and leached.

The concentrations of quartz in A horizons are substantially higher and vertically homogeneous in soils with endogeic earthworms (Figure 1.5a), reflecting the upward mixing of underlying loess material. The A horizon concentrations of total plagioclase and potassium feldspars behave similarly to quartz. Phyllosilicate clay minerals (illite/smectite, muscovite, and kaolinite) all show greater concentrations in the A horizon compared to the loess material (Table 2), and their A horizon depth profiles are homogenized in the rear group due to the mixing by endogeic earthworm species. We found high concentrations of opal (amorphous silicon oxide) in the A horizons of the frontal group soils (Figure 1.5d), which was greatly reduced in the rear group, and was not present in the loess across the entire transect. Sugar maple foliage contain opal phytoliths (Wilding and Drees 1971) which is likely the source of opal in our site soils.

3.4 Elemental concentrations of soils

Elemental concentrations – like mineralogy – in the loess material are remarkably constant along the studied transect (Table 4). Systematic changes in elemental compositions are only observed in the A horizons along the transect.

Distinct elemental depth profiles are observed between the frontal and rear groups of the soils. The concentrations of Si, the most abundant oxide element in the A horizons of frontal group visibly decrease with increasing degree of invasion (Figure 1.7a). The direction of change is reversed across the transition from the frontal to rear groups such that there is an abrupt increase of Si concentration from 150 meter to 100 meter. This increase in Si concentration is followed by the continued increase with the longer history of earthworm invasion. This trend of Si is almost opposite in the case of Fe (Figure 1.7b). A horizon concentration of Fe increases with the longer history of earthworm invasion in the frontal group but decreases to its lowest values in the rear group soils.

Such abrupt reversals in the directions of changes in the elemental concentrations between the frontal and rear group soils are even more evident for the nutrient elements: Ca, Mg, and P (Figure 1.7c, d) (for Mg, see Table 8). Their concentrations increase with the presence of epi-endogeic and epi-anecic earthworms the frontal group, until the arrival of the endogeic species in the rear group. Soils that have been mixed by rear group earthworms show an abrupt reduction of Ca, Mg, and P concentrations. The concentrations of potassium, however, do not show such a systematic trend along the invasion transect (Figure 1.7e).

Litter elemental concentrations

Foliar elemental concentrations of Fe, K, Ca, Mg, and P were analyzed for the materials collected from Oi and Oe horizons at each soil pit in 2009 (n=12). The Oi horizon is composed of fresh and fully recognizable tree leaf litter while the litter in the Oe horizon is moderately decomposed. The litter samples have largely constant elemental compositions across the earthworm invasion transect (Table 6 Appendix I).

3.5 Elemental Inventories

To obtain the abundance of an element in a given horizon, we multiply the elemental concentration, bulk density, and the horizons' thicknesses. This is necessary because of the earthworm driven modification of horizon thicknesses and bulk density (Table 3). The A horizons show abrupt reductions in the inventories of P and Ca after the arrival of endogeic species despite the increases in bulk density and the horizon thickness (Figure 1.8a, 1.8b). Potassium, in contrast, does not show such reduction and remains relatively constant across the transect (Figure 1.8c). The foliar inventories (using Oe and Oi elemental chemistry) of Ca and P decrease after the invasion by the endogeic forefront (distance 100 meter) although their sizes are negligible when compared to those of soil A horizon and loess layer.

3.6 Exchangeable chemistry

Exchangeable cations of Ca, K, and Mg show highly similar and systematic variations along the transect (Figure 1.9a, 1.9b; see Table 1.11 in appendix II for Mg).

Soils in the rear group have reduced and vertically homogeneous concentrations of exchangeable cations in their A horizons compared to the soils in the front group.

3.7 Results from Geochemical Mass Balance Calculations

Silicon

Silicon is enriched in the A horizon relative to the loess materials in the frontal group soils (Figure 1.10a). With initial invasion of epigeic and epi-endogeic species, the frontal group Si enrichment increases. Such enrichment, however, sharply disappears in the rear group soils. The soil at 0 meter behaves differently than the rest of the soils in the rear group, and the possible reasons for its deviation from the larger trend are noted in the discussion. The depth integrated absolute mass changes of Si in the A horizons (δ) (Figure 1.11a) range from 0.21 to 0.94 kg m^{-2} in the frontal group soils. The mass gains diminish in the rear group soils from 0.38 to a loss of 0.89 kg m^{-2}, except in the soil at 0 m.

Iron

Substantial fractional enrichments of Fe, relative to the loess material, are observed for the soils in the frontal group, which are reduced to negligible gains in the rear group (Figure 1.10b). The enrichment increases with longer period of invasion within the frontal group as observed for Si. When depth integrated over A horizons, absolute mass changes of Fe range from the gains of 0.05 to 0.16 kg m^{-2} in the frontal group and from 0.03 to 0.09 kg m^{-2} in the rear group with the exception of the soil at 0 meter (Figure 1.11b).

Calcium

In the frontal group soils, Ca is enriched in the top A horizon by the factor of 8 to 14 relative to the loess parent material (Figure 1.10c). Until the arrival of endogeic species, Ca enrichment increases with the presence of epigeic and epi-endogeic species. However, in the soils inhabited by endogeic species, little enrichment of Ca is found in the A horizons. The A horizons in the frontal group soils have acquired 0.39 to 0.54 kg m^{-2} of Ca on top of what they inherited from the loess material. Such mass gains of Ca, however, decrease in the rear group soils (Figure 1.11c) from 0.09 to 0.25 kg m^{-2}.

Phosphorous

In the frontal group soils, P is enriched in the top A horizon by a factor of 5 to 18 relative to the loess parent material (Figure 1.10d). Like Ca, soils inhabited by endogeic species no longer show significant P enrichment in the A horizon, and P enrichment increases with longer earthworm invasion in the frontal group. Absolute mass addition of P to the A horizon, in addition to the inherited mass from the underlying loess material, ranges from 0.02 to 0.04 kg m^{-2} in the frontal group but decreases to 0.01 to 0.02 kg m^{-2} in the rear group soils with the exception of the soil at 0 m (Figure 1.11d).

Potassium

In the frontal group soils, K is enriched in the A horizons relative to the loess material (Figure 1.10e). Until the arrival of endogeic species, K enrichment increases with the presence of epigeic and epi-anecic species. Potassium shows negligible enrichment or depletion in the rear group soils except in the soil at 0 meter. The A horizons in the frontal group soil have acquired 0.02 to 0.08 kg m^{-2} of K. This mass input however, decreased to a gain of 0.03 and finally shifted to a loss of 0.03 kg m^{-2} in the rear group soils with the exception of the soil at 0 meter (Figure 1.11e).

3.8 Total tau (τ) and volumetric strain (ε):

Total fractional mass changes (Eq. 1b) in the frontal group show enrichment by a factor of 250-450% at the top of A horizons (Figure 1.12). The soils undergoing mixing by endogeic species show total fractional enrichment by less than the factor of 1.

A horizon soils across the transect exhibit large volumetric dilation compared to the underlying loess material. The dilation, with the advent of epi-endogeic and epi-anecic species, increases by a factor of 8 to 14 at shallow A horizon depths in the frontal group (Figure 1.13). The degree of volumetric expansion greatly decreased to less than four in the rear group soils.

4.Discussion

4.1 Elemental Mass Fluxes along the Invasion Gradient

Elemental concentrations along the invasion chronosequence (Fig. 6) are derived by three major soil processes that are operating simultaneously. First, the elements that we examine are tightly coupled to biological processes. Second, the hydro-chemical dissolution of minerals that bear the elements we examined influences their concentrations. Lastly, the physical translocation of minerals and organic matter by earthworms can alter concentrations. All of these processes have different impacts on different elements, making their measured concentrations a poor window to calculate their losses and gains. This challenge is addressed by applying geochemical mass balance models (Eq. 1-3) to the soils along the invasion chronosequence (Figure 1.3).

Here, I first focus on key nutrient elements of Ca and P. In forested ecosystems, Ca cycles through plants and soils *via* litter fall and mineralization processes (Likens et al.

1997) and P is tightly cycled by biologic entities such as plants, mycorhizzal fungi, and microorganisms (Wood et al. 1984). The invasive earthworms are essential in understanding the dynamics of Ca and P because of the intense disturbance of the O horizon and upper soil horizons, and decrease in fine roots (Fisk et al. 2004) that may influence nutrient mineralization and cycling of important nutrient elements. Below I discuss the elemental behaviors in A horizons in response to different stages of earthworm invasion in the order of inorganic nutrient elements (Ca, P, and K) followed by Si and Fe. Largely based on the fractional enrichment or depletion of elements (Figure 1.10a-e), the invasion sequence is divided into the following stages. Stage 1 (S1) is the initial state as observed from the soil at 190 meters that is inhabited by small biomasses of epigeic species. Stage 2 (S2) is represented by the soils at 160 and 150 meters that are inhabited by epigeic, epi-endogeic, and epi-anecic species. Stage 3 (S3) is soil invaded the longest and is populated by rear group endogeic species, and anecic species at distances 50 and 0 meters.

4.1.1. Dynamics of Nutrient Elements (Ca, P, K) along the Invasion Chronosequence

4.1.1.1 Stage 1 (Initial State with epigeic species)

The soil at 190 meter shows a high level of Ca and P enrichment in the A horizon relative to its parent material, which is likely due to biological recycling of the key nutrient elements. It has been commonly observed that soils have Ca and P deposited into their A horizons as the plants shed leaves that contain the nutrients derived from the mineral soil (Wood et al. 1980, Likens et al. 1998). We looked to soil mineralogy in order to examine the possibility that some of the Ca is from carbonate minerals present in the glacial till, but Ca-bearing minerals, dolomite and calcite, were not found in the A horizons or loess parent material (Table 2).

4.1.1.2 Stage 2 (Epi-endogeic and epi-anecic species)

The dramatic increases in the level of fractional enrichments of Ca and P in A horizons (Figure 1.10c, d) at 160 and 150 meter may be linked to epi-endogeic and epi-anecic species feeding on litter fragments from the Oa and Oe subhorizons, and partially incorporating and leaching nutrients in the organic matter into A horizons (Holdsworth et al. 2006). This is also well reflected in decreased litter biomass in the frontal group from distances 190 meter to 150 meter (Lyttle et al. 2010). This exercise stresses the importance of normalizing elemental concentrations relative to immobile elements. The modest increase (7 to 10%) of Ca concentration (Fig. 6c), for example, actually accompanies the drastic enhancement of enrichment from the factor of 7 to 14 (Fig. 9c).

Litter fragments from the O subhorizons are more readily decomposed due to fragmentation (Hobbie et al. 2006) which may explain the short-lived nature of the greater enrichment of Ca and P over the 40 meter distance from 150-190 meter (approximately 8 years of invasion history given an 5 m yr^{-1} migration rate). Epi- and endogeic earthworms, by processing leaf litter, can expedite nutrient cycling and P leaching from the soil (Pelletier 2001), leading to P limitation (Lawrence et al. 2003). Sugar maple tree rings from earthworm invasion sites, including the Ottertail transect, show a three-part response to earthworm invasion. Trees may be initially shocked by the loss of the O horizon, but the combination of possible reestablishment of fine roots and mineralization of nutrients held in organic matter may influence a period of growth from a pulse of nutrients. The authors hypothesized that increased growth rates were short lived due to leaching of N and P (Larson et al. 2010). A brief window of further enrichment of Ca and P in the A horizons near the beginning of earthworm invasion may therefore be reflected in the growth of sugar maple trees.

4.1.1.3 Stage 3

The soils in the rear group, with endogeic and anecic species present, show that the Ca and P fractional enrichments found in the front group soils are drastically reduced (Fig. 9c and d) and also show homogenized depth profiles. Endogeic species consume larger amounts of soil organic matter and soil minerals in comparison to epi-anecic juveniles. Endogeic earthworms thus rapidly mineralize Ca and P in the organic matter, which is represented in the abrupt decrease of light density fraction organic matter in the rear group soils (Lyttle, in preparation). The newly released Ca and P from organic matter may result in leaching losses. The appearance of the endogeic forefront leads to vigorous A horizon mixing, which may negatively affect soil biology (i.e. plant roots and fungal mycelium networks) that is critical in retaining nutrients in the rhizosphere. The newly released Ca and P from organic matter may therefore be lost through leaching because of the low demand by diminished plant communities.

The loss of enriched biologically important Ca and P in the A horizons may affect the growth and sustainability of the forest over time. The nutrient imbalances of these elements (Ca and P) through weathering, for example, lead to foliar imbalances that result in altered sugar maple physiology and decline syndrome (St. Clair et al. 2008). The availability of soil base cations to sugar maples plays an important role in their health (Long et al 2009), and when limiting, they can negatively affect the sugar maple's photosynthetic function (Lui et al. 1997) and may impair primary metabolism (St. Clair

2004). For example, the soils in the northeastern United States affected by acid deposition were depleted of base cations, which resulted in reduced sugar maple tree growth and health (Bailey et la. 2004 and 2005). Invasive earthworms may play a role reducing the buffering capacity of the soils by reducing the enrichment of Ca in shallow soils, and therefore influencing sugar maple growth.

The observed decrease in P enrichment in A horizon differs from the observations made elsewhere. P dynamics may be impacted along our study site as soil morphology is fundamentally altered from a mor to mull soil after earthworm invasion. In mor soils, the organic horizon is distinctly delineated from the underlying mineral material. The fine roots in the organic horizon effectively work to uptake P released via mineralization (Wood 1980). However, in mull soils, soil fauna (e.g. earthworms) mix the organic horizon and mineral soil, where P from the litter layer comes in contact with inorganic constituents (Fe oxides), creating a sink for inorganic P, therefore reducing the availability for plants (Pare and Bernier 1989). Suarez et al. (2004) also noted that A horizon soil becomes more enriched in P after anecic species bring up the subsoil materials rich in P, which is not observed at our site.

4.1.1.4 Potassium

Potassium, an important plant nutrient, behaves similarly to Ca and P discussed above. Potassium also serves as an excellent example to illustrate the power of geochemical mass balance model. At the initial state, the concentration of K is lower in the A horizon relative to the loess material (Fig. 1.7e). Despite the K depth profile, it is still enriched in the A horizon relative to the loess layer (Fig. 1.10d). This seemingly contradictory result reveals an important part of the K cycle. The excess K is likely from the leaf litter, which also adds other elements (Ca, P, Si, etc) into the A horizon in greater quantities (Table 6), that result in lowering the concentration of K.

As the initial stage (S1) transitions to S2, epi-endogeic species incorporate more litter material harboring K into the shallow A horizon, which results in further enriching the A horizon K relative to the loess layer (Fig. 1.10d). The additional enrichment is achieved with little change in the K concentrations because the incorporated litter mass is composed of other elements as well.

In the S3 (except at 0 m), K concentrations in the shallow A horizon increases (Fig. 7e) probably because of (1) greater leaching losses of other elements like Ca, Mg, and Si as evidenced in their fractional mass changes (Fig. 1.10) and (2) physical incorporation of loess material that has higher K concentrations in the A horizons. The increasing concentration hides the fact that the K enrichment declines or nearly disappears in the S3 (Fig. 1.10d), which cannot be solely explained by physical mixing between the A horizon and loess material but has to involve the loss of pre-existing K enriched in the A horizon, possibly through leaching. The analysis above illustrates that without the use of the geochemical mass balance, actual mass gains and losses of K in the A horizons would not have been revealed.

4.1.1.5 *Exchangeable chemistry*

Exchangeable cations (Ca, K, Mg) in the frontal group are highest in the upper 10 cm (Figure 1.9a,b), likely because the cations are derived from sugar maple leaf litter (Finzi et al.1998). Exchangeable depth profiles of Ca and K are similar to the elemental depth profiles, with one notable difference at 100 meters, which clearly marks a transition between the frontal and rear group soils. The loss of exchangeable cations in the rear group is likely due to the combination of a short-turnover time of exchangeable cations, and the significant reduction of organic matter that functions as a major source of cations and cation exchange capacity. As endogeic earthworms ingest and facilitate the decomposition loss of particulate organic matter (Lyttle 2011), most cations mineralized from the organic matter may be leached (Fig. 1.8) and therefore do not replenish the exchangeable cation pools. Decreased exchangeable cations throughout the rear group soils further suggest that anecic species (present at 50 and 0 meters) negatively affect the supply of exchangeable cations by removing litter. Runoff erosion of *L. terrestris*'s casts enriched in exchangeable cations may also contribute to the losses.

Our results of exchangeable cations do not agree with other published measurements which focused on earthworm casts. Oyedele et al. (2006) investigated the chemistry of casts from the epi-endogeic *Hyperiodrilus africanus* earthworm, which were collected from the Lixisol and Luvisil soils at 3 different locations in Nigeria (Ogere, Ikenne, and Ibadan) under bush fallow. They found that the casts of *H. africanus* were enriched with dispersible clays and exchangeable Ca and Mg. Winsome and McColl (1997) also found similar results of enriched Ca, Mg, and K in casts compared to the bulk soil for an epi-endogeic species, *Argilophilus papillifer eisen*, in a microcosm study using the soils from a mixed conifer oak forest soil in the Cascade Mountains in northern Califonia, which generally agreed with other results from both temperate and tropical forests (Lund and Jacobson 1944, Nye 1955, De Vlesschauwer and Lal 1981, Kang et al. 1994).

This discrepancy between our results and published studies is likely derived from their focus on comparing earthworm casts to the bulk soil, while we target A horizon materials as they are actively mixed by invasive earthworms. The contrast of our results and those from previous studies highlights the potential pitfalls of projecting published earthworms' role in local biogeochemical cycles to assess the biogeochemical impacts of invasive earthworms.

4.1.1.6 Elemental inventory

The A horizon inventories of Ca (and P) decrease from 0.47±0.06 kg m^{-2} (0.04±0.005 kg m^{-2} for P) in the front group to 0.21±0.02 kg m^{-2} (0.02±0.002 kg m^{-2} for P) in the rear group. The mechanisms behind the reduction of their enrichment in A horizons is discussed above. The degree of reductions in the A horizon inventories of Ca and P are significantly less than what were shown in the losses of fractional enrichments. This is because endogeic earthworms, while reducing the elemental enrichment, also increase the bulk density and thickness of the A horizons. While the reduction in the biologically active A horizon's Ca inventory appears to be compensated by the increase in the Ca inventory in the loess horizon, such compensation does not occur for P. The inventory of P in the loess material is consistent across the transect (Fig. 1.8.).

The A horizon inventory of K offers another example to illustrate the power of the geochemical mass balance model which showed the loss of K enrichment in the A horizon, despite the obvious increase in its concentration during S3. The A horizon inventory of K shows a slight but still significant increase from 0.16±0.04 kg m^{-2} in the front group soils to 0.20±0.02 kg m^{-2} in the rear group soils. (Fig. 1.7c). Despite the loss of the pre-existing K, the A horizon is gradually filled with higher K concentration material. Additionally the A horizon bulk density and horizon thickness increases, which also contributes to the inventory calculation. The increase of K inventory is also clear for the loess material. Therefore, we suggest that the lost K from the A horizon could have been captured in the underlying loess layer.

Although O horizon Ca and P inventory pools also decrease with greater time length of earthworm invasion, their masses are negligible compared to the A horizon and loess pools. Although litter concentrations of Ca, P, and K are not altered, their foliar inventories are impacted because of the earthworm-driven reduction of litter.

4.1.2 Dynamics of Si along the invasion chronosequence

Si, like K, illustrates the value of adopting the geochemical mass balance approach. Once Si concentrations are normalized relative to Zr, we see that lower A horizon concentrations of Si in the frontal group A horizon relative to loess material (Fig. 1.6a) disguise the fact that the A horizons are enriched in Si relative to the loess material up to 80% (Fig. 1.9a). This enrichment is likely due to the phytolith-bearing leaves of sugar maple trees that have entered the A horizon. The enrichment of Si in A horizons is further enhanced by epi-endogeic and epi-anecic species within the frontal group (S2) which show fractional mass gain increases from 190 meter to 160 meter to 150 meter (Fig. 1.9a). This is probably due to earthworm activities that incorporate sugar maple leaves into the A horizons, which at the same time add other elements in greater quantities and thus lower the concentrations of Si (Fig. 1.7a).

With the arrival of endogeic species (S3), Si concentrations increase in the A horizon (Fig. 1.6a). However, fractional enrichment of Si relative to the loess material reveals an abrupt decrease. The increases in Si concentrations occur because of (1) additional incorporation of loess material which has higher Si concentration than the A horizon and (2) greater losses of other elements such as Ca (Fig. 1.4). With mixing, the materials in the A horizons become increasingly similar to the underlying loess parent material, which explains why the δ values move toward zero. However, dramatic reduction in Si enrichment still requires the loss of excess Si, which is in agreement with the significant reduction of opal in the rear group soils (Fig. 1.5d). Phytoliths are liberated from organics into the soils through a number of ways one of the most common pathways being death and decay of vegetation (organic matter) into A horizon soils (Piperno 2006), which would be influenced by the organic matter feeding endogeic species. Indeed, phytoliths produced from sugar maples are known to be highly fragile and susceptible to dissolution because of their geometric configuration and large surface area (Wilding and Drees 1971). Therefore, these observations lead to a conclusion that endogeic ingestion of A horizon materials result in the dissolution and leaching of phytoliths rather than redistribution, due to the absence of opal concentrations below the A horizons.

It is notable that the soil at 50 meter shows fractional depletion of Si relative to the loess material, which indicates that there are other sources of Si loss in addition to the opal. The primary silicate minerals mixed into the A horizons from the loess material may be experiencing chemical dissolution that leads to the subsequent leaching of Si. Given that the endogeic arrival at the site occurs within the last decade or so, the depletion of Si suggests a remarkably fast loss. Ingestion of minerals by earthworms may enhance the dissolution of the minerals. Suzuki et al. (2003), for instance, fed earthworms mixtures of potassium feldspar and quartz grains and found that earthworm consumption led to the physical break down and rounding of the mineral grains. Needham et al. (2004) suggested that earthworms may chemically influence mineralogy, after finding the formation of new minerals in the casts of *L.terrestris* (nightcrawler), which they attributed to the earthworm's harsh gut environment that degrades the crystal lattice of minerals and may enhance weathering. These published studies suggest that the degrees and rates of dissolution losses of the primary silicate minerals may be significantly altered by earthworm ingestion.

4.1.3 Dynamics of Fe along the invasion chronosequence

Like Si, Fe is enriched in A horizons in the soil at 190 meter (S1) and shows greater enrichment with the arrivals of epi-endogeic and epi-anecic (S2). However, such enrichments disappear in the soils inhabited by endogeic species, with the exception of the soil at 0 meter (S3). Conversely to Si, the concentrations of Fe decreased with the appearance of endogeic species and then stabilized through further arrivals of anecic species.

The earthworm gut is both organic rich and anoxic (Drake et al. 2007) which may play an important role in influencing pedogenic iron oxides as endogeic earthworms ingest A horizon materials. Windsome and McColl (1998) reported that casts deposited by epi-endogeic *A. papillifer* contained kaolinite which was not present in the soil. The authors attributed the source of the kaolinite to the dissolution of colloidal Fe and Al oxides during, or shortly after, earthworm ingestion of soil materials. Because our XRD results suggest that earthworm-derived production of new kaolinite is unlikely (Fig 1.5e), the declining enrichment of Fe in the A horizons must be associated with endogeic consumption of soil materials.

Despite the Fe enrichment declining with the arrival of endogeic earthworms, our earlier work (Resner et al. 2011) showed that extractable Fe pools ($Fe_{di,\ py,ox}$) were more abundant in the rear group soils (Table 7 Appendix 1). The reported increases in dithionite- citrate-extractable Fe (Fe_{di}) in rear group soils, which is interpreted to represent crystalline, pedogenic, iron oxides, may be due to the dissolution of Fe in earthworms' guts followed by re-oxidation. The greater sodium pyrophosphate extractable Fe (Fe_{py}) also suggests more effective contacts between Fe ions and the organic molecules in earthworm gut. In agreement with these results from our study, earthworm casts from a site in Nigeria showed higher amounts of extractable Fe_{di} and Al_{di} in comparison to the A horizon soils, and also higher Fe_{ox} which may indicate an alteration of the crystalline oxides to a more amorphous form of Fe and Al oxides (Oyedele et al. 2006).

4.2 Connection between Volumetric Changes and Mass Fluxes

It has been commonly observed that biologically active soils are volumetrically dilated because of the addition of low-density organic matter and new pores created by active bioturbation (Chadwick et al. 1990). Earthworms reduce low-density organic matter (Lyttle et al., in preparation) and also burrow into mineral soils. Calculated values of ε and τ for the soils along the invasion transect were plotted against each other to understand the potential relationship between organic matter cycle and volumetric changes in the A horizons.

Epsilon (ε in Eq.3) can be re-written as a function of total fractional mass change (in Eq.1b) as:

$\varepsilon_{i,w} = \left[\frac{\rho_p}{\rho_w}(\tau_{total} + 1)\right] - 1.$ (eq. 4).

Then, we use this equation in examining the relationship between the calculated values of total τ and ε (Figure 1.12 and 1.13).

Fig 1.14 shows the relative roles of organic matter and bulk density in the control of volumetric dilation in the A horizons. The strain has non-zero and positive y-intercept (where τ is zero). The value of the y-intercept (~2) represents the volumetric dilation that occurs purely because of the physical expansion of the parent material without additional mass inputs. The observed values of strains for the soil at 190 meter increase up to ~7 as the values of total fractional enrichment increase up to ~2.5. Therefore, as the A horizon mass increases by two and half fold by the addition of organic matter, the volume of the A horizon increases by seven fold, and less than one third of the volumetric extension is due to simple burrowing and restructuring of the material.

The three invasion stages we previously identified for elemental fluxes works well for describing the trends in volumetric expansion. In S2, epi-endogeic and epi-anecic species increase the total fractional enrichment up to 4.5, which results in further increasing the volumetric dilation up to a factor of 15. However, as the light-density organic matter dramatically decreases with the arrival of endogeic species (S2) (Lyttle et al., in preparation), the total fractional enrichment declines abruptly to the values less than 1, and the volumetric dilation accordingly decreases to the values less than 4. Therefore, most of the volumetric dilation is controlled by earthworms' impacts on the light-density organic matter. It is also notable that the y-intercept also decreased for the soils in the rear group. This indicates that endogeic earthworms, by altering the structure of the A horizon material, also lead to decreasing the degree of volumetric dilation.

Earthworms are commonly thought to aerate the soil and subsequently increase the flow of water, although this concept is largely limited to agricultural soils, where highly compacted soils by agricultural equipment may be loosened by earthworms' burrowing activities (Hale et al. 2005b). The loss of O horizon and volumetrically less expanded A horizons in the soils inhabited by endogeic earthworms may encourage surface runoff, therefore influencing the forest's hydrology and soil moisture. During the liquid extraction of earthworms along the transect, we noticed that heavily invaded soils had more surface runoff and less infiltration than the soils with few to no earthworms. Decreased infiltration of water should be one of the results from the loss of O horizon - which also increases evaporation loss of water (Hale et al. 2005b) - and volumetrically less dilated A horizons post invasion. Increased bulk densities due to earthworms' activities have been previously documented in Minnesota (Hale et al. 2005b, Alban and Berry, 1994), which we also find across the Ottertail transect (Table 3). Here, we quantitatively showed how the earthworms' impacts on soil biogeochemistry and physical structure are coupled. Our finding suggests the potentially significant role of earthworm invasion in altering the transport of gases and water, and thus moisture contents in the biologically critical shallow soil depths.

4.3 Implications for forest nutrient dynamics

Our observation that Ca and P enrichment in A horizons disappear with the arrival of endogeic species has far reaching implications for species richness in northern hardwood forests. In addition to the physical disturbance of the rooting zone, the depletion of biologically important elements seen in our results may also play a role in influencing plant communities post earthworm invasion. For example, earthworm invasion may favor plants with low nutrient demands and no mycohizzal associations (Frelich et al. 2006), such as *Carex pensylvanica (Pennsylvania sedge)*, an understory plant in sugar maple forests, that has no mycorhizzal associations (Brundrett and Kendrick 1988). *Carex pensylvanica* recolonizes post earthworm invasion across our invasion transect, in earthworm invaded soils with high degrees of rhizosphere disturbance (Hale 2006) although many other plants decrease in richness and abundance. The decreased demand of nutrient pools because of lower plant abundances may encourage further loss of soil elements and thus reinforce earthworms' influence on the productivity and diversity of understory plant communities.

Mycorhizzal fungi, which assist in nutrient acquisition, also decrease in sugar maple forests with the onset of earthworm invasion and may influence P dynamics within the soil (Lawrence et al. 2003). Lawrence et al. (2003) found that earthworm invaded plots at Arnot Forest in New York, had higher concentrations of labile P and higher P in litterfall, indicating enhanced P uptake and possibly higher P availability in the soils. Lawrence et al. (2013) attributed loss of fungal colonization and decreased abundances in sugar maple trees to increased nutrient availability that can reduce colonization, or secondly by the physical disturbance of earthworm driven soil mixing that disrupts mycelium and infection rates. This may be occurring in the frontal group soils at our site, which show increased P enrichment in A horizons, but our foliar chemistry do not show any trend in P concentration along the transect (Table 6 Appendix I).

The reduced inventory of A horizon Ca is compensated by the increased inventory in the underlying loess layer. However, as long as the source of Ca for the sugar maple trees is not certain, it is difficult to assess how sugar maples will respond to the changes in the soil Ca pool.We are interested in the declining enrichment of Ca because of sugar maple's sensitivity to Ca nutrition (Long et al., 1997) and its role in protecting against environmental stressors such as cold and disease (McLaughlin and Wimmer 1999). Ca can also influence the uptake of other biologically important nutrients, Mg, K, and P in sugar maple trees (Kobe et al. 2002).

4.4 Implications for Carbon Cycle

With major elemental cycles impacted by earthworm invasion, there may be repercussions for the soil C cycle. The data suggest that extractable Fe and Al oxides increase (Table 7 Appendix I). The pedogenic iron- and aluminum- oxides provide mineral surface area which can sorb and thus protect organic matter (Pronk et al. 2011, Kaiser & Guggenberger 2003, Eusterhues et al. 2005). Past studies have also found that polyvalent ions like Fe^{3+} and Ca^{2+} bridge soil organic matter and negatively charged clay minerals, which allows for the flocculation of organic matter and protection against microbial degradation (Chenu and Stotzky, 2002; von Lutzow 2006). Therefore, the observed alteration of major elemental budgets may play a significant role in mediating the interactions between organic matter and minerals.

Hobbie et al. (2006) suggested that hardwood forests are C sinks, but may turn into a C source with environmental disturbance. Though inorganic nutrient cycling and C dynamics are often studied separately, the interactions between organic and inorganic elemental cycles altered by earthworm invasion may have unique ecological consequences. For example, our results show that soils invaded by endogeic earthworms have decreased A horizon enrichments of Ca and P, which can decrease nutrients available for sugar maple and may negatively impact its photosynthesis (St. Clair 2004) and subsequently impact the larger C cycle. In addition to altered nutrient pools, we found that earthworms alter soil properties, (e.g. increased bulk density) which we observed to decrease water infiltration in earthworm invaded soils. The C cycle at our site may also be greatly impacted by warming due to the prediction that suitable habitat for sugar maple in Minnesota is likely to be eliminated within the next 100 years (Iverson et al. 2008) because of proposed climate change. With impending climate change, invasive earthworms may amplify the impacts of warming on the forests in central North America by eliminating the soil moisture barrier (O horizon) (Frelich and Reich 2009) and by altering the volumetric dilation of soil materials. The proposed ecological changes to the C cycle and large scale ecology reinforce the importance of policy and management strategies to reduce further spread of invasive earthworms into soils devoid of native earthworms.

4.5 Limitations of the Study

Our geochemical data and morphological observations showed that earthworm mixing is largely constrained to the A horizon and the upper boundary of the underlying loess material. We found that as earthworms invade, the A horizon expands at the expense of the O and the underlying loess parent material. Should the geochemical properties of the material underlying the A horizon have been different, we would likely have seen different geochemical results. We did not find *L. terrestris* below the loess material during our excavations. Either the silty loess material or the dense clay rich B horizon may have inhibited *L. terrestris* from deeper burrowing. If endogeic or anecic earthworms had access to the B horizons or calcareous till material, the geochemical results from this study could have been markedly different. Because of these issues, it is important to recognize that initial soil properties should have a strong influence on the degree to which soil biogeochemistry is impacted by invasive earthworms across different study sites.

Disrupting the biological retention of nutrient elements may increase their susceptibility to leaching. We predicted that an element's behavior would be governed by its biological demand and solubility, which is reflected in the greater losses of base cations (accompanying the loss of organic matter) in the A horizon compared to the less soluble Si and Fe. This observation demands the examination of how consistent the hydrology is along the studied transect. There is certainly a local scale variation in soil water. For example, the areas at distances of 20 and 30 meter show ponding after snow melt and the lysimeters installed in the soil at 50 meter collected the greatest volume of soil water. Although these variations in soil water occur due to local microtopography, we found few differences for the observed geochemical properties of the loess and the till materials along the transect. Therefore, we believe that the hydrological impacts on the observed elemental fluxes is not likely to be a major issue.

In our application of geochemical mass balance model, results from the soil at 0 meter were particularly challenging (Figure 1.11). Mineralogical and elemental compositions of the loess material at 0 meter are confirmed be similar to the rest of the transect. However, because of Zr profiles that showed lower concentrations than other rear group soils (Figure 1.15), we obtained several unusual results from the soil at 0 meter. The increase in soil bulk density in (S3) soils also plays a key role in the unusual results for soils at distance 0 meter.

5. Conclusions

This study confirms our major hypotheses that earthworms have measureable effects on soil biogeochemical cycles. The combination of monitored earthworm population, geochemical mass balance calculations, and soil carbon data lead us to conclude that earthworms affect soil elemental cycles through the following pathways. First, earthworms mineralize organic matter which results in the release of organically bound Ca, P, and K. Because earthworms simultaneously decrease plant abundances, these newly available cations are leached out rather than biologically retained. Such leaching losses of the nutrient elements outweigh the mixing driven incorporation of minerals comprised of these elements from the underlying loess layer. A similar process appears to be active for Si cycle, although the enhanced dissolution of phytoliths in the intestines of endogeic earthworms also plays a critical role.

On a fundamental level, our results reinforce the importance of bioturbation in nutrient dynamics of terrestrial ecosystems. Although the weathering supply of inorganic nutrients has been related to tectonically driven erosion of soil minerals in geologic time and continental spatial scales, our results show that the colonization by bioturbating organisms such as earthworms can cause a dramatic influence on the enrichment or depletion of major elements within the rhizosphere in a matter of years. At a more practical level, the unique outdoor laboratory used in this study allowed us to explicitly connect elemental fluxes to different ecological groups of earthworms. The result is a systematic connection between the geochemical evolution of soils and earthworm population, which could be useful in predicting how hardwood forests in the region will respond to earthworm invasions with the knowledge of the earthworm biomasses and species present.

REFERENCES

Alban, D.H. and Berry, E.C. (1994), Effects of earthworm invasion on morphology, carbon and nitrogen of a forest soil, Appl. Soil Ecol,1, 243–49, doi: 10.1016/0929-1393(94)90015-9

Bailey, S.W., Horsley, S.B., and Long, R.P. (2005), Thirty years of change in forest soils of the Allegheny Plateau, Pennsylvania, Soil Sci. Soc. Am. J, 69, 681–690, doi:10.2136/sssaj2004.0057

Baldock, J.A., and Skjemstad, J.O. (2000), Role of the soil matrix and minerals in protecting natural organic materials against biological attack, Organic Geochemistry, 31(7), 697-710, doi: 10.1016/S0146-6380(00)00049-8

Balogh-Brunstad, Z., Keller, C. K., Bormann, B. T., O'Brien, R., Wang, D., and Hawley, G. (2008), Chemical weathering and chemical denudation dynamics through ecosystem development and disturbance, Global Biogeochem. Cycles, 22, GB1007, doi: 10.1029/2007GB002957.

Bailey, S.W., Horsley, S.B., Long, R.P., and Hallett, R.A. (2004), Influence of edaphic factors on sugar maple nutrition and health on the Allegheny Plateau, Soil Science Society of America Journal, 68, 243-252, doi: 10.2136/sssaj2004.2430

Belote, R. T., and Jones, R. H. (2008), Tree leaf litter composition and nonnative earthworms influence plant invasion in experimental forest floor mesocosms, Biological Invasions, 11(4), 1045-1052, doi: 10.1007/s10530-008-9315-1.

Berner, R. A. (1992), Weathering, plants, and the long-term carbon cycle, Geochim. Cosmochim Acta, 56(8), 3225-3231, doi: 10.1016/0016-7037(92)90300-8

Bohlen, P.J., Groffman, P.M., Fahey, T.J., Fisk, M.C., Suarez , E., Pelletier, D.M., and Fahey, R.T. (2004a), Ecosystem consequences of exotic earthworm invasion of north temperate forests, Ecosystems, 7, 1–12, doi: 10.1007/s10021-003-0126-z

Bohlen, P.J., Scheu, S, Hale, C.M., McLean, M.A., Migge, S., Groffman, P.M., and Parkinson, D. (2004b), Non-native invasive earthworms as agents of change in northern temperate forests, Front Ecol Environ, 2, 427–435, doi: 10.1890/1540-9295(2004)002[0427:NIEAAO]2.0.CO;2

Brimhall, G.H., and Dietrich, W.E. (1987), Constitutive mass balance relations between chemical composition, volume, density, porosity, and strain in metasomatic hydrochemical systems: Results on weathering and pedogenesis, Geochimica et Cosmochimica Acta, 51, 567-587, doi: 10.1016/0016-7037(87)90070-6.

Brundrett, M. C. and Kendrick, B. (1988), The mycorrhizal status, root anatomy and phenology of plants in a sugar maple forest, Canadian Journal of Botany, 66, 1153-1173, doi: 10.1139/b88-166

Canti, M. G., and Piearce T.G. (2003), Morphology and dynamics of calcium carbonate granules produced by different earthworm species, Pedobiologia, 47, 511–521, doi: 10.1078/0031-4056-00221

Chadwick, O.A., Brimhall, G.H., Hendricks, D.M. (1990), From a black to a gray box- a mass balance interpretation of pedogenesis, Geomorphology, 3, 369-390, doi: 10.1016/0169-555X(90)90012-F.

Chenu, S., and Stotzky, G. (2002), Interactions between microorganisms and soil particles, an overview, Editors: Huang, P.M., Bollag, J.M., Senesi, N., Weinheim Wiley-VCH-Verlag,

Crang, M. G., Holsen R.C, and Hitt J. B. (1968), Calcite production in mitochondria of earthworm calciferous glands, BioScience, 18,299, doi:10.2307/1294220

Darwin, C. (1892), The formation of vegetable mould, through the action of worms, with observations on their habits, Murray, London, UK.

De Vleeschauwer, D., and Lal, R. (1981), Properties of worm casts under secondary tropical forest regrowth, Soil Science, 132, 175-181.

Drake, H. L., and Horn, M.A. (2007), As the worm turns: the earthworm gut as a transient habitat for soil microbial biomes, Annual review of microbiology, 61, 169-89, doi:10.1146/annurev.micro.61.080706.093139

Eisenhauer, N., Partsch, S., Parkinson, D., and Scheu, S. (2007), Invasion of a deciduous forest by earthworms: Changes in soil chemistry, microflora, microarthropods and vegetation, Soil Biology and Biochemistry, 39(5), 1099-1110, doi:10.1016/j.soilbio.2006.12.019

Eisenhauer, N., Milcu, A., Sabais, A. C. W., and Scheu, S. (2008), Animal ecosystem engineers modulate the diversity-invasibility relationship, PloS one, 3(10), e3489, doi:10.1371/journal.pone.0003489

Ellsworth, D.S., and Liu, X. (1994), Photosynthesis and canopy nutrition of four sugar maple forests on acid soils in northern Vermont, Canadian Journal of Forest Research, 24, 2118-2127, doi: 10.1139/x94-272

Eusterhues, K., Rumpel, C., and Kögel-Knabner, I. (2005), Organo-mineral associations in sandy acid forest soils: importance of specific surface area, iron oxides and micropores, European Journal of Soil Science, 56,753-763, doi: 10.1111/j.1365-2389.2005.00710.x

Essington, M.E. (2004), Soil and water chemistry: an integrative approach, Boca Raton (FL):CRC Press LLC.

Finzi, A.C., Canham, C.D., and Van Breemen, N. (1998), Canopy tree-soil interactions within temperate forests: species effects on pH and cations, Ecological Applications, 8(2), 447-454, doi: 10.1890/1051-0761(1998)008[0447:CTSIWT]2.0.CO;2

Fisk, M.C, Fahey, T.J., Groffman, P.M., and Bohlen, P.J. (2004), Earthworm invasion, fine root distribution and soil respiration in hardwood forests, Ecosystems, 7, 55-62. doi: 10.1007/s10021-003-0130-3

Frelich, L. E., Hale, C. M., Scheu, S., Holdsworth, A. R., Heneghan, L., Bohlen, P. J., and Reich, P. B. (2006), Earthworm invasion into previously earthworm-free temperate and boreal forests, Biological Invasions, 8(6), 1235-1245, doi:10.1007/s10530-006-9019-3

Frelich, L.E., and Reich, P.B. (2009), Will environmental changes reinforce the impact of global warming on the prairie-forest border of central North America?, Front Ecol Environ, 8, 371-378, doi: 10.1890/080191

Gabet, E. J., Reichman, O. J., and Seabloom, E. W. (2003), The effects of bioturbation on soil processes and sediment transport, Annual Review of Earth and Planetary Sciences, 31(1), 249-273, doi: 10.1146/annurev.earth.31.100901.141314

Gates, G. E. (1982), Farewell to North American megadriles, Megadrilogica, 4:77.

Gu, B., Schmitt, J., Chen, Z., Llang, L., and McCarthy, J.F. (1994), Adsorption and desporption of natural organic matter on iron oxide: mechanisms and models, Environ.Sci.Technol., 28, 38-46, doi: 10.1021/es00050a007

Hale, C.M. (2004), Ecological consequences of exotic invaders: interactions involving European earthworms and native plant communities in hardwood forests, PhD thesis, Department of Forest Resources, University of Minnesota, St. Paul, Minnesota, United States.

Hale, C.M., Frelich, L.E., and Reich, P.B. (2005), Exotic European earthworm invasion dynamics in northern hardwood forests of Minnesota, U.S.A., Ecol Appl., 15, 848–860, doi: 10.1890/03-5345

Hale, C.M., Frelich, L.E., and Reich, P.B. (2005), Effects of European earthworm invasion on soil characteristics in northern hardwood forests of Minnesota, Ecosystems, 8, 911–927, doi: 10.1007/s10021-005-0066-x

Hale, C.M, Frelich, L.E., and Reich, P.B. (2006), Changes in hardwood forest understory plant communities in response to European earthworm invasions, Ecology, 87(7), 1637-1649, doi: 10.1890/0012-9658(2006)87[1637:CIHFUP]2.0.CO;2

Hale, C. M.E., Reich, P. B., and Pastor, J. (2008), Exotic earthworm effects on hardwood forest floor, nutrient availability and native plants: a mesocosm study, Oecologia, 155(3), 509-18, doi:10.1007/s00442-007-0925-6

Hendrix, P.F., and Bohlen, P.J. (2002), Exotic earthworm invasions in North American: ecological and policy implications, BioScience, 52(9), 801-811, doi: 10.1641/0006-3568(2002)052[0801:EEIINA]2.0.CO;2

Hendrix, P.F., Callaham, M.A., Drake, J.M., Huang, C., James, S.W., Snyder, B.A., and Zhang, W. (2008), Pandora's box contained bait: the global problem of introduced earthworms, The Annual Review of Ecology, Evolution, and Systematics, 39, 593–613, doi: 10.1146/annurev.ecolsys.39.110707.173426

Hobbie, S.E., Reich, P.B., Oleksyn, J., Ogdahl, M., Zytkowiak, R., Hale, C., and Karolewski, P. (2007), Tree species effects on decomposition and forest floor dynamics in a common garden, 87, 2288-2297, doi: 10.1890/0012-9658(2006)87[2288:TSEODA]2.0.CO;2

Hobbie, S.E., Ogdahl, M., Chorover, J., Chadwick, O.A. Oleksyn, J., Zytkowiak, R., and Reich, P.B. (2007), Tree species effects on soil organic matter dynamics: the role of soil cation composition, Ecosystems, 10, 999-1018, doi: 10.1007/s 10021-007-9073-4

Hole, F.D. (1981), Effects of animals on soil, Geoderma, 25, 75-112.

Holdsworth, A. R., Frelich, L. E., and Reich, P. B. (2008), Litter decomposition in earthworm-invaded northern hardwood forests: Role of invasion degree and litter chemistry, Ecoscience, 15(4), 536-544, doi: 10.2980/15-4-3151

Iverson, L.R., Prasad, A.M, Matthews, S.N., and Peters, M. (2008), Estimating potential habitat for 134 eastern US tree species under six climate scenarios, Forest Ecology and Management, 254, 390-406, doi: 10.1016/j.foreco.2007.07.023

Kaiser, K., and Guggenberger, G. (2003), Mineral surfaces and soil organic matter, European Journal of Soil Science, 54, 219-236, doi:10.1046/j.1365-2389.2003.00544.x.

Kang, B. T., Akinnifesi, F.K., and Pleysier, J.L. (1994), Effect of agroforestry woody species on earthworm activity and physiochemical properties of worm casts, Soil and Fertility of Soils, 18, 193-199, doi: 10.1007/BF00647666

Kelly, E. F., O. A. Chadwick, and Hilinski, T.E. (1998), The effect of plants on mineral weathering, Biogeochem., 42, 21–53, doi: 10.1023/A:1005919306687

Kobe, R.K., Likens, G.E., and Eagar, C. (2002), Tree seedling growth and mortality responses to manipulations of calcium and aluminum in a northern hardwood forest, Canadian Journal of Forest Research, 32, 954-966, doi: 10.1139/X02-018

Kurtz, A. C., Derry, L. A., Chadwick, O. A., and Alfano, M. J. (2000), Refractory element mobility in volcanic soils, Geology, 28, 683-686, doi:10.1130/0091-7613(2000)28<683

Lawrence, B., Fisk, M.C., Fahey, T.J., and Suarez, E.R. (2003), Influence of nonnative earthworms on mycorrhizal colonization of sugar maple, New Phytologist, 157, 145-153, doi: 10.1046/j.1469-8137.2003.00649.x

Larson, E.R., Kipfmueller, K.F., Hale, C.M., Frelich, L.E. and Reich, P.B. (2009), Tree rings detect earthworm invasions and their effects in northern Hardwood forests, Biological Invasions, 12, 1053-1066, doi: 10.1007/s10530-009-9523-3

Le Bayon, R., and Milleret, R. (2009), Effect of earthworms on phosphorus dynamics-a review, Dynamic Soil, Dynamic Plant, 3 (Special Issue 2), 21-27.

Lee, K.E. (1985), Earthworms – Their ecology and relationships with soils and land use. Academic Press, Sydney, Australia.

Li, J., and Richter, D.D. (2012), Effects of two-century land use changes on soil iron crystallinity and accumulation in Southeastern Piedmont region, USA, Geoderma, 173, 184-191, doi: 10.1016/j.geoderma.2011.12.021

Likens, G.E., Bormann, F.H., Johnson, N.M., Fisher, D.W., and Pierce, R.S. (1970), Effects of forest cutting and herbicide treatment on nutrient budgets in the Hubbard Brook watershed-ecosystem, Ecol. Monogr.,40, 23, doi: 10.2307/1942440

Likens, G.E., Driscoll, C.T., Buso, D.C., Siccama, T.G., Johnson, C.E., Lovett, G.M., Fahey, T.J., Reiners, W.A., Ryan, D.F., Martin, C.W., and Bailey, S.W. (1998), The biogeochemistry of calcium at Hubbard Brook, Biogeochemistry, 41, 89-173, doi:10.1023/A:1005984620681

Long, R. P., Horsley, S. B., Hallett, R. A, and Bailey, S. W. (2009), Sugar maple growth in relation to nutrition and stress in the northeastern United States, Ecological Society of America, 19(6), 1454-66, doi: 10.1890/08-1535.1

Loss, S. R., and Blair, R.B. (2011), Reduced density and nest survival of ground-nesting songbirds relative to earthworm invasions in northern hardwood forests, Conservation Biology, 25(5), 983-992, doi: 10.1111/j.1523-1739.2011.01719.x

Lund, H.A., and Jacobson, H.G. (1944), The chemical composition of earthworm casts, Soil Science, 58, 367-375.

Lyttle, A., Yoo, K., Hale, C.M., Aufdenkampe, A., Sebestyen, S. (2011), Carbon-mineral interactions along an earthworm invasion gradient at a sugar maple forest in northern Minnesota, Applied Geochemistry, 26, S85-S88.

Maerz, J.C., Nuzzo, V.A., and Blossey, B. (2009), Declines in woodland salamander abundance associated with non-native earthworm and plant invasions, Conservation Biology, 23(4), 975-981, doi: 10.1111/j.1523-1739.2009.01167.x

McKeague, J.A., Brydon, J.E., and Miles, N.M. (1971), Differentiation of forms of extractable iron and aluminum in soils, Soil Sci. Soc. Am. J., 35, 33-38, doi: 10.2136/sssaj1971.03615995003500010016x

McLaughlin, S.B. and Wimmer, R. (1999), Tansley Review No. 104: calcium physiology and terrestrial ecosystem processes, New Phytologist, 142, 373-417, doi: 10.1046/j.1469-8137.1999.00420.x

Merritts, D.J., Chadwick, O.A., Hendricks, D.M., Brimhall, G.H., and Lewis, C.J. (1992), The mass balance of soil evolution on late quaternary marine terraces, northern California, Geological Society of America Bulletin, 104, 1456-1470, doi: 10.1130/0016-7606(1992)104<1456:TMBOSE>2.3.CO;2

Needham, S. J., Worden, R. H., and Mcilroy, D. (2004), Animal-sediment interactions : the effect of ingestion and excretion by worms on mineralogy, Biogeosciences, 1, 113-121, doi: 10.5194/bg-1-113-2004

Nye, P.H. (1955), Some soil-forming processes in the humid tropics IV. The action of soil fauna, Journal of Soil Science, 6, 73-83, doi: 10.1111/j.1365-2389.1954.tb02171.x

Oh, N.H., and Richter, D.D. (2005), Elemental translocation and loss from three highly weathered soil-bedrock profiles in the southeastern United States, Geoderma, 126, 5-25, doi: 10.1016/j.geoderma.2004.11.005

Oyedele, D.J., Schjonning, P., and Amusan, A.A. (2006), Physicochemical properties of earthworm casts and uningested parent material from selected sites in southwestern Nigeria, Ecological Engineering, 28, 106-113, doi: 10.1016/j.ecoleng.2006.05.002

Pare, D., and Bernier, B. (1989), Origin of the phosphorus deficiency observed in declining sugar maple stands in the Quebec Appalachians, Canadian Journal of Forest Research, 19(1), 24-34, doi: 10.1139/x89-004.

Pelletier, D.M. (2001), The effect of earthworm invasion on nutrient cycling and hydrologic losses in two northern hardwood forests., MS thesis, Cornell University, USA.

Piperno, D. (2006), Phytoliths: a comprehensive guide for archaeologists and paleoecologists. New York, Toronto, Oxford: AltaMira Press , Rowman Altamira.

Pronk, G.J., Heister, K., and Kögel-Knabner, I. (2011), Iron oxides as major available interface component in loamy arable topsoils, Soil Science Society of America Journal, 75,2158-2168, doi: 10.2136/sssaj2010.0455

Raymo, M.E., and Ruddiman, W.F. (1992), Tectonic forcing of late Cenozoic climate, Nature, 359, 117-122,doi: 10.1038/359117a0

Reich, P.B., Oleksyn, J., Modrzynski, J., Mrozinski, P., Hobbie, S.E., Eissenstat, D.M., Chorover, J., Chadwick, O.A., Hale, C.M., and Tjoelker, M.G. (2005), Linking litter calcium, earthworms, and soil properties: a common garden test with 14 tree species, Ecology Letters, 8, 811-818, doi, 10.1111/j.1461-0248.2005.00779.x

Resner, K., Yoo, K., Hale, C.M., Aufdenkampe, A., and Sebestyen, S. (2011), Elemental and mineralogical changes in soils due to bioturbation along an earthworm invasion chronosequence in Northern Minnesota, Applied Geochemistry, 26, S127-S131.

Riebe, C., Kirchener, J.W., and Finkel, R.C. (2003), Long-term rates of chemical weathering and physical erosion from cosmogenic nuclides and geochemical mass balance, Geochimica et Cosmochimica Acta, 67, 4411-4427, doi: 10.1016/S0016-7037(03)00382-X

Robertson, J. D. (1936), The function of calciferous glands of earthworms, Journal of Experimental Biology, 13:279–297.

Schaberg, P. G., Tilley, J. W., Hawley, G. J., DeHayes, D. H., and Bailey, S. W. (2006), Associations of calcium and aluminum with the growth and health of sugar maple trees in Vermont, Forest Ecology and Management, 223(1-3), 159-169. doi:10.1016/j.foreco.2005.10.067

Schaetzl, R., and Anderson, S. (2005), Soils: Genesis and Geomorphology, New York: Cambridge University Press.

Schaetzl, R.J., Johnson, D.L., Burns, S.F., and Small, T.W. (1989), Tree uprooting: review of terminology, process, and environmental implications. Can. J. For. Res, 19, 1-11

Scheu, S. (2003), Effects of earthworms on plant growth: patterns and perspectives: The 7th international symposium on earthworm ecology· Cardiff· Wales· 2002, Pedobiologia, 47, 846–856, doi: 10.1078/0031-4056-00270

Six, J., Bossuyt, H., Degryze, S., and Denef, K. (2004), A history on the link between (micro)aggregates, soil biota, and soil organic matter dynamics, Soil Tillage Research, 79, 7-31, doi: 10.1016/j.still.2004.03.008

Soil Survey Staff, Soil Taxonomy (Agriculture Handbook No. 436, Government Printing Office, Washington, D.C., 1975).

St.Clair, S.B. (2004), Factors and mechanisms underlying sugar maple sensitivity to edaphic stresses on Pennsylvania's Allegheny Plateau, PhD thesis, Department of Integrative Biosciences, Pennsylvania State University, University Park, Pennsylvania, United States.

Suarez, E. R., Pelletier, D.M., Fahey, T.J., Groffman, P.M., Bohlen, P.J., and Fisk, M.C. (2003), Effects of exotic earthworms on soil phosphorus cycling in two broadleaf temperature forest, Ecosystems, 7, 28-44, doi:10.1007/s10021-003-0128-x

Suzuki, Y., Matsubara, T., and Hoshino, M. (2003), Breakdown of mineral grains by earthworms and beetle larvae, Geoderma, 112(1-2), 131-142, doi:10.1016/S0016-7061(02)00300-230.

Thomas, G.W. (1982), Exhangeable cations, in Methods of soil Analysis, Part 2: Chemical and Microbiological Properties, 2nd edition, ASA, SSA, edited by Page, A. L. pp. 159-165, Madison, WI.

Wilding, L.P., Drees, L.R. (1971), Biogenic opal in Ohio soils, Soil Society of America Journal, 35(6), 1004-1010. doi: 10.2136/sssaj1971.03615995003500060041x

Winsome, T, and McColl, J.R. (1998), Changes in chemistry and aggregation of a California forest soil worked by the earthworm Agrilophilus papillifer eisen (megascolecidae), Soil Biology & Biochemistry, 30 (13), 1677-1687, doi: 10.1016/S0038-0717(97)00262-9

Wood, T., Bormann, F.H., and Voigt, G.K. (1984), Phosphorus cycling in a northern hardwood forest, biological and chemical control, Science, 223(4634), 391-393, doi: 10.1126/science.223.4634.391

von Lutzow, M., Kögel-Knabner, I., Ekschmitt, K., Matzner, E., Guggenberger, G., Marschner, B., and Flessa, H. (2006), Stabilization of organic matter in temperate soils: mechanisms and their relevance under different soil conditions – a review, European Journal of Soil Science, 57:426-445, doi: 10.1111/j.1365-2389.2006.00809.x

Figure 1.1. Recently glaciated part of the N. America (highlighted in blue) evolved without native earthworms until the recent arrival of exotic European earthworm species. The red diamond indicates the location of our study site. Map data source: Elsevier Quaternary Glaciations.

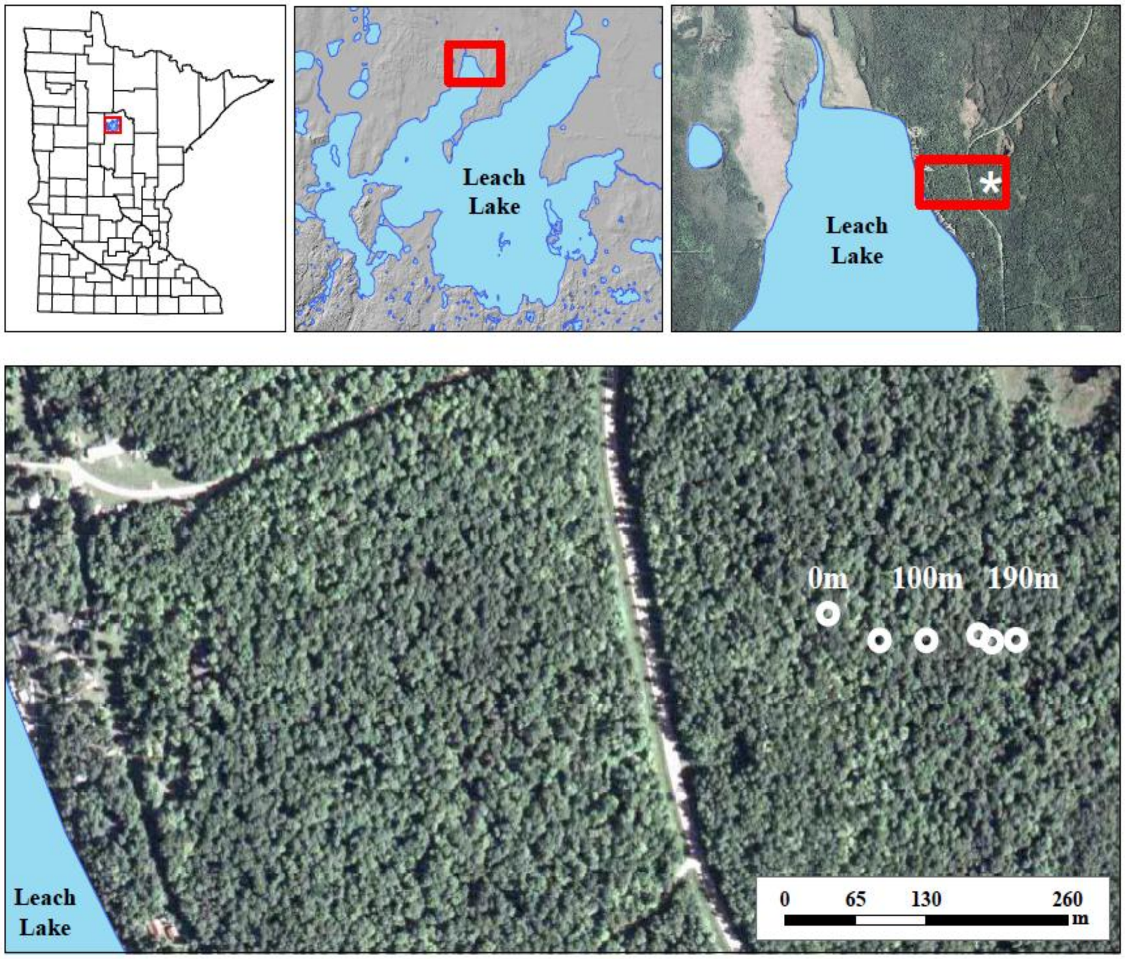

Figure 1.2. Ottertail earthworm invasion chronosequence, near Leech Lake, MN. The soil pit with the longest history of earthworm invasion (0 meter) is closest to the road. The farthest soil pit (190 meter) from the road has only few litter dwelling earthworms.

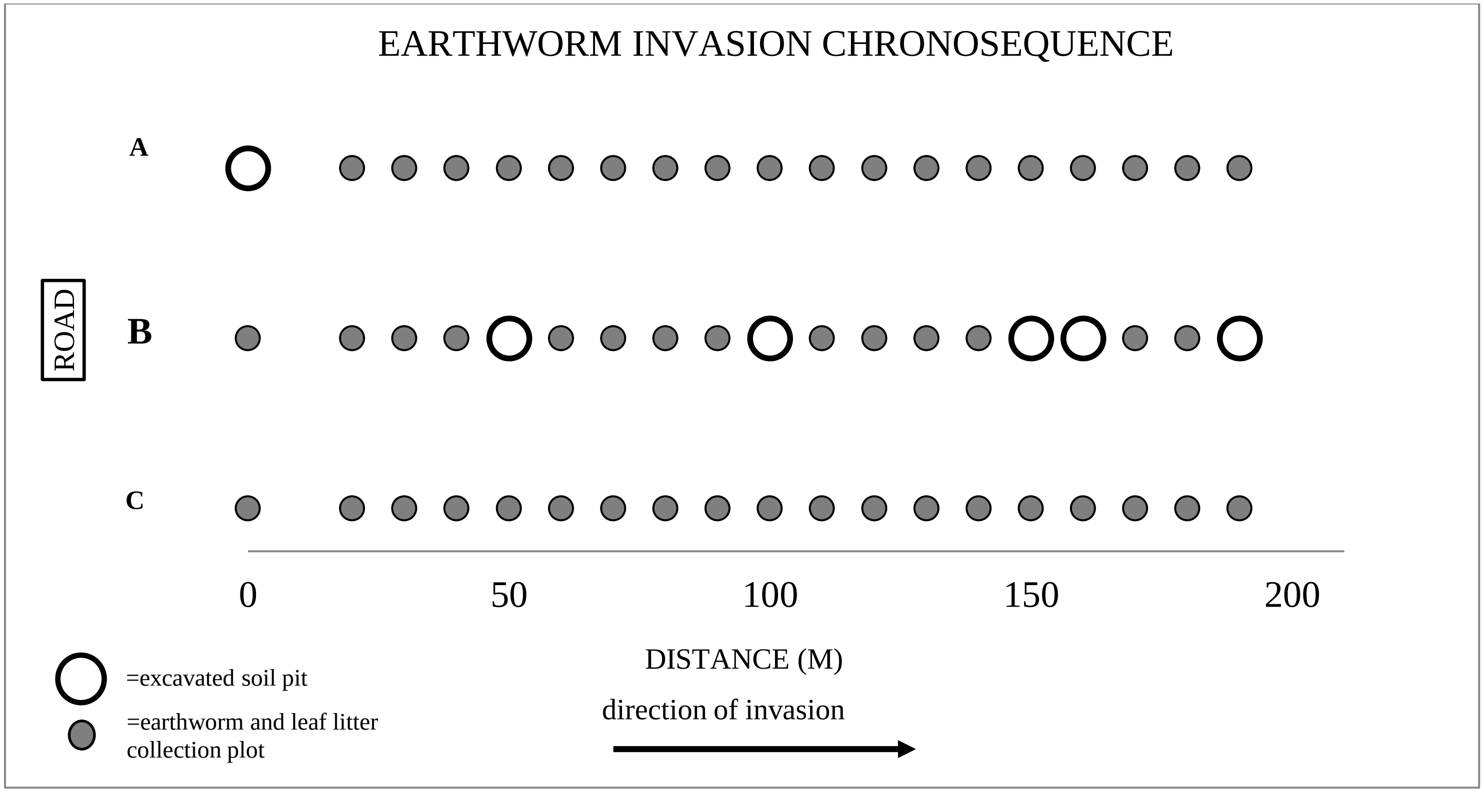

Figure 1.3. Earthworm invasion chronosequence transect sampling plots. The Ottertail sampling transect with 19 plots with three replicates. Open circles represent the soil pits that were excavated in 2009. Nineteen locations in gray circles along the transect B were used for earthworm sampling in 2009.

A B C

Figure 1.4. Removal of litter layer (O horizon) and thickening of A horizon with increasing degree of earthworm invasion are evident. From the left: Soil pit at the transect distance 190 meter (A), 100 meter (B), and 0 meter (C).

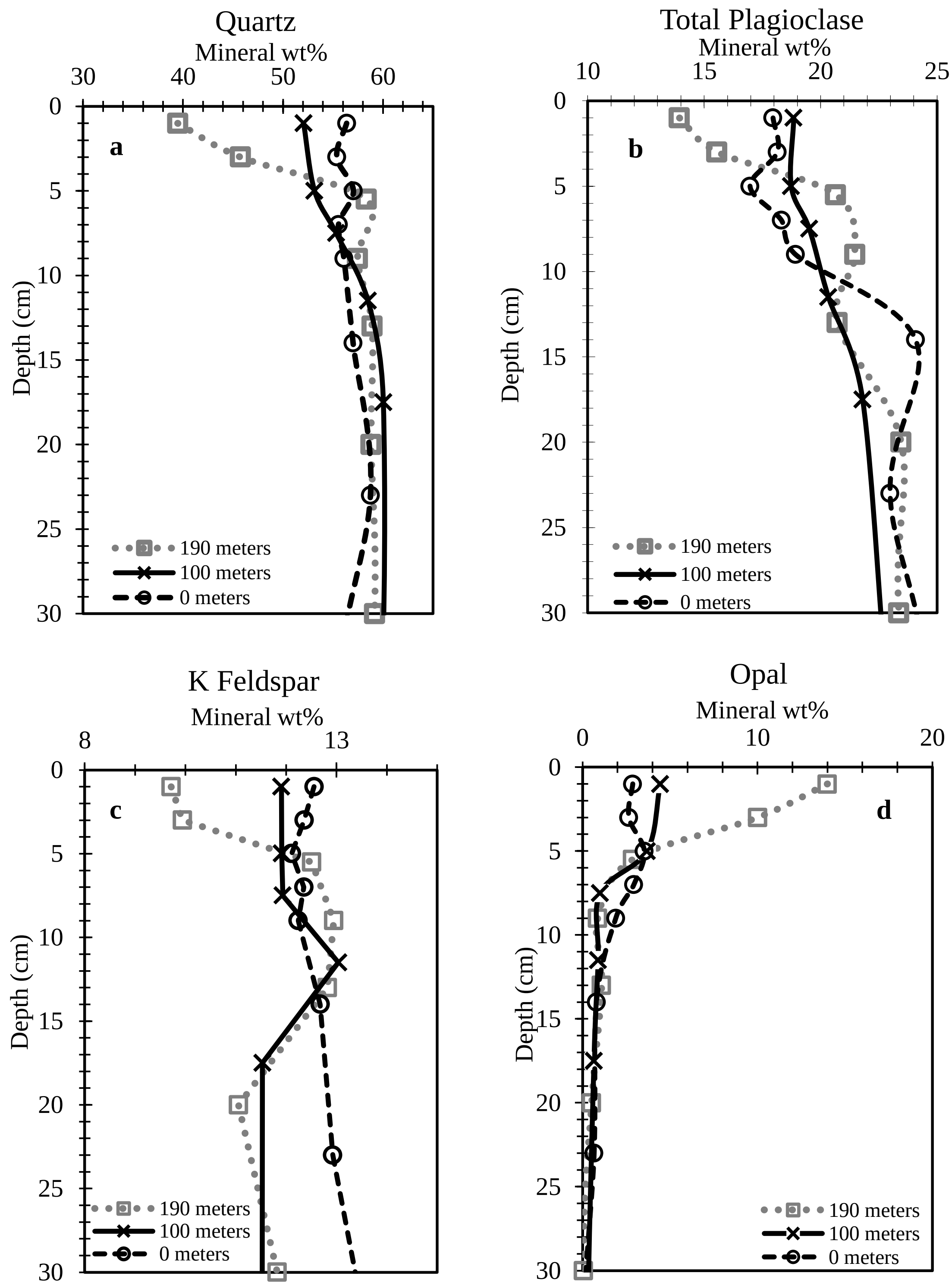
Quartz
Mineral wt%
30
40
50
60
0
5
10
15
20
25
30
Depth (cm)
a
190 meters
100 meters
0 meters
Total Plagioclase
Mineral wt%
10
15
20
25
b
K Feldspar
Mineral wt%
8
13
c
Opal
Mineral wt%
0
10
20
d

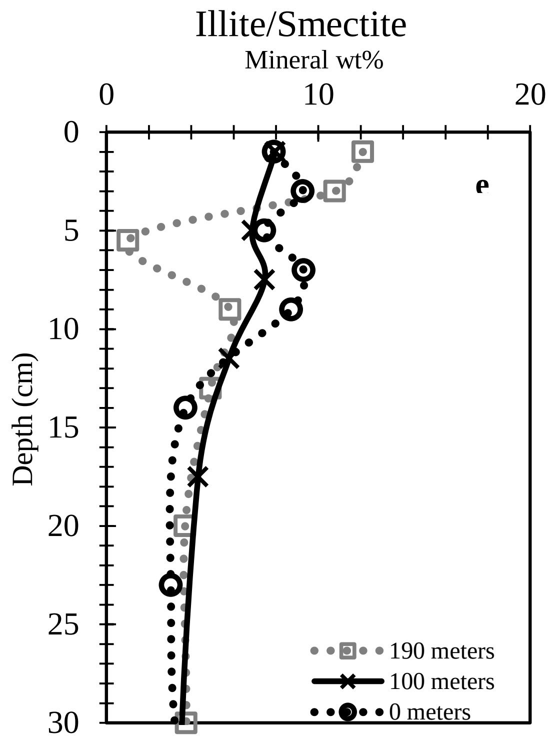

Figure 1.5. Mineralogical compositions based on quantitative XRD. XRD results show that the soil mineralogy is largely explained by quartz (A) plagioclase (B) K-feldspar (C). Other minerals of significant presence are opal (D), kaolinite (E), and illite/smectite (D). Though endogeic earthworms alter the vertical distribution of soil minerals in the upper 5cm of the soil (A horizons), mineralogical compositions in the underlying loess material show little change with depth and are remarkable consistent along the transect.

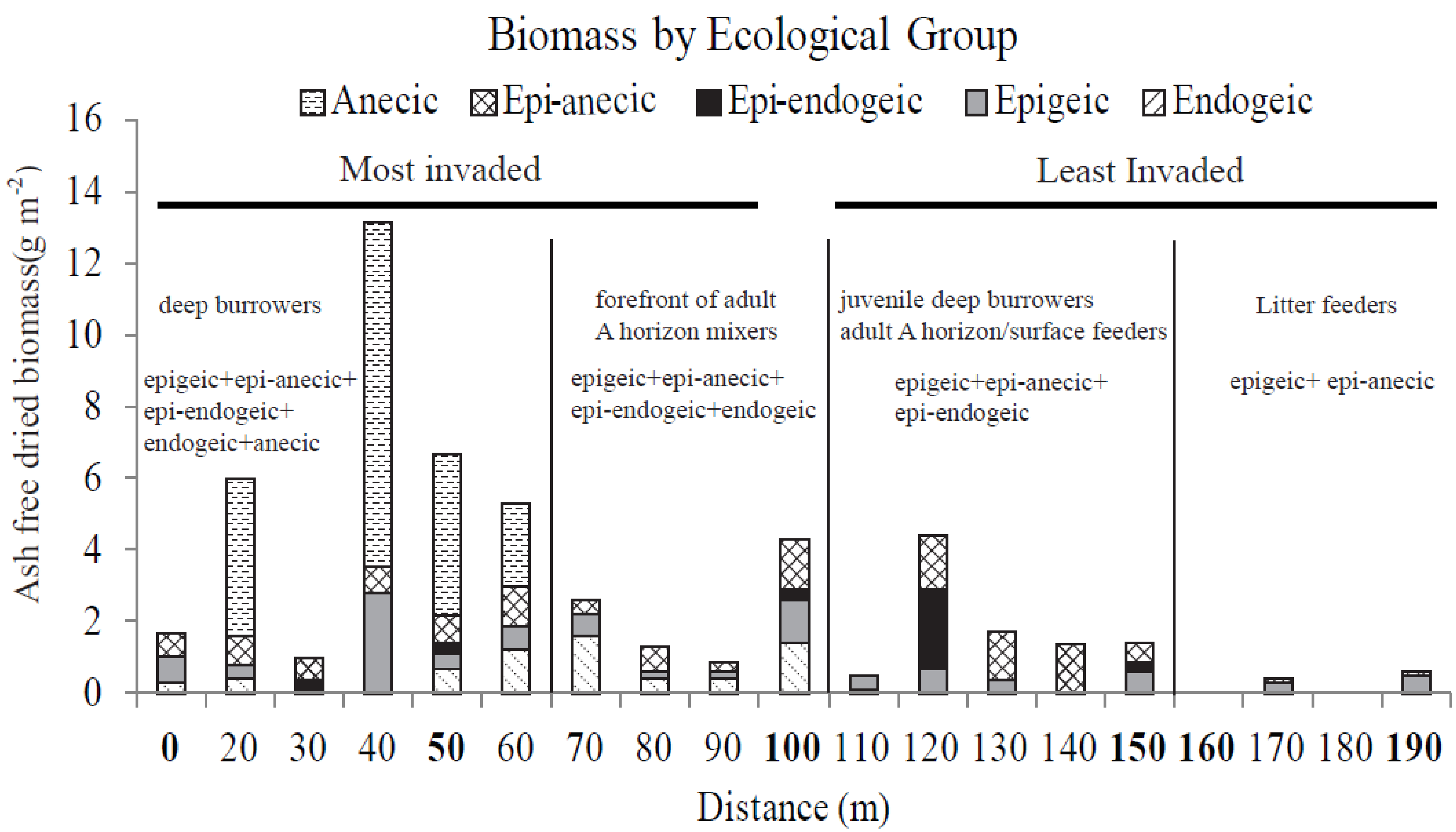

Figure 1.6. Earthworm biomass by ecological groups along the invasion chronosequence. Earthworm biomass is generally higher next to the fishing road and decreases with increasing distance from the road. Based on the earthworm biomass survey and identification and field observation of soil morphology (Fig. 1.4), the excavated soil pits (at 0, 50, 100, 150, 160, and 190 meters) are divided into two groups, the frontal and rear groups. Arrival of endogeic earthworm species largely divides the two groups. In each group, the soils are further distinguished by different associations of functional groups.

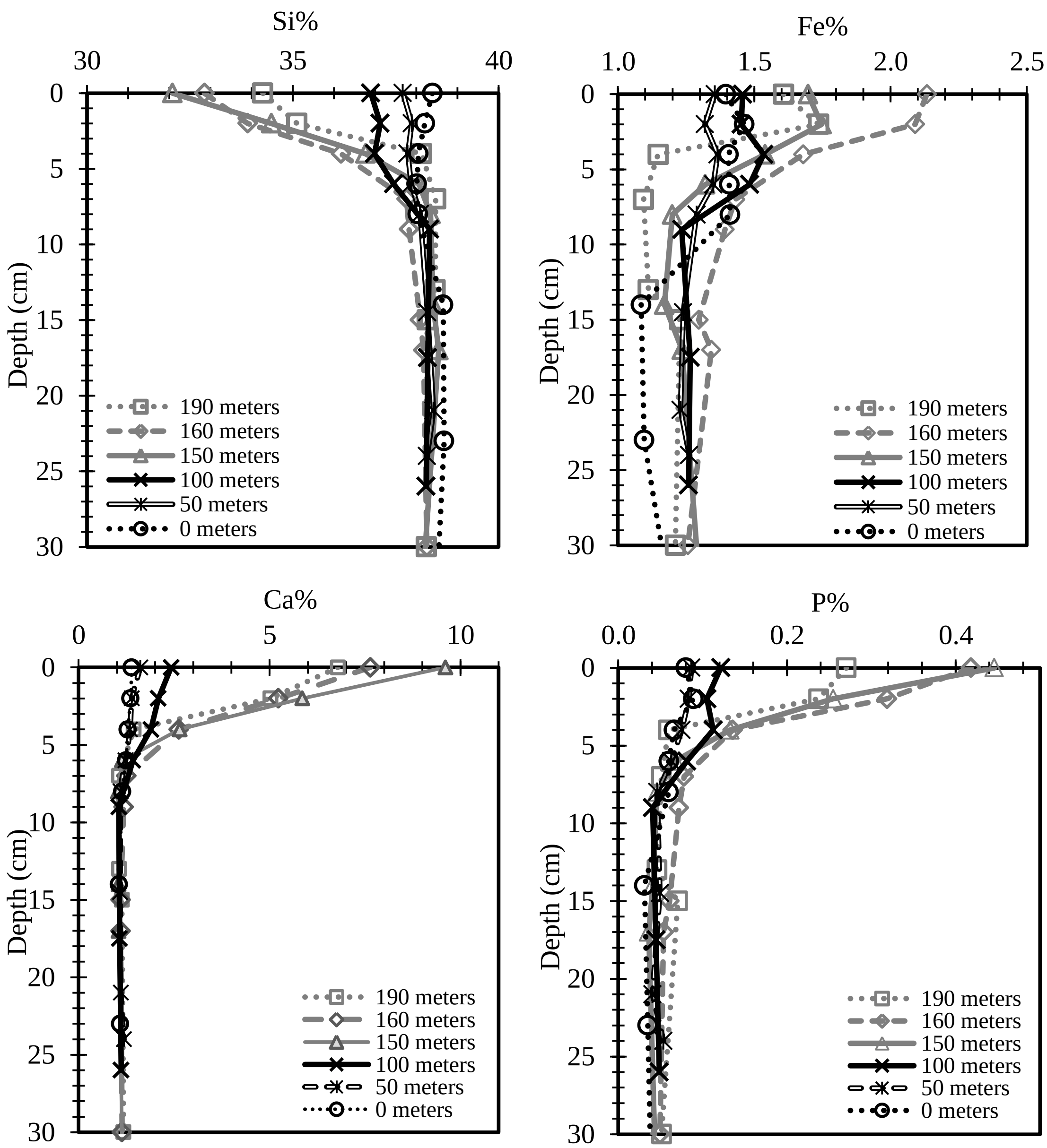
Si%
30
35
40
Depth (cm)
0
5
10
15
20
25
30
190 meters
160 meters
150 meters
100 meters
50 meters
0 meters
Fe%
1.0
1.5
2.0
2.5
Depth (cm)
190 meters
160 meters
150 meters
100 meters
50 meters
0 meters
Ca%
0
5
10
Depth (cm)
190 meters
160 meters
150 meters
100 meters
50 meters
0 meters
P%
0.0
0.2
0.4
Depth (cm)
190 meters
160 meters
150 meters
100 meters
50 meters
0 meters

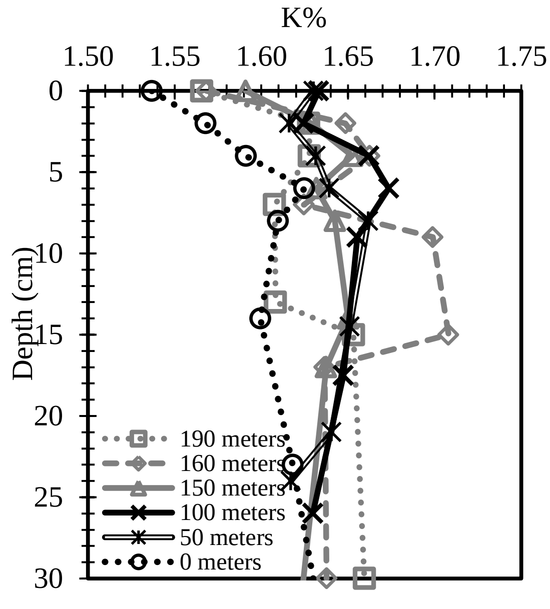

Figure 1.7. Depth profiles of Si (a), Fe(b), Ca (c), P (d), and K(e) along the earthworm invasion chronosequence.

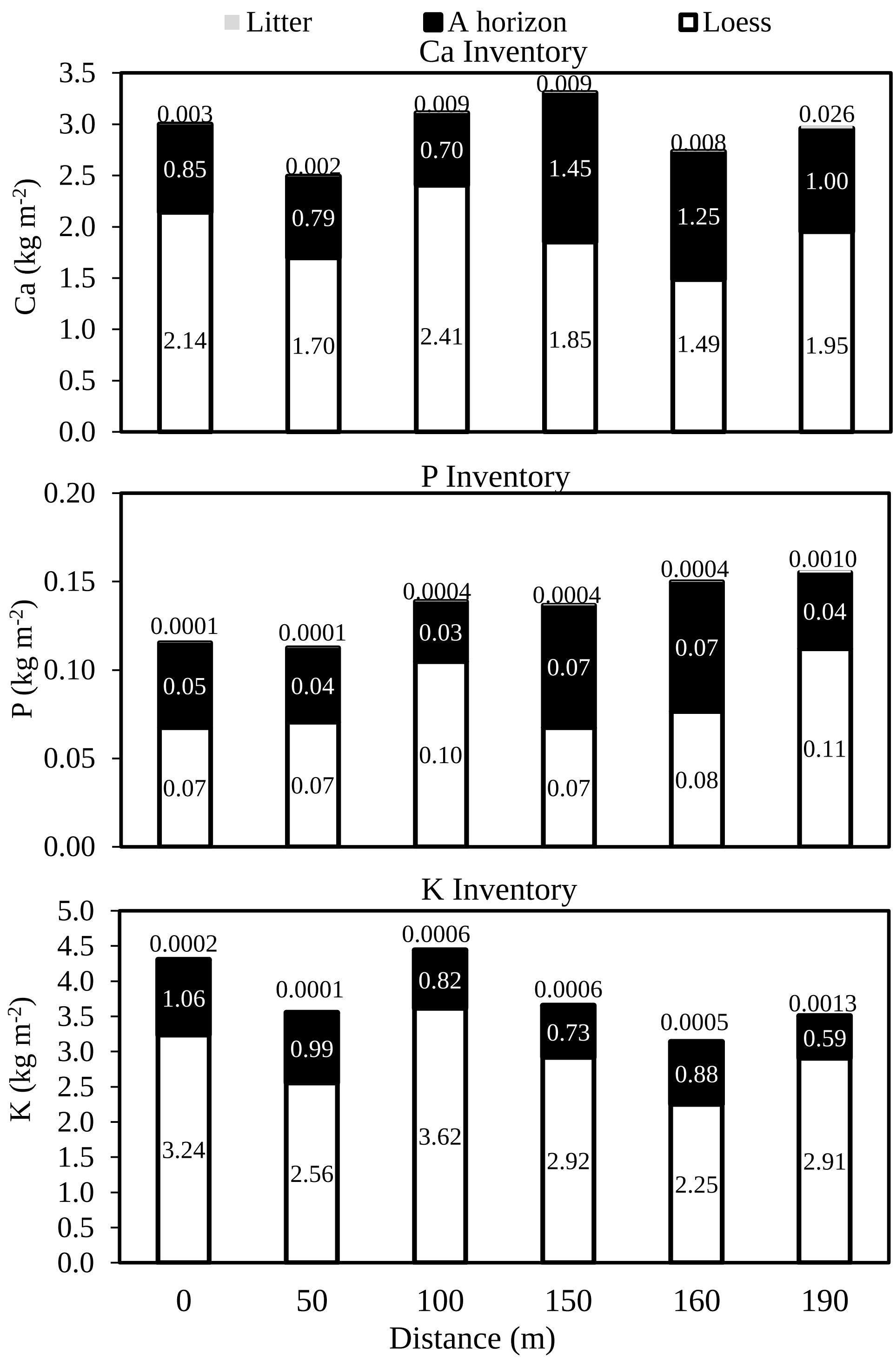

Figure 1.8. Elemental inventories by soil horizons. Ca (a), P (b), K (c). Elemental inventories of O horizons show a decrease with the longer history of earthworm invasion, but their sizes are negligible when compared to those in the A horizons and the loess layer.

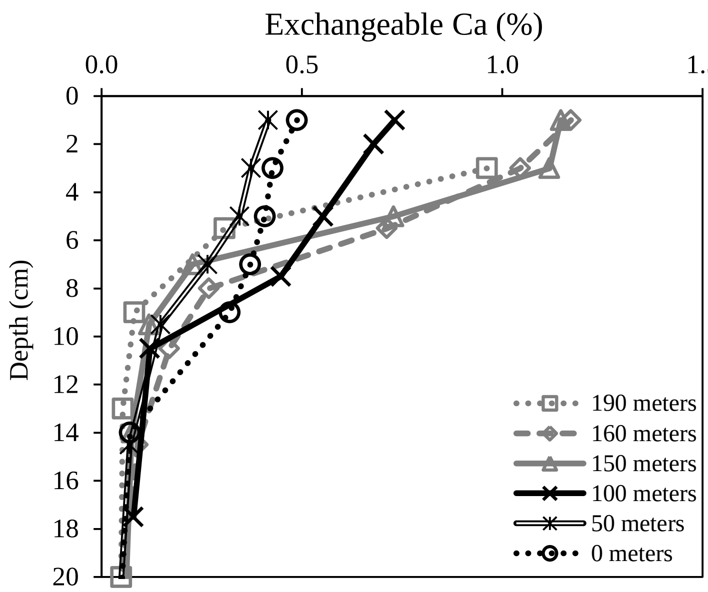

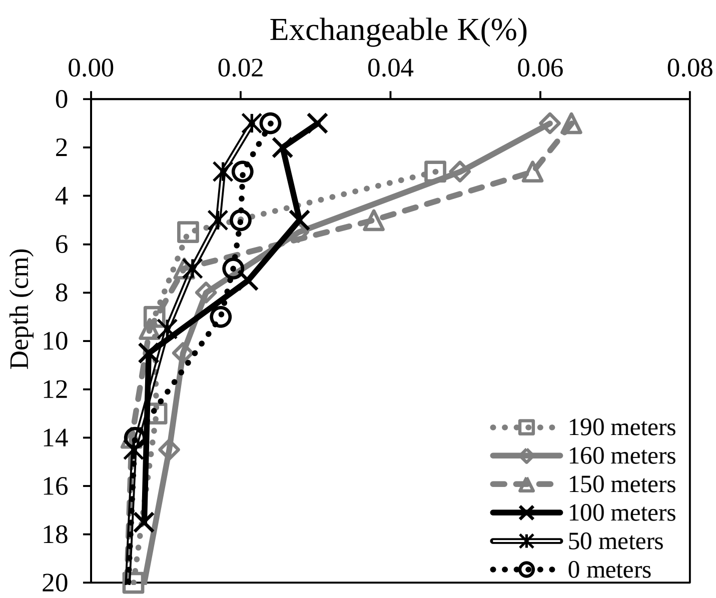

Figure 1.9. Depth profiles of exchangeable Ca (a) and K (b) concentration (%) along the studied earthworm invasion chronosequence.

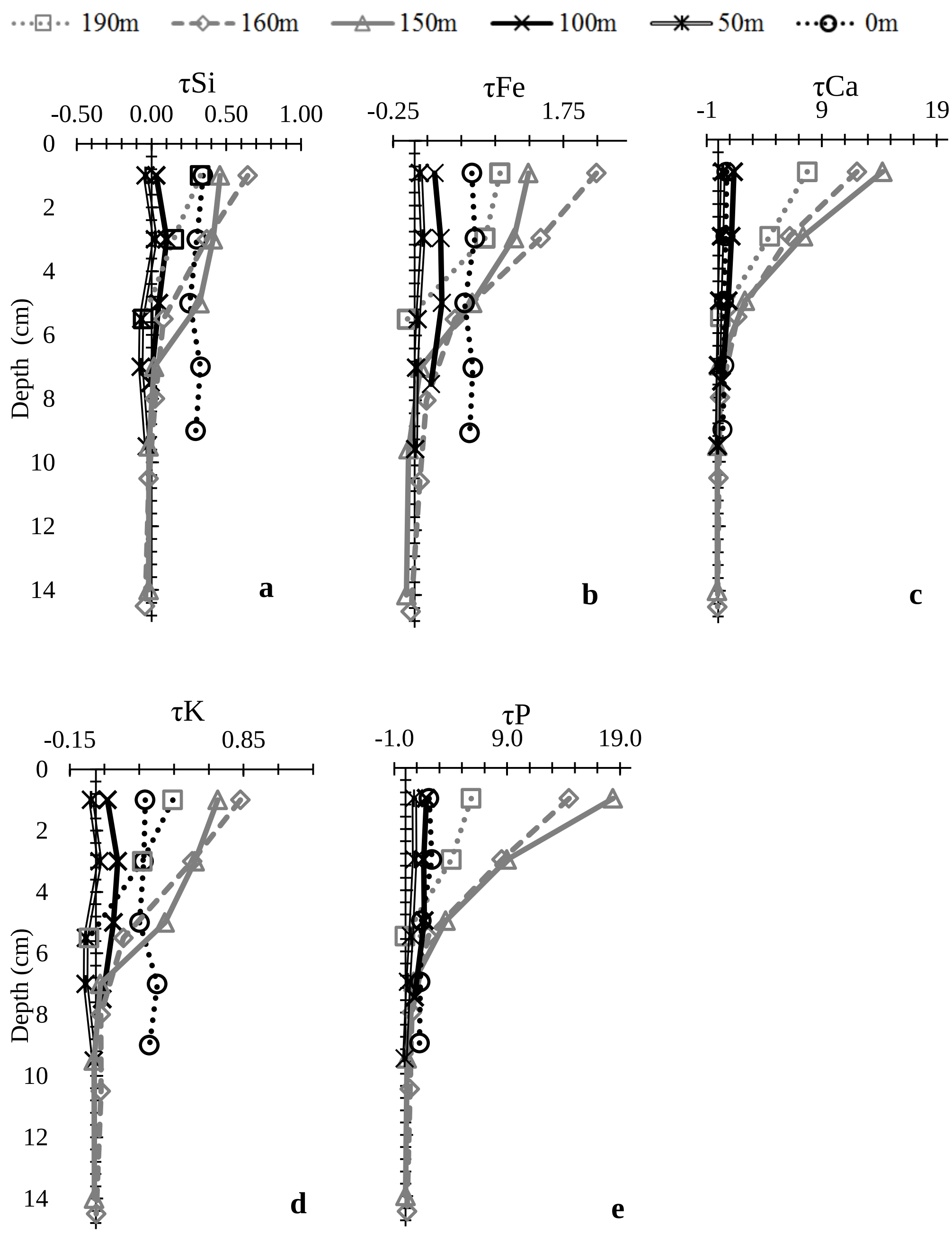

Figure 1.10. A horizon depth profiles of fractional mass gains (positive values) or losses (negative values) (τ) of Si (a) Fe (b) Ca (c) P (d) and K (e) along the earthworm invasion chronosequence. The vertical line indicates no mass gains or losses.

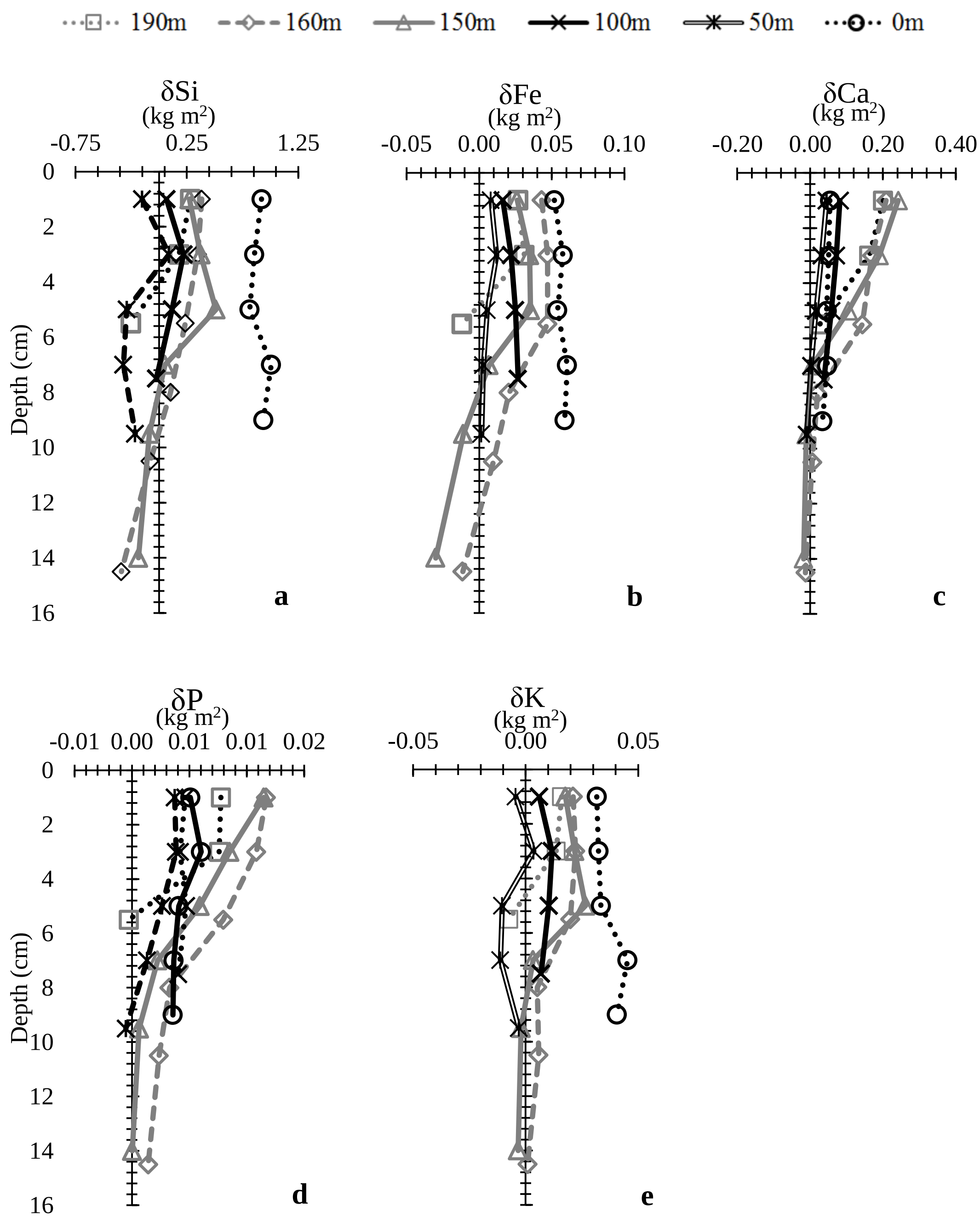

Figure 1.11. Soil A horizon depth profiles of absolute mass gains (positive values) and losses (negative values) of Si (a) Fe (b) Ca (c) P (d) and K (e) along the earthworm invasion chronosequence. The vertical line indicates no mass gains or losses.

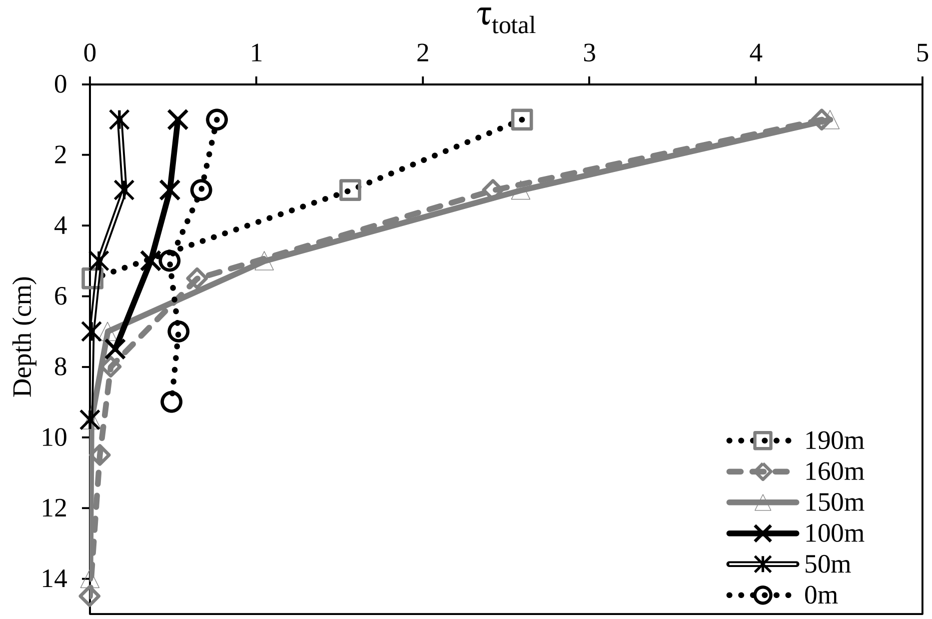

Figure 1.12. Depth profiles of total fractional mass losses along the earthworm invasion chronosequence.

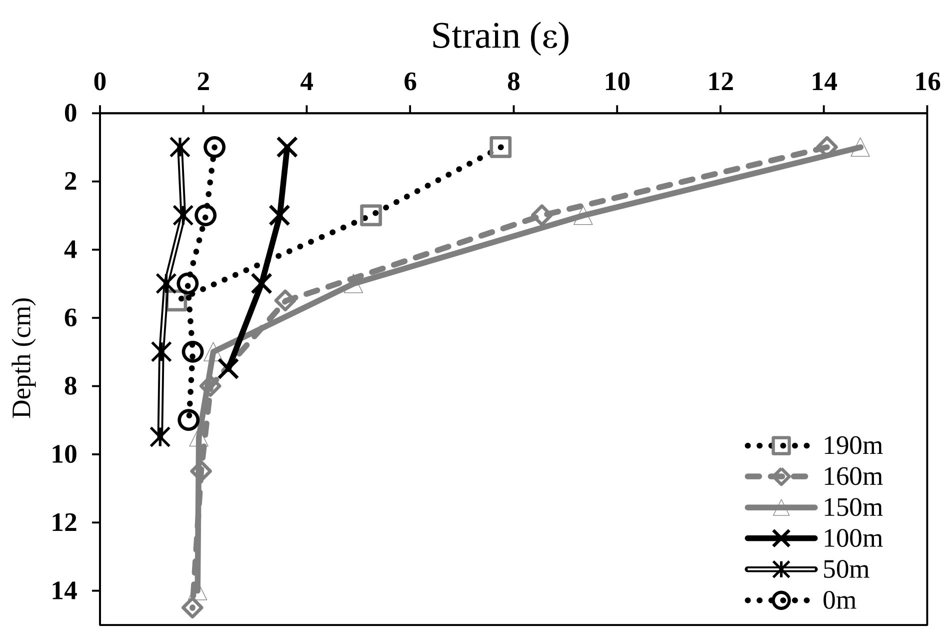

Figure 1.13: Depth profiles of volumetric strains along the earthworm invasion chronosequence. Positive values indicate volumetric dilation, while negative values indicate volumetric collapse.

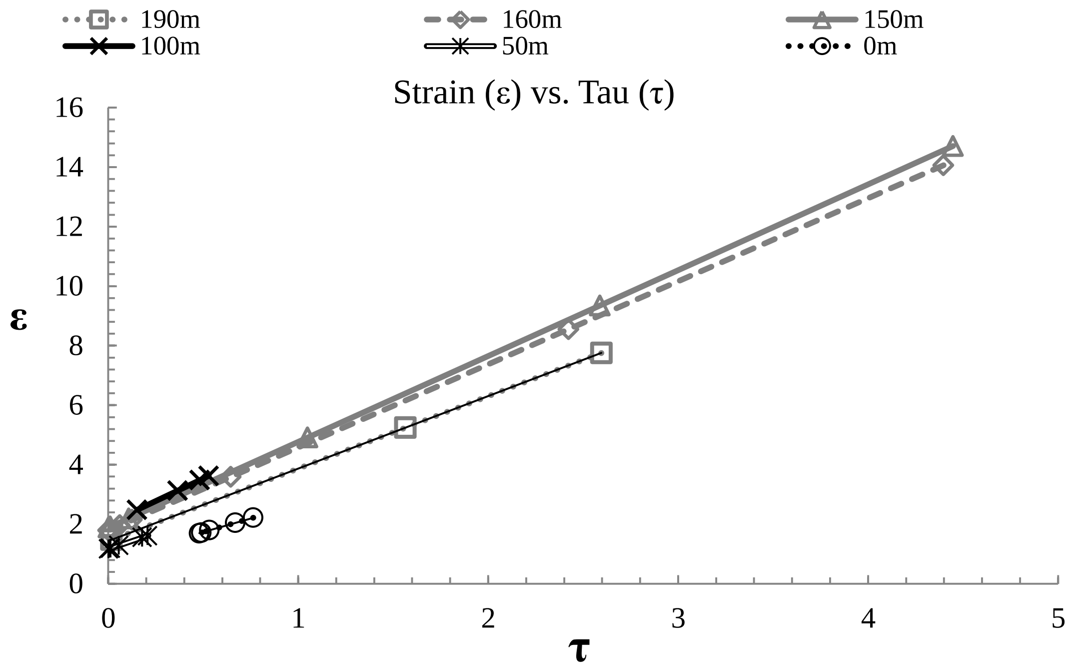

Figure 1.14. Soil epsilon (ε) versus tau (τ). Profiles in the frontal group are both enriched and dilated, but undergo a depletion (τ) and collapse in rear soil groups.

Equation 4 regression lines for distance 190m(a), 100m(b), and 0m(c)

a. $y = 2.43x + 1.43$

b. $y = 3.02x + 2.02$

c. $y= 1.83x + 0.83$

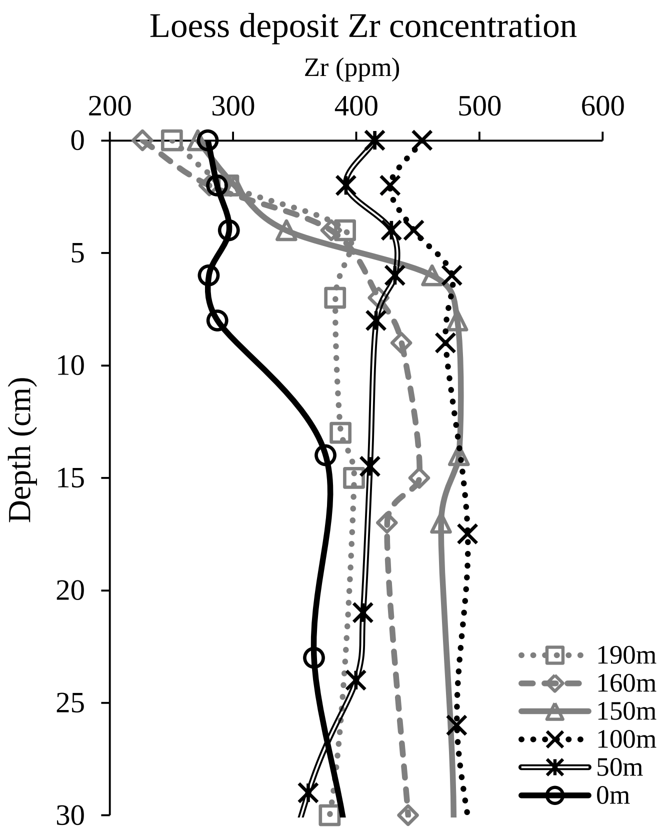

Figure 1.15. Zr concentration (ppm) throughout the loess deposit. Loess deposit concentrations of Zr for depths across the transect are narrowly constrained, and do not show an earthworm invasion trend.

Chapter 2

Elemental and mineralogical changes in soils due to bioturbation along an earthworm invasion chronosequence in northern Minnesota.

This chapter was published in *Applied Geochemistry* in 2011.
Full citation information is:
Resner,K., Yoo K, Hale CM, Aufdenkampe A, Sebestyen. 2011. Elemental and mineralogical changes in soils due to bioturbation along an earthworm invasion chronosequence in Northern Minnesota. Applied Geochemistry 26: S127-S131.

Chapter overview

Minnesota forested soils have evolved without the presence of earthworms since the last glacial retreat. When exotic earthworms arrive, enhanced soil bioturbation often results in dramatic morphological and chemical changes in soils with negative implications for the forests' sustainability. However, the impacts of earthworm invasion on geochemical processes in soils are not well understood. This study attempts to quantify the role of earthworm invasion in mineral chemical weathering and nutrient dynamics along an earthworm invasion chronosequence in a sugar maple forest in northern Minnesota. Depth and rates of soil mixing can be tracked with atmospherically derived short lived radioisotopes ^{210}Pb and ^{137}Cs. Their radioactivities increase in the lower A horizon at the expense of the peak activities near the soil surface, which indicate that soil mixing rate and its depth reach have been enhanced by earthworms. Enhanced soil mixing by earthworms is consistent with the ways that the vertical profiles of elemental and mineralogical compositions were affected by earthworm invasion. Biologically cycled Ca and P have peak concentrations near the soil surface prior to earthworm invasion. However, these peak abundances significantly declined in the earthworm invaded soils presumably due to enhanced soil mixing. It is clear that enhanced soil mixing due to earthworms also profoundly altered the vertical distribution of most mineral species within A horizons. Though the mechanisms are not clear yet, earthworm invasion appears to have contributed to net losses of clay mineral species and opal from the A horizons. As much as earthworms vertically relocated minerals and elements, they also intensify the contacts between organic matter and cations as shown in the increased amount of Ca and Fe in organically complexed and in exchangeable pools.

With future studies on soil mixing rates and elemental leaching, this study will quantitatively and mechanically address the role of earthworms in geochemical evolution of soils and forests' nutrient dynamics.

Introduction:

Since the last glacial retreat, the forests in Northern Minnesota have evolved without the presence of earthworms. Over the last century, however, earthworm invasion of the forests has been progressing due to the expansion of agriculture, use of earthworms for fishing bait, and logging activities. Earthworms have long been thought to be beneficial to agriculture, and thus most studies on the earthworms' impacts on soil processes have been conducted on agricultural soils, however, a number of studies show that earthworms' impacts on soils in previously earthworm free regions often negatively affect forest sustainability. Here, preliminary results are shown for elemental and mineralogical compositions in soils and extraction chemistry along a 200 meter long earthworm invasion chronosequence within a sugar maple forest located in Northern Minnesota. The most heavily invaded soils occur next to a road close to a popular fishing lake. All soil pits along the transect have an aeolian deposit over glacial till. Along the transect, the population dynamics of earthworm invasion had been documented in Hale (2004), and the population monitoring resumed in 2009. It has been shown that earthworm invasion occurs as different ecological groups of earthworms arrive at different stages of invasion. Each group exhibits a unique burrowing habit associated with different mixing depths. Anecic species, such as the night crawler, are deep burrowers, epi-anecic species are A horizon to deep burrowers, epi-endogeic are A horizon mixers, and endogeic species only dwell in the litter layer (Hale, 2007).

The least invaded soils on the transect contain a thick litter layer (6–9 cm) underlain by A, E, and Bt horizons. As the invasion intensity increases, the litter layer disappears because earthworms disperse the organic material into underlying mineral horizons. With increased earthworm activities, A horizons thicken, and an A /E horizon is formed. Prior to the earthworm invasion, the A horizons were made of structureless single grains to weak small granules. However, with the earthworm ingestion of soil materials and deposition of their castings, the materials become strongly aggregated. The ultimate goal is to quantify how physical (e.g., soil mixing) and chemical (e.g., oxidation change) activities of the invading earthworms affect the rates of chemical weathering and nutrient dynamics in soils. Toward this goal, this abstract focuses on presenting basic geochemistry data on the vertical distributions of elemental and extraction chemistry and mineralogical compositions along the invasion gradient. The findings presented here will guide the ongoing research activities that focus on physical movement of minerals (^{210}Pb and optically stimulated luminescence) and the leaching rates of cations and anions (chemical composition of soil water collected from lysimeters).

2. Results

2.1. Short lived isotopes

Atmospherically derived ^{137}Cs and ^{210}Pb were used to determine the depth reach and intensity of earthworm-driven soil mixing. Because the short lived isotopes strongly bind to organic matter and clays, their activities are expected to be highest in the upper centimeters of the soil, which was confirmed at a least invaded soil pit. An earthworm invaded soil, however, shows significant vertical intrusion of the radioisotopes (Fig. 1), suggesting that organic matter and clays have been incorporated to deeper depths via mixing.

2.1.1. Elemental compositions

Depending on the initial depth profiles of the elemental concentrations, vertical homogenization by earthworm-driven soil mixing produced different effects. Biologically cycled Ca and P, which abruptly decrease in their concentrations with increasing soil depth in the pre-invaded soil, experienced the reduction in their concentrations near the soil surface due to earthworm-driven soil mixing. In contrast, shallow A horizons showed significant gains in the concentrations of other cations such as K, Na, Al and Fe (Fig. 2). The abundances of these elements had depth profiles that were the reverse of Ca and P (Fig. 3).

2.2. X-ray diffraction

In agreement with visual observation, XRD reveals the presence of calcite and dolomite in the C horizon made of glacial till (Fig. 4). Overlying the glacial till, the Bt and E horizons, despite their dramatically different morphology, share similar mineralogy. Up to 95% of the soil materials were explained by quartz, feldspars and plagioclase. There are subtle differences in mineralogy that suggest the significant role of earthworm activities in modulating mineral weathering. Significant presence of the mineral opal was found only in the pre-invaded soil (Fig. 6). It also appears that the abundances of phyllosilicate clay minerals such as kaolinite and illite/smectite declined with the presence of earthworms (Fig. 7).

2.3. Extraction chemistry (Fe)

Dithionite and pyrophosphate extracts from 8 of 9 soil pits along the chronosequence were analyzed for Fe. Both the pedogenic crystalline form of Fe (dithionite extracts) and organically bound Fe (pyrophosphate) were greater in the earthworm invaded soil (Figs. 8 and 9).

2.4. Cation Exchange Capacity

Cation exchange capacity (CEC) is initially higher at the subsurface for the least invaded soils than in the invaded soils. With the earthworm invasion, CEC increases with depth compared to the least invaded. This trend is also seen in the exchangeable Ca data (Fig 5).

3. Discussion

Overall, mineralogical and elemental compositions of the soils are remarkably consistent along the earthworm invasion chronosequence. This supports the basic assumption that the soils along the transect share virtually identical parent materials and soil minerals, and the only variable is the degree of earthworm invasion. Likewise, there is a strong vertical consistency in mineral compositions within the soils. This is particularly surprising because the silty homogeneous E horizon materials look very different from the underlying clay rich Bt horizon with strong pedogenic structure. This result suggests that the E horizons were derived from an aeolian deposit.

During study site visits there was concern about the fact that the depth to carbonate varies significantly from 80 cm to over 150 cm along the transect. This concern was due to the possibility that deep burrowing anecic species may reach the deep soil zone and cause an added complexity due to the variation of the carbonate depths. However, XRD analysis, which is highly sensitive to calcite and dolomite, did not detect the carbonate minerals above the C horizons. This indicates that incorporation of C horizon materials into soils via deep burrowers does not occur along the transect. The elemental chemistry data suggests that biological retention of Ca and P in the soil surface proceeds at rates significantly slower than soil mixing by earthworms, which exemplifies the capacity of earthworms to disrupt nutrient cycles in the forest. However, probably reflecting the intense contacts between Ca ions and organic matter within earthworms' intestines, the sizes of exchangeable and organically complexed Ca pools were greater in the earthworm invaded soils. An increase in the organically bound Ca and Fe pools may contribute to C stability. From a pedogenic perspective, secondary Fe oxides may inhibit mineral dissolution by coating the reactive surface, therefore, interfering with weathering processes. It also appears that the combination of sugar maple and earthworm invasion may have significant impacts on the forest's silicon cycle. It is likely that the opal in the soil is from phytoliths of sugar maples which are dominant tree species at the site. Phytoliths are plant bodies, most commonly siliceous, and are found in the leaves of sugar maples. In the invaded soil, the opal contents were significantly lower, despite the likely presence of excess phytoliths as the litter layers were introduced into the A horizons. Whether the earthworm activities contributed to the dissolution of opal remains to be tested with detailed soil water chemistry data.

4. Conclusions and future work

This study confirms the major assumptions in the chronosequence approach. Because the solid state chemistry reveals the cumulative effects of earthworm invasion on soil geochemistry over the last several years to decades, they are highly informative in setting priorities in the next efforts. The data suggests that earthworm activities can affect mineral weathering through two major pathways. First, their burrowing activities physically relocated minerals and elements, thus exposing them to altered geochemical environments. Such physical relocation of elements and minerals are clear throughout the data. Second, more intimate contacts between cations, minerals, and organic matter, which occur within earthworms' intestines, appear to affect the exchangeable and organically bound pools of cations. To constrain the physical relocation of minerals and elements, detailed measurements of ^{210}Pb activities will be conducted. In addition, major cations and anions will be determined in soil water collected from the already installed lysimeters along the transect. This will allow connecting the soil mixing with mineral dissolution and leaching. In parallel, organic C analysis will be made in conjunction with cations and minerals that are associated with them. Such integration will allow prediction of the impacts of exotic earthworms on the biogeochemistry of hardwood ecosystems in Northern Minnesota.

References

Hale, C.M. (2007), Earthworms of the Great Lakes, Kollath and Sensaas Publishing, Duluth.

Hale, C.M. (2004), Ecological Consequences of Exotic Invaders: Interactions Involving European, Earthworms and Native Plant Communities in Hardwood Forests, PhD diss. Univ. Minnesota, Dept of Forest Resources, St. Paul, MN.

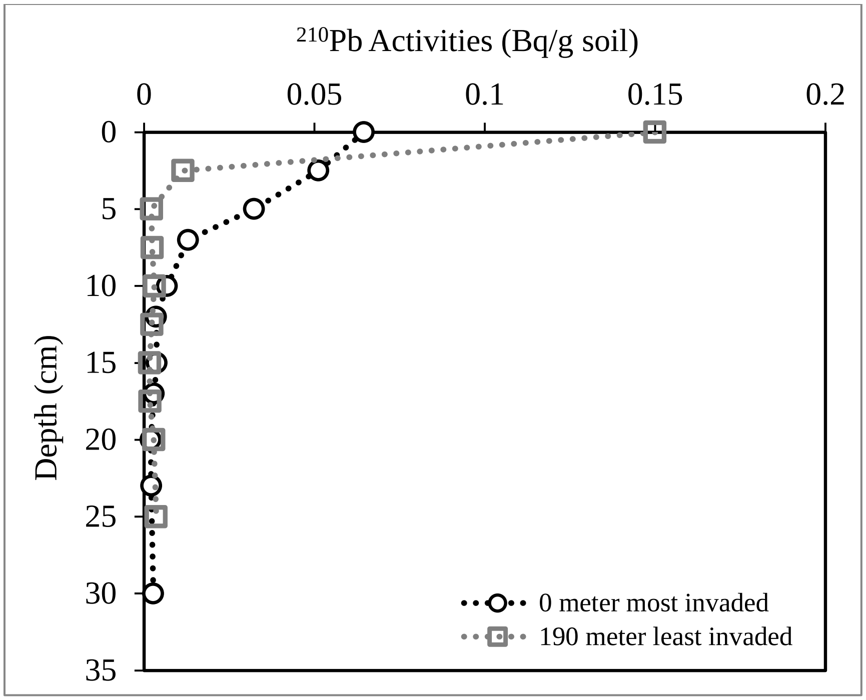

Figure 2.1. ^{210}Pb activities in the soils prior to and post earthworm invasion. Note the vertical intrusion of ^{210}Pb in the earthworm invaded soil.

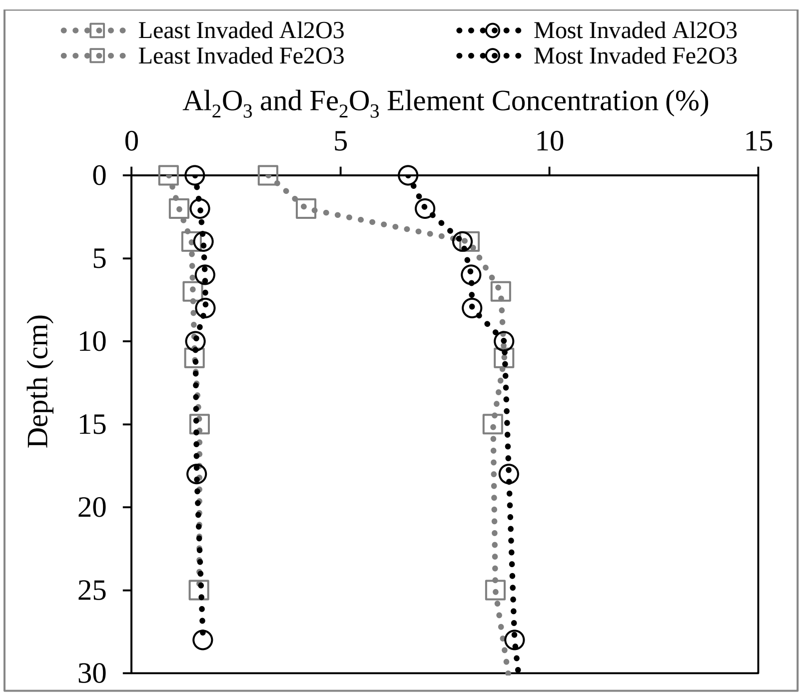

Figure 2.2. Depth profiles of Al_2O_3 and Fe_2O_3 in soils prior to and post earthworm invasion

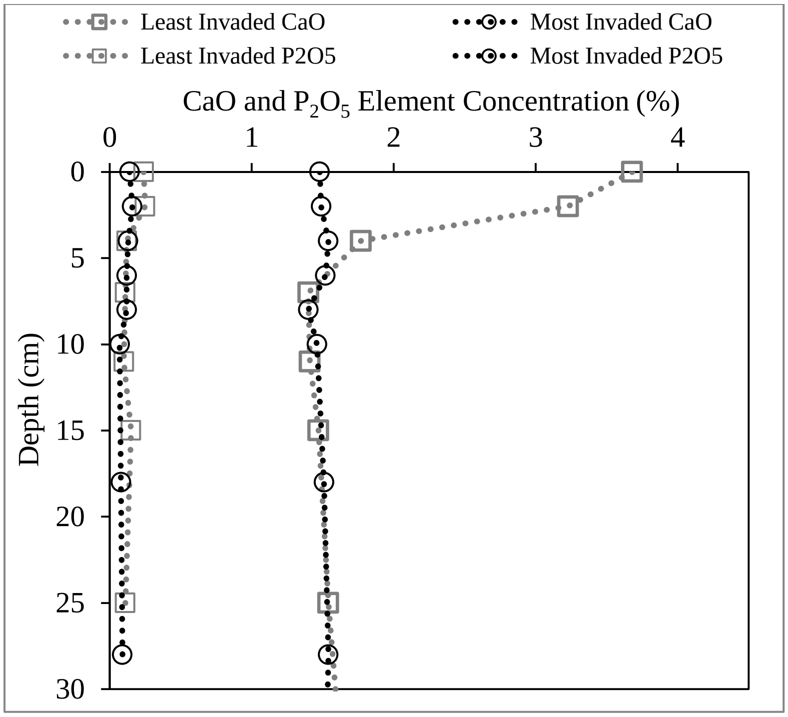

Figure 2.3. Depth profiles of CaO and P_2O_5 in soils prior to and post earthworm invasion

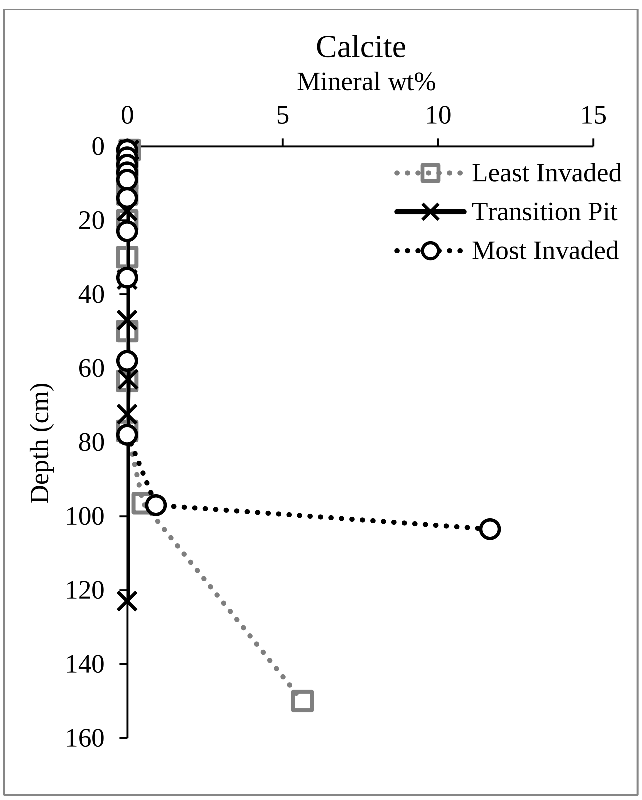

Figure 2.4. Calcite depth profiles. No measureable amounts of calcite were found above the C horizon.

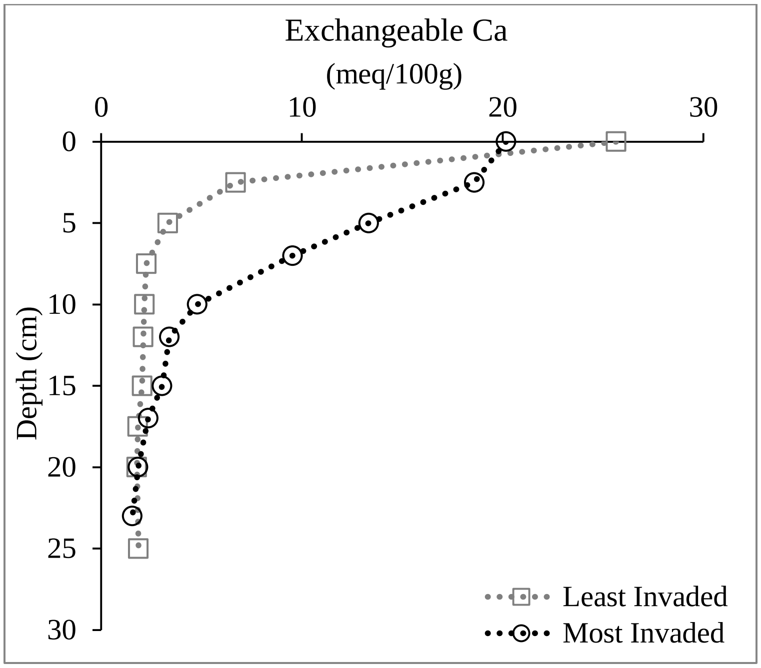

Figure 2.5. Depth profiles of exchangeable Ca (meq/100g).

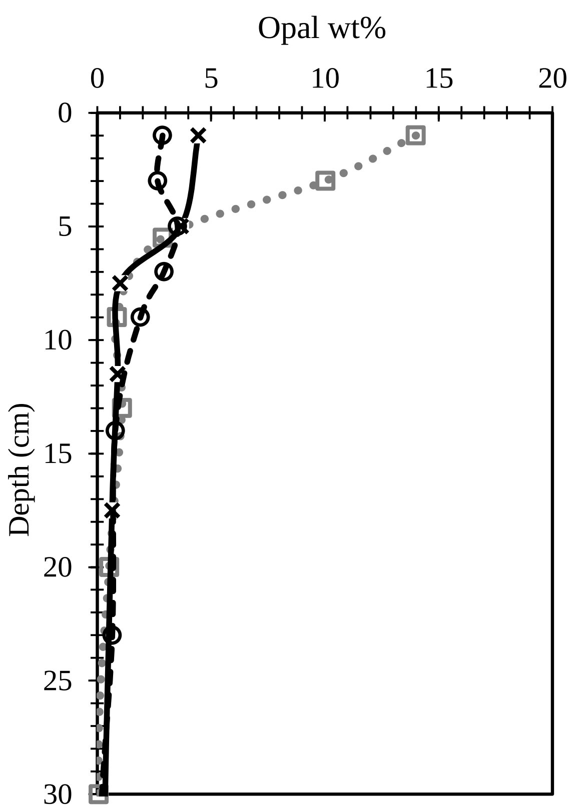

Figure 2.6. Depth profiles of opal (wt%) that is considered to have originated from phytoliths of sugar maple trees at our site

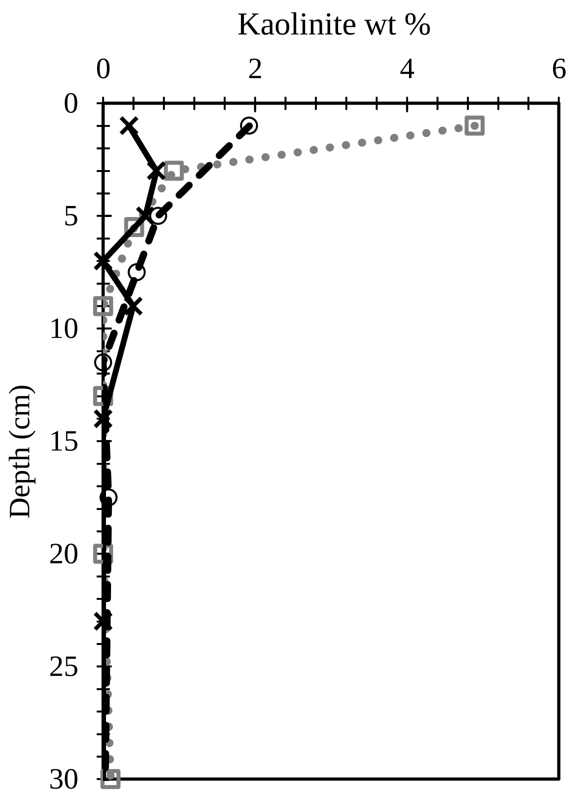

Figure 2.7. Depth profiles of kaolinite concentrations (wt%)

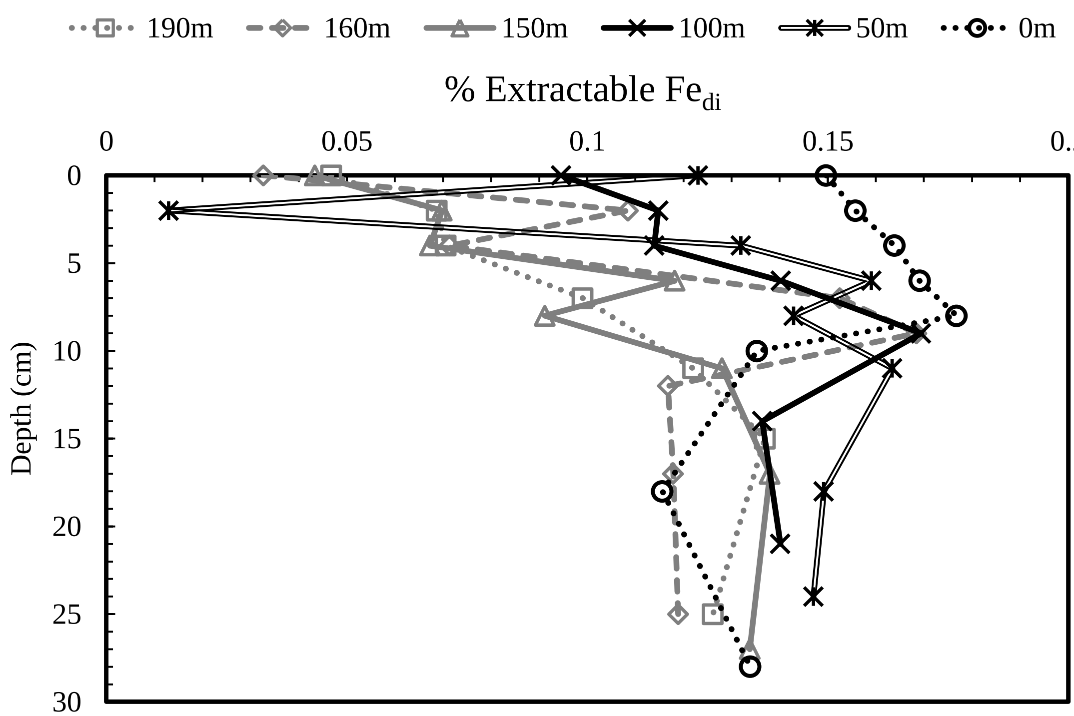

Figure 2.8. Depth profiles of pedogenic crystalline iron oxides (%)

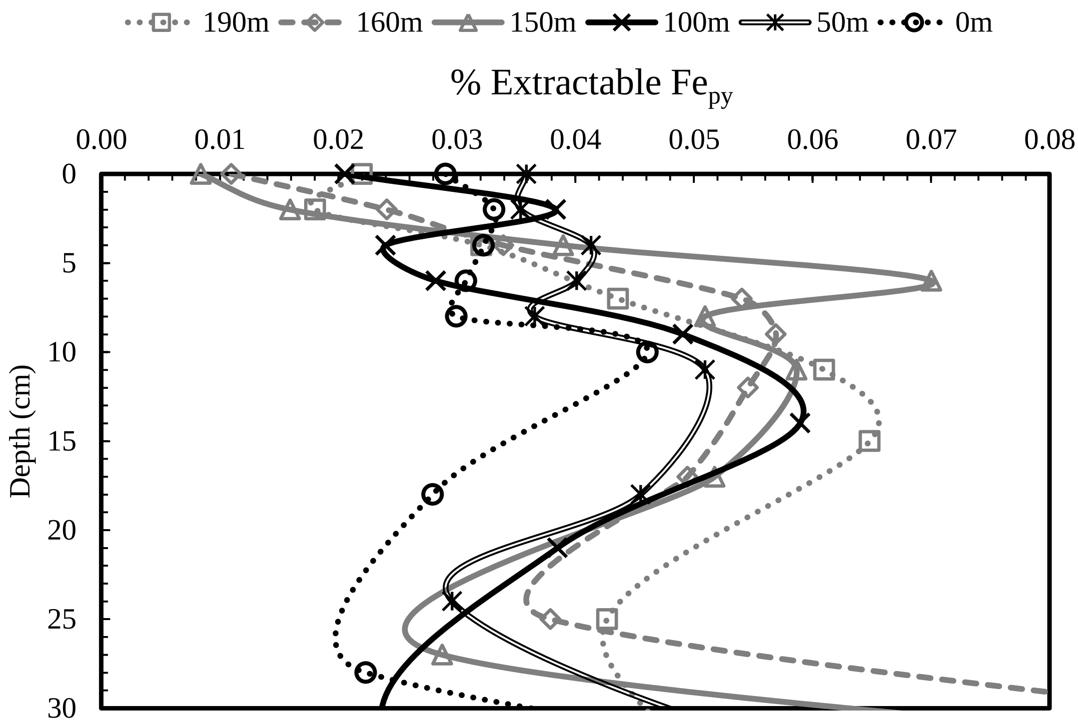

Figure 2.9. Depth profiles of organically complexed iron oxides (%)

Bibliography

Alban, D.H. and Berry, E.C. (1994), Effects of earthworm invasion on morphology, carbon and nitrogen of a forest soil, Appl. Soil Ecol.1, 243–49, doi, 10.1016/0929-1393(94)90015-9

April, R., Newton, R., and Coles, L.T. (1986), Chemical weathering in two Adirondack watersheds: Past and present-day rates, Geol. Soc. Am. Bull., 97, 1232– 1238, doi: 10.1130/0016-7606(1986)97<1232:CWITAW>2.0.CO;2

Bailey, S.W., S.B. Horsley, and R.P. Long. (2005), Thirty years of change in forest soils of the Allegheny Plateau, Pennsylvania, Soil Sci. Soc. Am. J, 69, 681–690, doi:10.2136/sssaj2004.0057

Baldock, J.A., and Skjemstad, J.O. (2000), Role of the soil matrix and minerals in protecting natural organic materials against biological attack, Organic Geochemistry, 31(7), 697-710, doi: 10.1016/S0146-6380(00)00049-8

Bailey, S.W., Horsley, S.B., Long, R.P., and Hallett, R.A. (2004), Influence of edaphic factors on sugar maple nutrition and health on the Allegheny Plateau, Soil Science Society of America Journal, 68, 243-252, doi: 10.2136/sssaj2004.2430

Belote, R. T., and Jones, R. H. (2008), Tree leaf litter composition and nonnative earthworms influence plant invasion in experimental forest floor mesocosms, Biological Invasions, 11(4), 1045-1052, doi: 10.1007/s10530-008-9315-1.

Berner, R. A. (1992), Weathering, plants, and the long-term carbon cycle, Geochim. Cosmochim Acta, 56(8), 3225-3231, doi: 10.1016/0016-7037(92)90300-8

Borggaard, O.K. (1982), The influence of iron oxides on the surface area of soil, Journal of Soil Science, 33, 443-449. doi: 10.1111/j.1365-2389.1982.tb01779.x

Bohlen, P.J., Groffman, P.M., Fahey, T.J., Fisk, M.C., Suarez, E., Pelletier, D.M., and Fahey, R.T. (2004a), Ecosystem consequences of exotic earthworm invasion of north temperate forests, Ecosystems, 7, 1–12, doi: 10.1007/s10021-003-0126-z

Bohlen, P.J., Scheu, S., Hale, C.M., McLean, M.A., Migge, S., Groffman, P.M., and Parkinson, D. (2004b), Non-native invasive earthworms as agents of change in northern temperate forests, Front Ecol Environ, 2, 427–435, doi: 10.1890/1540-9295(2004)002[0427:NIEAAO]2.0.CO;2

Brimhall, G.H., and Dietrich, W.E. (1987), Constitutive mass balance relations between chemical composition, volume, density, porosity, and strain in metasomatic hydrochemical systems: Results on weathering and pedogenesis, Geochimica et Cosmochimica Acta, 51, 567-587, doi: 10.1016/0016-7037(87)90070-6.

Brundrett, M. C., and Kendrick, B. (1988), The mycorrhizal status, root anatomy and phenology of plants in a sugar maple forest, Canadian Journal of Botany, 66, 1153-1173.

Brunstad, Z., Keller, C. K., Bormann, B. T., O'Brien, R., Wang, D., and Hawley, G. (2008), Chemical weathering and chemical denudation dynamics through ecosystem development and disturbance, Global Biogeochem. Cycles, 22, GB1007, doi: 10.1029/2007GB002957.

Burtelow, A. E., Bohlen, P.J., and Groffman, P.M. (1998), Influence of exotic earthworm invasion on soil organic matter, microbial biomass and denitrification potential in forest soils of the northeastern United States, Appl Soil Ecol, 9, 197-202, doi: 10.1016/S0929-1393(98)00075-4,

Canti, M. G., and Piearce T.G. (2003), Morphology and dynamics of calcium carbonate granules produced by different earthworm species, Pedobiologia, 47, 511–521, doi: 10.1078/0031-4056-00221

Chadwick, O.A., Brimhall, G.H., and Hendricks, D.M. (1990), From a black to a gray box- a mass balance interpretation of pedogenesis, Geomorphology, 3, 369-390, doi: 10.1016/0169-555X(90)90012-F.

Chenu, S., and Stotzky, G. (2002), Interactions between microorganisms and soil particles, an overview, Editors: Huang, P.M., Bollag, J.M., Senesi, N., Weinheim Wiley-VCH-Verlag.

Cornell, R.M., and Schwertmann, U. (2003), The iron oxides: structure, properties, reactions, occurrences and uses, Weinheim (DE): Wiley-VCH.

Crang, M. G., Holsen, R.C, and Hitt, J. B. (1968), Calcite production in mitochondria of earthworm calciferous glands, BioScience, 18,299, doi:10.2307/1294220

Darwin, C. (1892), The formation of vegetable mould, through the action of worms, with observations on their habits, Murray, London, UK.

De Vleeschauwer, D., and Lal, R. (1981), Properties of worm casts under secondary tropical forest regrowth, Soil Science, 132, 175-181.

Drake, H. L., and Horn, M.A. (2007), As the worm turns: the earthworm gut as a transient habitat for soil microbial biomes, Annual review of microbiology, 61, 169-89, doi:10.1146/annurev.micro.61.080706.093139

Eisenhauer, N., Partsch, S., Parkinson, D., and Scheu, S. (2007), Invasion of a deciduous forest by earthworms: Changes in soil chemistry, microflora, microarthropods and vegetation, Soil Biology and Biochemistry, 39(5), 1099-1110, doi:10.1016/j.soilbio.2006.12.019

Eisenhauer, N., Milcu, A., Sabais, A. C. W., and Scheu, S. (2008), Animal ecosystem engineers modulate the diversity-invasibility relationship, PloS one, 3(10), e3489, doi:10.1371/journal.pone.0003489

Ellsworth, D.S., Liu, X. (1994), Photosynthesis and canopy nutrition of four sugar maple forests on acid soils in northern Vermont, Canadian Journal of Forest Research, 24, 2118-2127, doi: 10.1139/x94-272

Eusterhues, K., Rumpel, C., and Kögel-Knabner, I. (2005), Organo-mineral associations in sandy acid forest soils: importance of specific surface area, iron oxides and micropores, European Journal of Soil Science, 56,753-763., doi: 10.1111/j.1365-2389.2005.00710.x

Essington, M.E. (2004), Soil and water chemistry: an integrative approach, Boca Raton (FL): CRC Press LLC.

Finzi, A.C., Canham, C.D., and Van Breemen, N. (1998), Canopy tree-soil interactions within temperate forests: species effects on pH and cations, Ecological Applications, 8(2), 447-454, doi: 10.1890/1051-0761(1998)008[0447:CTSIWT]2.0.CO;2

Fisk, M.C, Fahey, T.J., Groffman, P.M., and Bohlen, P.J. (2004), Earthworm invasion, fine root distribution and soil respiration in hardwood forests, Ecosystems, 7, 55-62. doi: 10.1007/s10021-003-0130-3

Frelich, L. E., Hale, C. M., Scheu, S., Holdsworth, A. R., Heneghan, L., Bohlen, P. J., and Reich, P. B. (2006), Earthworm invasion into previously earthworm-free temperate and boreal forests, Biological Invasions, 8(6), 1235-1245, doi:10.1007/s10530-006-9019-3

Frelich, L.E., and Reich, P.B. (2009), Will environmental changes reinforce the impact of global warming on the prairie-forest border of central North America?, Front Ecol Environ, 8, 371-378, doi: 10.1890/080191

Gabet, E. J., Reichman, O. J., and Seabloom, E. W. (2003), The effects of bioturbation on soil processes and sediment transport, Annual Review of Earth and Planetary Sciences, 31(1), 249-273, doi: 10.1146/annurev.earth.31.100901.141314

Gates, G. E. (1982), Farewell to North American megadriles, Megadrilogica, 4:77.

Gu, B., Schmitt, J., Chen, Z., Llang, L., McCarthy, J.F. (1994), Adsorption and desporption of natural organic matter on iron oxide: mechanisms and models, Environ.Sci.Technol., 28, 38-46, doi: 10.1021/es00050a007

Hale, C.M. (2004), Ecological consequences of exotic invaders: interactions involving European earthworms and native plant communities in hardwood forests, PhD thesis, Department of Forest Resources, University of Minnesota, St. Paul, Minnesota, United States.

Hale, C.M., Frelich, L.E., and Reich, P.B. (2005), Exotic European earthworm invasion dynamics in northern hardwood forests of Minnesota, U.S.A., Ecol Appl., 15, 848–860, doi: 10.1890/03-5345

Hale, C.M., Frelich L.E., and Reich P.B. (2005), Effects of European earthworm invasion on soil characteristics in northern hardwood forests of Minnesota, Ecosystems, 8, 911–927, doi: 10.1007/s10021-005-0066-x

Hale, C.M., Frelich, L.E., and Reich, P.B. (2006), Changes in hardwood forest understory plant communities in response to European earthworm invasions, Ecology, 87(7), 1637-1649, doi: 10.1890/0012-9658(2006)87[1637:CIHFUP]2.0.CO;2

Hale, C.M. (2007), Earthworms of the Great Lakes Region. Kollath & Stensaas Publishing. 36 pages.

Hale, C.M. (2008), Evidence for Human-Mediated Dispersal of Exotic Earthworms: support for exploring strategies to limit further spread, Molecular Ecology Perspectives 17(5), 1165-1169, doi: 10.1111/j.1365-294X.2007.03678.x

Hale, C. M.E., Reich, P. B., and Pastor, J. (2008), Exotic earthworm effects on hardwood forest floor, nutrient availability and native plants: a mesocosm study. Oecologia, 155(3), 509-18, doi:10.1007/s00442-007-0925-6

Hendrix P.F., and Bohlen P.J. (2002), Exotic earthworm invasions in North American: ecological and policy implications, BioScience, 52(9), 801-811, doi: 10.1641/0006-3568(2002)052[0801:EEIINA]2.0.CO;2

Hendrix, P.F., Callaham, M.A., Drake, J.M., Huang, C., James, S.W., Snyder, B.A., and Zhang, W. (2008), Pandora's box contained bait: the global problem of introduced earthworms, The Annual Review of Ecology, Evolution, and Systematics, 39, 593–613, doi: 10.1146/annurev.ecolsys.39.110707.173426

Hobbie, S.E., Reich, P.B., Oleksyn, J., Ogdahl, M., Zytkowiak, R., Hale, C., and Karolewski, P. (2007), Tree species effects on decomposition and forest floor dynamics in a common garden, 87, 2288-2297, doi: 10.1890/0012-9658(2006)87[2288:TSEODA]2.0.CO;2

Hobbie, S.E., Ogdahl, M., Chorover, J., Chadwick, O.A. Oleksyn, J., Zytkowiak, R., and Reich, P.B. (2007), Tree species effects on soil organic matter dynamics: the role of soil cation composition, Ecosystems, 10, 999-1018, doi: 10.1007/s 10021-007-9073-4

Hole, F.D. (1981), Effects of animals on soil, Geoderma, 25, 75-112.

Holdsworth, A. R., Frelich, L. E., and Reich, P. B. (2008), Litter decomposition in earthworm-invaded northern hardwood forests: Role of invasion degree and litter chemistry, Ecoscience, 15(4), 536-544, doi: 10.2980/15-4-3151

Iverson, L.R., Prasad, A.M., Matthews, S.N., and Peters, M. (2008), Estimating potential habitat for 134 eastern US tree species under six climate scenarios, Forest Ecology and Management, 254, 390-406, doi: 10.1016/j.foreco.2007.07.023

Johnson, D. L. (1990), Biomantle evolution and the redistribution of earth materials and artifacts, Soil Science, 149(2), 84-102.

Kaiser, K., and Guggenberger, G. (2003), Mineral surfaces and soil organic matter, European Journal of Soil Science, 54,219-236, doi: 10.1046/j.1365-2389.2003.00544.x.

Kang, B. T., Akinnifesi, F.K., and Pleysier, J.L. (1994), Effect of agroforestry woody species on earthworm activity and physiochemical properties of worm casts, Soil and Fertility of Soils, 18, 193-199, doi: 10.1007/BF00647666

Kelly, E. F., O. A. Chadwick, and Hilinski, T. E. (1998), The effect of plants on mineral weathering, Biogeochem., 42, 21–53, doi: 10.1023/A:1005919306687

Kobe, R.K., Likens, G.E., and Eagar, C. (2002), Tree seedling growth and mortality responses to manipulations of calcium and aluminum in a northern hardwood forest, Canadian Journal of Forest Research, 32, 954-966, doi: 10.1139/X02-018

Kolka, R. K., Grigal, D.F., and Nater, E.A. (1996), Forest soil mineral weathering rates: Use of multiple approaches, Geoderma, 73, 1 –21, doi: 10.1016/0016-7061(96)00037-7

Kurtz, A. C., Derry, L. A., Chadwick, O. A., and Alfano, M. J. (2000), Refractory element mobility in volcanic soils, Geology, 28, 683-686, doi:10.1130/0091-7613(2000)28<683

Land, M., Ingri, J., and O¨ hlander, B. (1999), Past and present weathering rates in northern Sweden, Appl. Geochem., 14, 761– 774, doi: 10.1016/S0883-2927(98)00098-5

Lawrence, B., Fisk, M.C., Fahey, T.J., and Suarez, E.R. (2003), Influence of nonnative earthworms on mycorrhizal colonization of sugar maple, New Phytologist, 157, 145-153, doi: 10.1046/j.1469-8137.2003.00649.x

Larson, E.R., Kipfmueller, K.F., Hale, C.M., Frelich, L.E. and Reich, P.B. (2009), Tree rings detect earthworm invasions and their effects in northern Hardwood forests, Biological Invasions, 12, 1053-1066, doi: 10.1007/s10530-009-9523-3

Le Bayon, R., and Milleret, R. (2009), Effect of earthworms on phosphorus dynamics-a review, Dynamic Soil, Dynamic Plant, 3 (Special Issue 2), 21-27.

Lee, K.E. (1985), Earthworms – Their ecology and relationships with soils and land use. Academic Press, Sydney, Australia.

Li, J., and Richter, D.D. (2012), Effects of two-century land use changes on soil iron crystallinity and accumulation in Southeastern Piedmont region, USA, Geoderma, 173, 184-191, doi: 10.1016/j.geoderma.2011.12.021

Likens, G.E., Bormann, F.H., Johnson, N.M., Fisher, D.W., and Pierce, R.S. (1970), Effects of forest cutting and herbicide treatment on nutrient budgets in the Hubbard Brook watershed-ecosystem, Ecol. Monogr.,40, 23, doi: 10.2307/1942440

Likens, G.E., Driscoll, C.T., Buso, D.C., Siccama, T.G., Johnson, C.E., Lovett, G.M., Fahey, T.J., Reiners, W.A., Ryan, D.F., Martin, C.W., and Bailey, S.W. (1998), The biogeochemistry of calcium at Hubbard Brook, Biogeochemistry, 41, 89-173, doi:10.1023/A:1005984620681

Long, R. P., Horsley, S. B., Hallett, R. A, and Bailey, S. W. (2009), Sugar maple growth in relation to nutrition and stress in the northeastern United States, Ecological Society of America, 19(6), 1454-66, doi: 10.1890/08-1535.1

Loss, S. R., and Blair, R.B. (2011), Reduced density and nest survival of ground-nesting songbirds relative to earthworm invasions in northern hardwood forests, Conservation Biology, 25(5), 983-992, doi: 10.1111/j.1523-1739.2011.01719.x

Lund, H.A., and Jacobson, H.G. (1944), The chemical composition of earthworm casts, Soil Science, 58, 367-375.

Lyttle, A., Yoo, K., Hale, C.M., Aufdenkampe, A., Sebestyen, S. (2011), Carbon-mineral interactions along an earthworm invasion gradient at a sugar maple forest in northern Minnesota, Applied Geochemistry, 26, S85-S88.

Lyttle, A.M. (2013), Carbon-mineral interactions and bioturbation: an earthworm invasion chronosequence in a sugar maple forest in Northern Minnesota, MS thesis, Department of Soil, Water, and Climate, University of Minnesota, St. Paul, Minnesota, United States, in press.

Maerz, J.C., Nuzzo, V.A., and Blossey, B. (2009), Declines in woodland salamander abundance associated with non-native earthworm and plant invasions, Conservation Biology, 23(4), 975-981. 10.1111/j.1523-1739.2009.01167.x

McKeague, J.A., Brydon, J.E., and Miles, N.M. (1971), Differentiation of forms of extractable iron and aluminum in soils, Soil Sci. Soc. Am. J., 35, 33-38, doi: 10.2136/sssaj1971.03615995003500010016x

McLaughlin, S.B. and Wimmer, R. (1999), Tansley Review No. 104: calcium physiology and terrestrial ecosystem processes, New Phytologist, 142, 373-417, doi: 10.1046/j.1469-8137.1999.00420.x

Merritts, D.J., Chadwick, O.A., Hendricks, D.M., Brimhall, G.H., and Lewis, C.J. (1992), The mass balance of soil evolution on late quaternary marine terraces, northern California, Geological Society of America Bulletin, 104, 1456-1470, doi: 10.1130/0016-7606(1992)104<1456:TMBOSE>2.3.CO;2

Needham, S. J., Worden, R. H., and Mcilroy, D. (2004), Animal-sediment interactions : the effect of ingestion and excretion by worms on mineralogy, Biogeosciences, 1, 113-121, doi: 10.5194/bg-1-113-2004

Neilson, G.E., and Hole, F.D. (1964), Earthworms and the development of coprogenous Al horizons in forest soils of Wisconsin, Soil Sci Soc Am Pro, 28, 426-30, doi: 10.2136/sssaj1964.03615995002800030037x

Nye, P.H. (1955), Some soil-forming processes in the humid tropics IV. The action of soil fauna, Journal of Soil Science, 6, 73-83, doi: 10.1111/j.1365-2389.1954.tb02171.x

Oh, N.H., and Richter, D.D. (2005), Elemental translocation and loss from three highly weathered soil-bedrock profiles in the southeastern United States, Geoderma, 126, 5-25, doi: 10.1016/j.geoderma.2004.11.005

Oyedele, D.J., Schjonning, P., and Amusan, A.A. (2006), Physicochemical properties of earthworm casts and uningested parent material from selected sites in southwestern Nigeria, Ecological Engineering, 28, 106-113, doi: 10.1016/j.ecoleng.2006.05.002

Pare, D., and Bernier, B. (1989), Origin of the phosphorus deficiency observed in declining sugar maple stands in the Quebec Appalachians, Canadian Journal of Forest Research, 19(1), 24-34, doi: 10.1139/x89-004.

Pelletier, D.M. 2001, The effect of earthworm invasion on nutrient cycling and hydrologic losses in two northern hardwood forests., MS thesis, Cornell University, USA.

Piperno, D. (2006), Phytoliths: a comprehensive guide for archaeologists and paleoecologists. New York, Toronto, Oxford: AltaMira Press , Rowman Altamira.

Pronk, G.J., Heister, K., Kögel-Knabner, I. (2011), Iron oxides as major available interface component in loamy arable topsoils, Soil Science Society of America Journal, 75,2158-2168, doi:10.2136/sssaj2010.0455

Raymo, M.E., and Ruddiman, W.F. (1992), Tectonic forcing of late Cenozoic climate, Nature, 359, 117-122, doi: 10.1038/359117a0

Reich, P.B., Oleksyn, J., Modrzynski, J., Mrozinski, P., Hobbie, S.E., Eissenstat, D.M., Chorover, J., Chadwick, O.A., Hale, C.M., and Tjoelker, M.G. (2005), Linking litter calcium, earthworms, and soil properties: a common garden test with 14 tree species, Ecology Letters, 8, 811-818, doi, 10.1111/j.1461-0248.2005.00779.x

Resner,K., Yoo, K., Hale, C.M., Aufdenkampe, A., Sebestyen, S. (2011), Elemental and mineralogical changes in soils due to bioturbation along an earthworm invasion chronosequence in northern Minnesota, Applied Geochemistry, 26, S127-S131.

Riebe, C., Kirchener, J.W., and Finkel, R.C. (2003), Long-term rates of chemical weathering and physical erosion from cosmogenic nuclides and geochemical mass balance, Geochimica et Cosmochimica Acta, 67, 4411-4427, doi: 10.1016/S0016-7037(03)00382-X

Robertson, J. D. (1936), The function of calciferous glands of earthworms, Journal of Experimental Biology, 13:279–297.

Schaberg, P. G., Tilley, J. W., Hawley, G. J., DeHayes, D. H., and Bailey, S. W. (2006), Associations of calcium and aluminum with the growth and health of sugar maple trees in Vermont, Forest Ecology and Management, 223(1-3), 159-169, doi:10.1016/j.foreco.2005.10.067

Schaetzl, R., and Anderson, S. (2005), Soils: Genesis and Geomorphology, New York: Cambridge University Press.

Schaetzl, R.J., Johnson, D.L., Burns, S.F., and Small, T.W. (1989), Tree uprooting: review of terminology, process, and environmental implications. Can. J. For. Res, 19, 1-11.

Scheu, S. (2003), Effects of earthworms on plant growth: patterns and perspectives: The 7th international symposium on earthworm ecology· Cardiff· Wales· 2002, Pedobiologia, 47, 846–856, doi: 10.1078/0031-4056-00270

Six, J., Bossuyt, H., Degryze, S., Denef, K., (2004), A history on the link between (micro)aggregates, soil biota, and soil organic matter dynamics, Soil Tillage Research, 79, 7-31, doi: 10.1016/j.still.2004.03.008

Soil Survey Staff, Soil Taxonomy (Agriculture Handbook No. 436, Government Printing Office, Washington, D.C., 1975).

St. Clair, S.B., (2004), Factors and mechanisms underlying sugar maple sensitivity to edaphic stresses on Pennsylvania's Allegheny Plateau, PhD thesis, Department of Integrative Biosciences, Pennsylvania State University, University Park, Pennsylvania, United States.

Suarez, E. R., Pelletier, D.M., Fahey, T.J., Groffman, P.M., Bohlen, P.J., and Fisk, M.C. (2003), Effects of exotic earthworms on soil phosphorus cycling in two broadleaf temperature forest, Ecosystems, 7, 28-44, doi:10.1007/s10021-003-0128-x

Suzuki, Y., Matsubara, T., and Hoshino, M. (2003), Breakdown of mineral grains by earthworms and beetle larvae, Geoderma, 112(1-2), 131-142, doi:10.1016/S0016-7061(02)00300-230.

Thomas, G.W. (1982), Exhangeable cations, in Methods of soil Analysis, Part 2: Chemical and Microbiological Properties, 2nd edition, ASA, SSA, edited by Page, A. L. pp. 159-165, Madison, WI.

Watmough, S. A., and Dillon P, J. (2003), Base cation and nitrogen budget for seven forested catchments in central Ontario, 1983– 1999, For. Ecol. Manage., 177, 155– 177, doi: 10.1007/s10021-002-0164-y

Wilding, L.P., and Drees, L.R. (1971), Biogenic opal in ohio soils, Soil Society of America Journal, 35(6), 1004-1010.

Winsome, T, and McColl, J.R. (1998), Changes in chemistry and aggregation of a California forest soil worked by the earthworm Agrilophilus papillifer eisen (megascolecidae), Soil Biology & Biochemistry, 30 (13), 1677-1687, doi: 10.1016/S0038-0717(97)00262-9

Wood, T., Bormann, F.H., and Voigt, G.K. (1984), Phosphorus cycling in a northern hardwood forest, biological and chemical control, Science, 223(4634), 391-393, doi: 10.1126/science.223.4634.391

Vitousek, P. M., and Reiners, W.A. (1975), Ecosystem succession and nutrient retention: A hypothesis, Bioscience, 25, 376– 381.

von Lutzow, M., Kögel-Knabner, I., Ekschmitt, K., Matzner, E., Guggenberger, G., Marschner, B., and Flessa, H. (2006), Stabilization of organic matter in temperate soils: mechanisms and their relevance under different soil conditions – a review, European Journal of Soil Science, 57:426-445, doi: 10.1111/j.1365-2389.2006.00809.x

Table 1-A. Textural properties of fine fraction (<2mm) soils collected from the excavated soil pit at the distance of 190 m in 2009.

distance (m)	depth (cm)	horizon	soil texture
190	0-2	1A1	NSS
190	2-4	1A1	NSS
190	4-7	1A2	loam
190	7-11	loess	silt loam
190	11-15	loess	silt loam
190	15-25	loess	silt loam
190	25-35	loess	silt loam
190	35-45	loess	silt loam
190	45-55	loess	silt loam
190	56-71	1Bw	silt loam
190	71-83	2Bw	sandy clay
190	83-110	2C1	sandy clay/sandy clay loam
190	105-130	2C2	coarse sandy loam

Table 1-B. Textural properties of fine fraction (<2mm) soils collected from the excavated soil pit at the distance of 150 m in 2009.

distance (m)	depth (cm)	horizon	soil texture
150	0-2	1A1	loam
150	2-4	1A1	loam
150	4-6	1A1	sandy loam
150	6-8	1A2	silt loam
150	8-11	1A2	silt loam
150	11-17	A-loess	silt loam
150	17-27	loess	silt loam
150	27-37	loess	silt loam
150	37-44	1Bw1	silty clay loam
150	44-54	1Bw2	silt loam
150	54-64	1Bw2	silty clay loam
150	64-74	1Bw2	silty clay loam
150	74-90	1Bw3	sandy clay loam
150	90-100	2Bw3	sandy clay loam
150	100-113	2Bw3	sandy clay loam
150	113-130	2C1	sandy clay loam
150	130-160	2C2	loamy sand

Table 1-C. Textural properties of fine fraction (<2mm) soils collected from the excavated soil pit at the distance of 100 m in 2009.

distance (m)	depth (cm)	horizon	soil texture
100	0-2	1A	loam
100	2-4	1A	sandy loam
100	4-6	1A	sandy loam
100	6-9	1A	sandy loam
100	9-14	loess-A	silt loam
100	14-21	loess	silt loam
100	21-31	loess	silt loam
100	31-41	loess	silt loam
100	41-53	loess-B	silt loam
100	53-58	2Bw1	silty clay loam
100	58-68	2Bw1	silt loam
100	68-77	2Bw2	sandy clay
100	77-87	2Bw2	sandy clay
100	87-97	2Bw3	sandy clay
100	97-107	2Bw3	-
100	107-123	2Bw3	sandy clay
100	123-130	2C	-

Table 1-D. Textural properties of fine fraction (<2mm) soils collected from the excavated soil pit at the distance of 50 m in 2009.

distance (m)	depth (cm)	horizon	soil texture
50	0-2	1A	Loam
50	2-4	1A	sandy loam
50	4-6	1A	sandy loam
50	6-8	1A	sandy loam
50	8-11	1A	sandy loam
50	11-18	loess/A	silt loam
50	18-24	loess	silt loam
50	24-34	loess	silt loam
50	34-43	1Bw1	silt loam
50	43-53	1Bw2	silty clay loam
50	53-63	2Bw2	sandy clay loam
50	63-73	2Bw2	sandy clay
50	73-83	2Bw2	sandy clay
50	83-93	2Bw2	sandy clay
50	93-103	2Bw2	sandy clay
50	103-113	2Bw3	sandy clay
50	113-123	2Bw3	sandy clay
50	123-133	2Bw3	sandy clay
50	133-150	2Bw3	sandy clay
50	150-180	2C	sandy clay

Table 2-A. Mineral compositions of soils collected from the excavated soil pit at the distance of 190 m in 2009. Mineral compositions were determined using quantitative XRD.

distance (m)	depth (cm)	kaolinite (wt %)	illite smectite (wt %)	muscovite (wt %)	clays (wt %)
190	0-2	4.9	12.1	5.0	22.0
190	2-4	0.9	10.8	6.4	18.1
190	4-7	0.4	1.0	3.6	5.1
190	7-11	0.0	5.8	0.0	5.8
190	11-15	0.0	4.9	0.0	4.9
190	15-25	0.0	3.7	1.0	4.7
190	25-35	0.1	3.8	0.0	3.9
190	45-55	0.1	3.6	0.0	3.7
190	56-71	0.0	6.7	0.0	6.7
190	71-83	0.2	16.2	0.7	17.0
190	83-110	0.2	9.8	1.3	11.2
190	144-156	0.3	7.3	0.8	8.4

Table 2-A. **continued:** Mineral compositions of soils collected from the excavated soil pit at the distance of 190 m in 2009. Mineral compositions were determined using quantitative XRD.

distance (m)	depth (cm)	quartz (wt %)	K spar (wt %)	plagioclase (wt %)	calcite (wt %)	dolomite (wt %)	amphibole (wt %)	Fe oxides (wt %)
190	0-2	39.5	9.7	13.9	0.1	0.2	0.7	0.0
190	2-4	45.7	9.9	15.5	0.0	0.1	0.5	0.1
190	4-7	58.3	12.5	20.6	0.0	0.0	0.5	0.1
190	7-11	57.5	12.9	21.5	0.0	0.0	1.4	0.0
190	11-15	58.9	12.8	20.7	0.0	0.1	1.4	0.1
190	15-25	58.8	11.1	23.5	0.0	0.2	1.3	0.1
190	25-35	59.2	11.8	23.4	0.0	0.1	1.6	0.0
190	45-55	57.4	11.4	24.9	0.0	0.2	1.4	0.1
190	56-71	57.1	10.2	24.0	0.0	0.1	1.5	0.2
190	71-83	48.9	9.6	21.4	0.0	0.1	1.9	0.6
190	83-110	47.5	9.5	18.5	0.5	3.3	1.5	0.2
190	144-156	42.4	7.9	16.3	5.6	5.8	0.8	0.2

Table 2-B. Mineral compositions of soils collected from the excavated soil pit at the distance of 100 m in 2009. Mineral compositions were determined using quantitative XRD.

distance (m)	depth (cm)	kaolinite (wt %)	illite smectite (wt %)	muscovite (wt %)	clays (wt %)
100	0-2	1.9	8.0	1.8	11.7
100	4-6	0.7	6.9	3.6	11.2
100	6-9	0.4	7.5	3.0	10.9
100	9-14	0.0	5.8	0.0	5.8
100	14-21	0.1	4.3	0.2	4.6
100	31-41	0.0	3.5	0.4	3.9
100	41-53	0.2	4.8	0.6	5.6
100	58-68	0.0	5.5	0.5	6.0
100	68-77	0.3	7.8	3.0	11.1
100	123	0.1	14.9	1.7	16.8

Table 2-B. **continued:** Mineral compositions of soils collected from the excavated soil pit at the distance of 100 m in 2009. Mineral compositions were determined using quantitative XRD.

distance (m)	depth (cm)	quartz (wt %)	K spar (wt %)	plagioclase (wt %)	calcite (wt %)	dolomite (wt %)	amphibole (wt %)	Fe oxides (wt %)
100	0-2	52.1	11.9	18.8	0.1	0.0	0.9	0.0
100	4-6	53.2	11.9	18.7	0.0	0.1	1.0	0.2
100	6-9	55.3	11.9	19.5	0.0	0.1	1.1	0.1
100	9-14	58.5	13.0	20.3	0.0	0.2	1.2	0.0
100	14-21	60.0	11.5	21.8	0.0	0.1	1.2	0.0
100	31-41	59.7	11.5	22.9	0.0	0.2	1.3	0.2
100	41-53	56.7	11.3	24.0	0.0	0.1	1.3	0.2
100	58-68	56.1	10.9	24.7	0.0	0.2	1.7	0.1
100	68-77	46.4	9.7	31.0	0.0	0.0	0.9	0.2
100	123	43.5	8.1	18.4	0.0	0.2	0.8	0.1

Table 2-C. Mineral compositions of soils collected from the excavated soil pit at the distance of 0 m in 2009. Mineral compositions were determined using quantitative XRD.

distance (m)	depth (cm)	kaolinite (wt %)	illite smectite (wt %)	muscovite (wt %)	clays (wt %)
0	0-2	0.3	7.9	1.0	9.2
0	2-4	0.7	9.3	0.6	10.6
0	4-6	0.6	7.4	1.8	9.8
0	6-8	0.0	9.3	0.6	9.9
0	8-10	0.4	8.7	0.7	9.9
0	10-18	0.0	3.7	0.0	3.7
0	18-28	0.0	3.0	0.0	3.0
0	28-43	0.0	4.0	0.2	4.3
0	53-63	0.3	10.2	0.0	10.5
0	73-83	0.3	10.1	0.0	10.5
0	94-100	0.0	2.6	0.0	2.6
0	100-107	0.3	11.9	2.9	15.2

Table 2-C. **continued:** Mineral compositions of soils collected from the excavated soil pit at the distance of 0 m in 2009. Mineral compositions were determined using quantitative XRD.

distance (m)	depth (cm)	quartz (wt %)	K spar (wt %)	plagioclase (wt %)	Calcite (wt %)	dolomite (wt %)	amphibole (wt %)	Fe oxides (wt %)
0	0-2	56.4	12.6	18.0	0.0	0.1	0.7	0.2
0	2-4	55.4	12.4	18.1	0.0	0.0	0.8	0.1
0	4-6	57.0	12.1	17.0	0.0	0.0	0.4	0.1
0	6-8	55.6	12.4	18.3	0.0	0.0	0.8	0.1
0	8-10	56.1	12.2	18.9	0.0	0.1	0.7	0.1
0	10-18	57.0	12.7	24.1	0.0	0.2	1.3	0.1
0	18-28	58.7	12.9	23.0	0.0	0.1	1.3	0.2
0	28-43	55.0	13.7	24.5	0.0	0.2	2.0	0.3
0	53-63	53.0	12.0	22.2	0.0	0.1	1.5	0.1
0	73-83	52.6	10.8	23.1	0.0	0.2	1.8	0.1
0	94-100	49.7	10.0	22.7	0.9	11.0	1.6	0.1
0	100-107	29.3	7.1	11.8	11.7	7.0	0.6	0.1

Table 3-A. Soil properties of fine fraction (<2mm) soils collected from the excavated soil pit at the distance of 190 m in 2009.

distance (m)	depth (cm)	horizon	bulk density (g/cm^3)	pH	<2mm (g)	>2mm (g)
190	0-2	1A1	0.27	-	166.1	20.9
190	2-4	1A1	0.27	6.11	270.5	26.9
190	4-7	1A2	0.86	5.74	575.4	2.4
190	7-11	loess	0.81	5.32	679.2	1
190	11-15	loess	0.81	5.09	895.7	1.8
190	15-25	loess	1.13	5.36	1004.3	1.5
190	25-35	loess	1.13	5.53	864.7	0
190	35-45	loess	1.2	5.76	1013.8	0
190	45-55	loess	1.2	-	930.3	0
190	56-71	1Bw1	1.22	-	778.4	176.5
190	71-83	2Bw2	1.13	-	453	316.4
190	83-110	2C1	1.21	-	780.4	298.3
190	105-130	2C2	1.21	-	644.9	146.9
190	144-156	2Ck	1.21	-	566.5	277.9

Table 3-B. Soil properties of fine fraction (<2mm) soils collected from the excavated soil pit at the distance of 160 m in 2009.

distance (m)	depth (cm)	horizon	bulk density (g/cm^3)	pH	<2mm (g)	>2mm (g)
160	0-2	1A1	0.24	6.21	279.7	25.3
160	2-4	1A1	0.24	6.49	318	24
160	4-7	1A2	0.24	6.47	430.8	27.2
160	7-9	1A2	0.61	5.91	673.8	6
160	9-12	A-loess	0.61	6.2	918.5	16.9
160	12-17	loess	1	6.04	1045.2	0
160	17-25	loess	1.2	5.73	1034	0
160	25-35	1Bw1	1.31	5.75	1150	90.8
160	35-44	1Bw1	1.31	5.65	640.4	528.3
160	44-54	1Cox	1.31	-	472.9	604.2
160	54-64	1Cox	1.31	-	1033.2	151.3
160	64-74	1Cox	1.31	-	933.8	313.1
160	74-84	1Cox	1.31	-	894.5	269.3
160	84-94	1Cox	1.31	-	1118.5	144.3
160	94-104	1Cox	1.31	-	874.4	221.2
160	104-114	2Cox	1.31	-	783.9	216.4
160	114-126	C2	1.37	-	873.7	570.5
160	126-140	C3	1.37	-	478.7	257.9
160	140-167	Bw2		-	-	-

Table 3-C. Soil properties of fine fraction (<2mm) soils collected from the excavated soil pit at the distance of 150 m in 2009.

distance (m)	Depth (cm)	horizon	bulk density (g/cm^3)	pH	<2mm (g)	>2mm (g)
150	0-2	1A1	0.33	6.86	172	13.7
150	2-4	1A1	0.33	6.48	248.3	33.2
150	4-6	1A1	0.33	5.83	387.6	31.1
150	6-8	1A2	0.5	5.14	663	13.2
150	8-11	1A2	0.5	5.29	917.5	13.3
150	11-17	A-loess	0.9	5.83	1023.3	0
150	17-27	loess	1.24	6.14	1303.7	0
150	27-37	loess	1.24	6.32	1172.6	27.2
150	37-44	1Bw1	1.19	6.09	546.7	628.5
150	44-54	1Bw2	1.14	-	1349.7	0.4
150	54-64	1Bw2	1.14	-	1217.4	1.3
150	64-74	1Bw2	1.14	-	1112	47.1
150	74-90	1Bw3	1.17	-	1192	0
150	90-100	2Bw3	1.17	-	1028.5	45.5
150	100-113	2Bw3	1.54	-	1073.5	128.4
150	113-130	2C1	1.54	-	746.6	155.8
150	130-160	2C2	1.54	-	775.4	213.1

Table 3-D. Soil properties of fine fraction (<2mm) soils collected from the excavated soil pit at the distance of 100 m in 2009.

distance (m)	depth (cm)	horizon	bulk density (g/cm^3)	pH	<2mm (g)	>2mm (g)
100	0-2	1A	0.24	6.06	383.3	86.1
100	2-4	1A	0.24	6.17	412.3	83
100	4-6	1A	0.24	6.12	534.5	90.4
100	6-9	1A	0.24	6.16	6983	78.4
100	9-14	loess-A	0.56	6.23	844.8	102.8
100	14-21	loess	1.3	6.26	1148.7	0
100	21-31	loess	1.3	6.22	1195.2	0
100	31-41	loess	1.3	6.2	1156.2	51.7
100	41-53	1EB	1.3	6.05	1093.2	198
100	53-58	2Bw1	1.35	-	333.8	718.4
100	58-68	2Bw1	1.35	-	807.5	357.6
100	68-77	2Bw2	1.28	-	294.7	807.1
100	77-87	2Bw2	1.28	-	585.2	784.8
100	87-97	2Bw3	1.28	-	461.7	580.9
100	97-107	2Bw3	1.28	-	359.4	727.7
100	107-123	2Bw3	1.28	-	267.9	646.6
100	123-130	2C	1.28	-	414.6	618.6

Table 3-E. Soil properties of fine fraction (<2mm) soils collected from the excavated soil pit at the distance of 50 m in 2009.

distance (m)	depth (cm)	horizon	bulk density (g/cm^3)	pH	<2mm (g)	>2mm (g)
50	0-2	1A	0.55	5.61	485.8	69.6
50	2-4	1A	0.55	6.19	560	132.4
50	4-6	1A	0.55	6	607.6	95.5
50	6-8	1A	0.55	5.95	729.7	100.6
50	8-11	1A	0.55	6.12	868	65
50	11-18	loess/A	1.09	5.96	1176.7	0
50	18-24	loess	1.32	5.84	1257.3	0
50	24-34	loess	1.32	5.98	1569.3	54
50	34-43	1Bw1	1.16	5.3	635.1	614.2
50	43-53	1Bw2	1.16	-	537.3	809.1
50	53-63	2Bw2	1.16	-	379.5	890.5
50	63-73	2Bw2	1.16	-	325.6	778.4
50	73-83	2Bw2	1.16	-	327.1	771.7
50	83-93	2Bw2	1.16	-	541.2	600.4
50	93-103	2Bw2	1.16	-	507.5	594.7
50	103-113	2Bw3	1.16	-	374.1	716.5
50	113-123	2Bw3	1.16	-	467.3	600.5
50	123-133	2Bw3	1.41	-	436.7	554.9
50	133-150	2Bw3	1.41	-	350.8	695.1
50	150-180	2C	1.41	-	364.1	712.1

Table 3-F. Soil properties of fine fraction (<2mm) soils collected from the excavated soil pit at the distance of 0 m in 2009.

distance (m)	depth (cm)	horizon	bulk density (g/cm^3)	pH	<2mm (g)	>2mm (g)
0	0-2	1A	0.67	6.44	534.9	58.3
0	2-4	1A	0.67	6.31	633.1	42.6
0	4-6	1A	0.67	6.36	737.4	33.6
0	6-8	1A	0.67	6.42	773.7	32.4
0	8-10	1A	0.67	6.48	972.9	28.9
0	10-18	loess/A	1.14	5.76	1126.9	7
0	18-28	loess	1.1	5.99	1246.9	4.4
0	28-43	loess	1.1	5.97	1213.9	0.8
0	43-53	1Bw	1.28	6.38	1191	55
0	53-63	1Bw	1.28	-	919.8	294.4
0	63-73	1Bw	1.28	-	1116	60.9
0	73-83	1Bw	1.28	-	1093.3	0
0	83-94	1Bw	1.28	-	701.3	369.9
0	94-100	1C	1.32	-	1378.6	28.9
0	100-107	2C	1.25	-	592.4	543.3

Table 4. Averaged elemental concentrations (kg kg^{-1}) of parent materials (loess cap) collected from excavated soil pits at the distance of 190, 160, 150, 100, 50, 0 meter in 2009 from transect distance. These are used as parent material values for mass balance calculations.

distance (m)	depths averaged (cm)	Zr (ppm)	Si (kg kg^{-1})	Fe (kg kg^{-1})	Ca (kg kg^{-1})	P (kg kg^{-1})	K (kg kg^{-1})
190	7-55	348.83	0.36	0.01	0.01	0.00056	0.02
160	17-35	421	0.37	0.01	0.01	0.00051	0.02
150	17-37	463	0.38	0.01	0.01	0.0004	0.02
100	9-41	472.5	0.37	0.01	0.01	0.00045	0.02
50	11-34	393.67	0.37	0.01	0.01	0.00047	0.02
0	10-43	221.5	0.39	0.01	0.01	0.00035	0.02

Appendix I

Table 5-A. Soil A and B horizon depth profiles of fractional mass (τ) losses and gains of major soil elements at the transect distance 190 meter.The loess cap chemistry was used as the parent material for the A horizon, and the C horizon chemistry was used as a parent material for the B horizon.

distance (m)	depth (cm)	horizon	Zr soil (ppm)	τ(Fe)	τ(Al)	τ(Si)	τ(Ca)	τ(Mg)	τ(K)	τ(Na)	τ(P)
190	0-2	A	250.65	1.00	0.33	0.33	7.76	2.62	0.44	-0.01	5.81
190	2-4	A	296.30	0.83	0.21	0.15	4.48	1.64	0.27	-0.13	4.06
190	4-7	A	391.11	-0.08	-0.07	-0.05	0.19	0.05	-0.04	-0.14	-0.04
190	56-71	Bw1	356.15	-0.44	-0.40	-0.44	-0.77	-0.77	-0.37	-0.36	0.03
190	71-83	Bw1	321.09	0.10	-0.25	-0.40	-0.72	-0.57	-0.33	-0.35	-0.26

Table 5-B. Soil A and B horizon depth profiles of fractional mass (τ) losses and gains of major soil elements at the transect distance 160 meter. The loess cap chemistry was used as the parent material for the A horizon, and the C horizon chemistry was used as a parent material for the B horizon.

distance (m)	depth (cm)	horizon	Zr soil (ppm)	τ(Fe)	τ(Al)	τ(Si)	τ(Ca)	τ(Mg)	τ(K)	τ(Na)	τ(P)
160	0-2	A	226.74	2.14	0.92	0.64	12.07	3.89	0.83	-0.06	14.49
160	2-4	A	280.82	1.48	0.62	0.37	6.23	2.10	0.56	-0.09	8.53
160	4-7	A	379.82	0.48	0.20	0.08	1.68	0.59	0.16	-0.10	2.00
160	7-9	A	418.30	0.14	0.08	0.02	0.16	0.16	0.03	-0.07	0.57
160	9-12	A	436.89	0.06	0.01	-0.02	0.05	0.07	0.03	-0.04	0.38
160	12-17	A-loess	451.23	-0.04	-0.04	-0.04	-0.05	0.01	0.00	-0.04	0.13
160	44-54	Bw1	363.41	0.02	-0.04	-0.11	-0.44	-0.77	-0.02	-0.17	-0.77

Table 5-C. Soil A and B horizon depth profiles of fractional mass (τ) losses and gains of major soil elements at the transect distance 150 meter. The loess cap chemistry was used as the parent material for the A horizon, and the C horizon chemistry was used as a parent material for the B horizon.

distance (m)	depth (cm)	horizon	Zr soil (ppm)	τ(Fe)	τ(Al)	τ(Si)	τ(Ca)	τ(Mg)	τ(K)	τ(Na)	τ(P)
150	0-2	A	271.57	1.34	0.61	0.46	14.29	4.69	0.70	-0.07	18.38
150	2-4	A	301.40	1.17	0.56	0.41	7.40	2.99	0.57	-0.01	8.98
150	4-6	A	343.47	0.68	0.41	0.32	2.33	1.23	0.40	0.07	3.56
150	6-8	A2	461.67	0.07	0.05	0.02	0.06	0.13	0.03	-0.06	0.72
150	8-11	A2	482.11	-0.07	-0.01	-0.02	-0.08	-0.01	-0.01	-0.06	0.12
150	11-17	A-loess	483.42	-0.09	-0.02	-0.02	-0.09	-0.02	-0.01	-0.02	0.00
150	37-44	1Bw1	438.36	-0.40	-0.48	-0.58	-0.78	-0.80	-0.47	-0.49	-0.03
150	44-54	1Bw2	418.51	-0.48	-0.48	-0.55	-0.76	-0.81	-0.46	-0.42	0.16
150	54-64	1Bw2	417.14	-0.43	-0.47	-0.55	-0.76	-0.80	-0.46	-0.43	0.10
150	64-74	1Bw2	420.03	-0.35	-0.45	-0.56	-0.76	-0.78	-0.46	-0.44	0.08
150	74-90	1Bw2	345.89	-0.33	-0.38	-0.45	-0.72	-0.75	-0.38	-0.31	0.28
150	90-100	2Bw3	414.25	-0.36	-0.45	-0.55	-0.76	-0.76	-0.46	-0.44	0.03
150	100-113	2Bw3	378.45	-0.31	-0.43	-0.52	-0.58	-0.53	-0.42	-0.38	0.00

Table 5-D. Soil A and B horizon depth profiles of fractional mass (τ) losses and gains of major soil elements at the transect distance 100 meter. The loess cap chemistry was used as the parent material for the A horizon, and the C horizon chemistry was used as a parent material for the B horizon.

distance (m)	depth (cm)	horizon	Zr soil (ppm)	τ(Fe)	τ(Al)	τ(Si)	τ(Ca)	τ(Mg)	τ(K)	τ(Na)	τ(P)
100	0-2	A	453.74	0.24	0.08	0.03	1.36	0.44	0.07	-0.09	1.84
100	2-4	A	427.61	0.31	0.15	0.10	1.16	0.43	0.13	-0.02	1.60
100	4-6	A	447.03	0.32	0.12	0.05	0.87	0.34	0.10	-0.07	1.67
100	6-9	A	477.86	0.20	0.04	-0.01	0.32	0.16	0.04	-0.09	0.80
100	53-58	2Bw1	398.21	-0.55	-0.46	-0.47	-0.77	-0.85	-0.44	-0.30	0.59
100	58-68	2Bw1	383.28	-0.65	-0.49	-0.43	-0.75	-0.87	-0.43	-0.22	1.27
100	68-77	2Bw2	304.47	-0.38	-0.20	-0.33	-0.64	-0.74	-0.30	0.21	-2.69
100	77-87	2Bw2	300.71	-0.34	-0.30	-0.30	-0.69	-0.75	-0.32	-0.08	3.24
100	87-97	2Bw3	335.69	-0.39	-0.39	-0.36	-0.75	-0.78	-0.40	-0.27	0.50
100	97-107	2Bw3	220.37	-0.07	-0.03	-0.04	-0.63	-0.62	-0.08	0.04	-3.29
100	107-123	2Bw3	228.82	-0.10	-0.04	-0.08	-0.61	-0.59	-0.09	0.04	-3.22

Table 5-E. Soil A and B horizon depth profiles of fractional mass (τ) losses and gains of major soil elements at the transect distance 50 meter. The loess cap chemistry was used as the parent material for the A horizon, and the C horizon chemistry was used as a parent material for the B horizon.

distance (m)	depth (cm)	horizon	Zr soil (ppm)	τ(Fe)	τ(Al)	τ(Si)	τ(Ca)	τ(Mg)	τ(K)	τ(Na)	τ(P)
50	0-2	A	415.16	0.06	0.00	-0.04	0.40	0.24	-0.03	-0.14	0.77
50	2-4	A	391.83	0.10	0.07	0.02	0.28	0.06	0.02	-0.07	0.81
50	4-6	A	428.74	0.04	-0.02	-0.07	0.13	0.11	-0.06	-0.15	0.48
50	6-8	A	431.60	0.02	-0.03	-0.07	0.02	0.04	-0.06	-0.15	0.23
50	8-11	A	416.31	0.01	0.00	-0.03	-0.05	0.03	-0.01	-0.07	-0.06
50	34-43	Bw1	361.09	-0.70	-0.57	-0.50	-0.86	-0.91	-0.48	-0.07	6.08
50	43-53	Bw1	290.92	-0.52	-0.42	-0.39	-0.84	-0.85	-0.36	0.05	-8.34
50	53-63	2Bw2	254.56	-0.42	-0.33	-0.31	-0.84	-0.81	-0.28	0.04	-7.43
50	63-73	2Bw2	187.58	-0.02	-0.04	-0.07	-0.81	-0.66	-0.03	0.06	-1.41
50	73-83	2Bw2	165.35	0.14	0.10	0.05	-0.79	-0.59	0.09	0.14	-0.52
50	83-93	2Bw2	161.36	0.16	0.12	0.08	-0.78	-0.57	0.11	0.10	-0.20
50	93-103	2Bw2	158.42	0.14	0.13	0.10	-0.75	-0.56	0.13	0.23	-0.57
50	103-113	2Bw3	162.85	0.08	0.07	0.07	-0.73	-0.56	0.10	0.17	-0.56
50	113-123	2Bw3	148.40	0.16	0.17	0.17	-0.59	-0.38	0.19	0.31	-0.60
50	123-133	2Bw3	169.08	-0.05	0.00	0.00	-0.36	-0.18	0.02	0.15	-0.91
50	133-150	2Bw3	158.64	-0.01	0.01	0.06	-0.10	-0.09	0.04	0.01	1.75

Table 5-F. Soil A and B horizon depth profiles of fractional mass (τ) losses and gains of major soil elements at the transect distance 0 meter. The loess cap chemistry was used as the parent material for the A horizon, and the C horizon chemistry was used as a parent material for the B horizon.

distance (m)	depth (cm)	horizon	Zr soil (ppm)	τ(Fe)	τ(Al)	τ(Si)	τ(Ca)	τ(Mg)	τ(K)	τ(Na)	τ(P)
0	0-2	A	279.71	0.68	0.29	0.34	0.74	0.48	0.28	-0.07	2.09
0	2-4	A	287.17	0.71	0.30	0.30	0.65	0.52	0.28	-0.10	2.34
0	4-6	A	296.90	0.59	0.30	0.26	0.52	0.53	0.25	0.01	1.40
0	6-8	A	280.48	0.69	0.38	0.33	0.55	0.58	0.35	0.09	1.30
0	8-10	A	287.47	0.65	0.34	0.30	0.39	0.50	0.31	0.08	1.24
0	43-53	Bw1	321.21	-0.16	-0.14	-0.16	-0.77	-0.84	-0.09	-0.05	1.01
0	53-63	Bw1	332.57	-0.22	-0.20	-0.18	-0.77	-0.86	-0.18	-0.13	0.56
0	63-73	Bw1	311.13	-0.08	-0.10	-0.14	-0.77	-0.82	-0.09	0.03	-4.84
0	73-83	Bw1	353.83	-0.17	-0.20	-0.25	-0.72	-0.83	-0.21	-0.09	1.69
0	83-94	Bw1	355.25	-0.29	-0.24	-0.25	-0.60	-0.74	-0.22	-0.07	2.70

Table 6-A. Foliar elemental concentrations (mg/kg) for leaf litter Oe and Oi horizons collected at transect distances 190, 160, 150, 100, 50, and 0 meter in the year 2009. The Oi horizon is composed of fresh and fully recognizable tree leaf litter, while the litter in the Oe horizon is moderately decomposed.

distance (m)	sub horizon	Fe (mg/kg)	Al (mg/kg)	Ca (mg/kg)	P (mg/kg)	K (mg/kg)	Mg (mg/kg)
0	Oi	597.58	664.50	24809.00	1179.20	2240.70	1473.30
50	Oi	1460.70	1391.10	18650.00	933.91	783.48	1212.70
100	Oi	223.80	245.89	29539.00	1491.60	3044.90	1913.80
150	Oi	325.98	443.89	33250.00	1673.70	2925.40	2883.50
160	Oi	167.95	165.06	27050.00	1530.10	2573.30	1867.30
190	Oi	241.35	249.89	31270.00	1428.20	2217.10	1775.10
0	Oe	1371.20	1254.70	16357.00	734.99	766.51	889.97
50	Oe	455.21	568.85	33693.00	1740.60	3025.90	2537.80
100	Oe	781.96	912.61	28433.00	1173.60	958.58	1436.40
150	Oe	712.00	844.73	36436.00	1387.00	1358.90	2595.60
160	Oe	594.14	693.58	31451.00	1322.50	1123.30	1816.30
190	Oe	777.00	732.06	34144.00	1197.60	1061.40	1705.50

Table 7-A. Amorphous Fe oxides (Fe_{ox}) as determined as ammonium oxalate extraction, pedogenic crystalline Fe, Al, and Ca oxides (Fe_{di}, Al_{di}, Ca_{di}) as determined as citrate-biocarbonate-dithionite extraction, and organically complexed Fe, Al, and Ca oxides (Fe_{py}, Al_{py}, Ca_{py}) as determined by a sodium pyrophosphate extraction from the excavated soil at the distance 190 meter in 2009.

distance (m)	depth (cm)	Fe_{ox} (%)	Fe_{di} (%)	Al_{di} (%)	Ca_{di} (%)	Fe_{py} (%)	Al_{py} (%)	Ca_{py} (%)
190	0-2	0.24	0.05	0.01	0.90	0.02	0.04	0.06
190	2-4	0.24	0.07	0.02	1.00	0.02	0.03	0.28
190	4-7	0.17	0.07	0.02	0.19	0.03	0.03	0.26
190	7-11	0.20	0.10	0.02	0.06	0.04	0.03	0.09
190	11-15	0.22	0.12	0.03	0.04	0.06	0.10	0.06
190	15-25	0.26	0.14	0.04	0.04	0.06	0.04	0.06
190	25-35	0.25	0.13	0.02	0.03	0.04	0.05	0.05
190	35-45	0.25	0.13	0.02	0.03	0.05	0.04	0.05
190	45-55	-	0.12	0.02	0.03	0.03	0.03	0.04
190	56-71	-	0.23	0.04	0.06	0.13	0.14	0.09
190	71-83	-	0.35	0.05	0.12	0.21	0.20	0.15
190	83-110	-	0.19	0.03	0.16	0.01	0.01	0.15
190	105-130	-	0.20	0.03	0.17	0.05	0.05	0.10
190	144-156	-	0.21	0.02	0.55	0.01	0.01	0.23

Table 7-B. Amorphous Fe oxides (Fe_{ox}) as determined as ammonium oxalate extraction, pedogenic crystalline Fe, Al, and Ca oxides (Fe_{di}, Al_{di}, Ca_{di}) as determined as citrate-biocarbonate-dithionite extraction, and organically complexed Fe, Al, and Ca oxides (Fe_{py}, Al_{py}, Ca_{py}) as determined by a sodium pyrophosphate extraction from the excavated soil at the distance 160 meter in 2009.

distance (m)	depth (cm)	Fe_{ox} (%)	Fe_{di} (%)	Al_{di} (%)	Ca_{di} (%)	Fe_{py} (%)	Al_{py} (%)	Ca_{py} (%)
160	0-2	0.24	0.03	0.02	1.23	0.01	0.02	0.26
160	2-4	0.30	0.11	0.03	0.95	0.02	0.03	0.39
160	4-7	0.30	0.07	0.04	0.66	0.03	0.02	0.41
160	7-9	0.34	0.15	0.04	0.20	0.05	0.04	0.26
160	9-12	0.36	0.17	0.04	0.14	0.06	0.03	0.16
160	12-17	0.32	0.12	0.04	0.06	0.05	0.05	0.09
160	17-25	0.30	0.12	0.03	0.03	0.05	0.07	0.04
160	25-35	0.25	0.12	0.03	0.02	0.04	0.05	0.04
160	35-44	-	0.27	0.04	0.07	0.15	0.14	0.10
160	44-54	-	0.30	0.05	0.08	0.22	0.20	0.13
160	54-64	-	0.19	0.04	0.05	0.08	0.07	0.07
160	64-74	-	0.16	0.03	0.04	0.07	0.05	0.06
160	74-84	-	0.22	0.05	0.07	0.07	0.07	0.07
160	84-94	-	0.16	0.03	0.04	0.05	0.04	0.06
160	94-104	-	0.18	0.04	0.04	0.05	0.03	0.06
160	104-114	-	0.24	0.04	0.05	0.05	0.04	0.07
160	114-126	-	0.44	0.02	0.16	0.01	0.04	0.13
160	126-140	-	0.15	0.02	0.14	0.01	0.16	0.14
160	140-167	-	0.23	0.05	0.30	0.02	0.04	0.19

Table 7-C. Amorphous Fe oxides (Fe_{ox}) as determined as ammonium oxalate extraction, pedogenic crystalline Fe, Al, and Ca oxides (Fe_{di}, Al_{di}, Ca_{di}) as determined as citrate-biocarbonate-dithionite extraction, and organically complexed Fe, Al, and Ca oxides (Fe_{py}, Al_{py}, Ca_{py}) as determined by a sodium pyrophosphate extraction from the excavated soil at the distance 150 meter in 2009.

distance (m)	depth (cm)	Fe_{ox} (%)	Fe_{di} (%)	Al_{di} (%)	Ca_{di} (%)	Fe_{py} (%)	Al_{py} (%)	Ca_{py} (%)
150	0-2	0.14	0.04	0.01	0.78	0.01	0.00	0.35
150	2-4	0.20	0.07	0.02	0.57	0.02	0.00	0.51
150	4-6	0.19	0.07	0.03	0.68	0.04	0.02	0.75
150	6-8	0.23	0.12	0.04	0.14	0.07	0.04	0.20
150	8-11	0.25	0.09	0.02	0.04	0.05	0.02	0.11
150	11-17	0.24	0.13	0.03	0.05	0.06	0.02	0.07
150	17-27	0.28	0.14	0.03	0.03	0.05	0.03	0.05
150	27-37	-	0.13	0.03	0.03	0.03	0.03	0.05
150	37-44	-	0.31	0.05	0.09	0.16	0.16	0.14
150	44-54	-	0.22	0.04	0.05	0.08	0.08	0.08
150	54-64	-	0.25	0.05	0.05	0.14	0.15	0.08
150	64-74	-	0.31	0.06	0.06	0.21	0.20	0.09
150	74-90	-	0.27	0.05	0.05	0.09	0.09	0.07
150	90-100	-	0.31	0.06	0.08	0.13	0.13	0.11
150	100-113	-	0.33	0.04	0.11	0.03	0.02	0.12
150	113-130	-	0.19	0.04	0.14	0.02	0.01	0.17
150	130-160	-	0.16	0.03	0.23	0.02	0.02	0.16

Table 7-D. Amorphous Fe oxides (Fe_{ox}) as determined as ammonium oxalate extraction, pedogenic crystalline Fe, Al, and Ca oxides (Fe_{di}, Al_{di}, Ca_{di}) as determined as citrate-biocarbonate-dithionite extraction, and organically complexed Fe, Al, and Ca oxides (Fe_{py}, Al_{py}, Ca_{py}) as determined by a sodium pyrophosphate extraction from the excavated soil at the distance 100 meter in 2009.

distance (m)	depth (cm)	Fe_{ox} (%)	Fe_{di} (%)	Al_{di} (%)	Ca_{di} (%)	Fe_{py} (%)	Al_{py} (%)	Ca_{py} (%)
100	0-2	0.28	0.09	0.02	0.56	0.02	0.03	0.50
100	2-4	0.24	0.11	0.00	0.42	0.04	0.04	0.38
100	4-6	0.32	0.11	0.03	0.27	0.02	0.02	0.36
100	6-9	0.30	0.14	0.03	0.08	0.03	0.02	0.28
100	9-14	0.31	0.17	0.02	0.05	0.05	0.02	0.13
100	14-21	0.37	0.14	0.03	0.04	0.06	0.01	0.07
100	21-31	0.24	0.14	0.03	0.04	0.04	0.01	0.06
100	31-41	-	0.15	0.02	0.03	0.02	0.01	0.08
100	41-53	-	0.30	0.03	0.09	0.05	0.02	0.07
100	53-58	-	0.16	0.04	0.04	0.11	0.08	0.13
100	58-68	-	0.23	0.03	0.09	0.04	0.06	0.07
100	68-77	-	0.25	0.03	0.09	0.09	0.15	0.13
100	77-87	-	0.27	0.04	0.09	0.08	0.13	0.14
100	87-97	-	0.25	0.04	0.09	0.06	0.03	0.14
100	97-107	-	0.27	0.05	0.12	0.05	0.02	0.16
100	107-123	-	0.34	0.05	0.24	0.02	0.06	0.21
100	123-123	-	0.31	0.07	0.15	0.05	0.09	0.19

Table 7-E. Amorphous Fe oxides (Fe_{ox}) as determined as ammonium oxalate extraction, pedogenic crystalline Fe, Al, and Ca oxides (Fe_{di}, Al_{di}, Ca_{di}) as determined as citrate-biocarbonate-dithionite extraction, and organically complexed Fe, Al, and Ca oxides (Fe_{py}, Al_{py}, Ca_{py}) as determined by a sodium pyrophosphate extraction from the excavated soil at the distance 50 meter in 2009.

distance (m)	depth (cm)	Fe_{ox} (%)	Fe_{di} (%)	Al_{di} (%)	Ca_{di} (%)	Fe_{py} (%)	Al_{py} (%)	Ca_{py} (%)
50	0-2	0.28	0.12	0.03	0.31	0.04	0.01	0.35
50	2-4	0.29	0.01	0.01	0.12	0.04	0.02	0.29
50	4-6	0.29	0.13	0.03	0.24	0.04	0.09	0.28
50	6-8	0.35	0.16	0.04	0.19	0.04	0.05	0.22
50	8-11	0.27	0.14	0.03	0.10	0.04	0.04	0.12
50	11-18	0.28	0.16	0.03	0.05	0.05	0.02	0.06
50	18-24	0.21	0.15	0.02	0.03	0.05	0.02	0.04
50	24-34	-	0.15	0.02	0.03	0.03	0.04	0.03
50	34-43	-	0.24	0.03	0.05	0.07	0.09	0.06
50	43-53	-	0.28	0.05	0.08	0.14	0.12	0.12
50	53-63	-	0.30	0.05	0.11	0.09	0.12	0.15
50	63-73	-	0.40	0.10	0.17	0.11	0.13	0.18
50	73-83	-	0.39	0.10	0.17	0.12	0.10	0.19
50	83-93	-	0.37	0.08	0.19	0.12	0.11	0.21
50	93-103	-	0.38	0.09	0.20	0.09	0.08	0.22
50	103-113	-	0.38	0.06	0.23	0.05	0.05	0.21
50	113-123	-	0.38	0.08	0.27	0.08	0.08	0.26
50	123-133	-	0.31	0.06	0.33	0.03	0.04	0.25
50	133-150	-	0.30	0.04	0.45	0.03	0.04	0.29
50	160-180	-	0.31	0.04	0.61	0.04	0.05	0.31

Table 7-F. Amorphous Fe oxides (Fe_{ox}) as determined as ammonium oxalate extraction, pedogenic crystalline Fe, Al, and Ca oxides (Fe_{di}, Al_{di}, Ca_{di}) as determined as citrate-biocarbonate-dithionite extraction, and organically complexed Fe, Al, and Ca oxides (Fe_{py}, Al_{py}, Ca_{py}) as determined by a sodium pyrophosphate extraction from the excavated soil at the distance 0 meter in 2009.

distance (m)	depth (cm)	Fe_{ox} (%)	Fe_{di} (%)	Al_{di} (%)	Ca_{di} (%)	Fe_{py} (%)	Al_{py} (%)	Ca_{py} (%)
0	0-2	0.30	0.15	0.03	0.39	0.03	0.02	0.43
0	2-4	0.37	0.16	0.04	0.32	0.03	0.03	0.35
0	4-6	0.35	0.16	0.04	0.30	0.03	0.03	0.32
0	6-8	0.33	0.17	0.04	0.28	0.03	0.02	0.30
0	8-10	0.00	0.18	0.04	0.24	0.03	0.02	0.27
0	10-18	0.24	0.14	0.02	0.05	0.05	0.02	0.06
0	18-28	0.17	0.12	0.02	0.02	0.03	0.02	0.04
0	28-43	-	0.13	0.02	0.03	0.02	0.01	0.04
0	43-53	-	0.26	0.04	0.08	0.16	0.15	0.10
0	53-63	-	0.26	0.04	0.07	0.12	0.11	0.09
0	63-73	-	0.28	0.04	0.07	0.14	0.13	0.11
0	73-83	-	0.26	0.04	0.07	0.10	0.09	0.10
0	83-94	-	0.20	0.02	0.07	0.02	0.01	0.10
0	94-100	-	0.09	0.01	0.16	0.00	0.00	0.09
0	100-107	-	0.17	0.02	1.32	0.03	0.03	0.52

Appendix II

Table 8-A. Soil elemental oxide percent (fine fraction <2mm) with LOI% removed and renormalized to 100% collected from the excavated soil pit at the distance of 190 m in 2009.

distance (m)	horizon	depth (cm)	CaO (%)	MgO (%)	Na_2O (%)	K_2O (%)	P_2O_5 (%)	LOI (%)	total (%)	total-LOI (%)	renormalized (%)
190	A	0-2	9.51	1.14	1.42	1.89	0.62	59.90	98.60	38.70	100
190	A	2-4	7.04	0.98	1.48	1.96	0.54	53.50	99.40	45.90	100
190	A	4-7	2.02	0.51	1.94	1.96	0.14	11.20	98.90	87.70	100
190	loess	7-11	1.49	0.45	1.99	1.94	0.12	3.64	97.60	93.96	100
190	loess	11-15	1.48	0.44	2.01	1.94	0.11	2.84	97.80	94.96	100
190	loess	15-25	1.58	0.47	2.17	1.99	0.16	1.72	94.60	92.88	100
190	loess	25-35	1.65	0.47	2.22	2.00	0.12	1.17	94.70	93.53	100
190	loess	35-45	1.69	0.46	2.13	1.87	0.15	1.06	98.20	97.14	100
190	loess	45-55	1.77	0.49	2.28	1.89	0.15	1.38	92.50	91.12	100
190	1Bw	56-71	1.77	0.61	2.09	1.79	0.15	1.85	99.00	97.15	100
190	2Bw	71-83	1.83	1.01	1.91	1.73	0.19	3.91	98.90	94.99	100
190	2C	83-110	2.90	1.44	1.78	1.60	0.12	4.61	101.00	96.39	100
190	2C	105-130	3.12	0.99	1.97	1.61	0.09	3.40	99.50	96.10	100
190	2C	144-156	5.97	1.89	1.65	1.51	0.09	7.26	100.00	92.74	100

Table 8-A. continued: Soil elemental oxide percent (fine fraction <2mm) with LOI% removed and renormalized to 100% collected from the excavated soil pit at the distance of 190 m in 2009.

distance (m)	horizon	depth (cm)	Hf (ppm)	Zr (ppm)	SiO_2 (%)	MnO (%)	Al_2O_3 (%)	Fe_2O_3 (%)	total (%)	total-LOI (%)	renormalized (%)
190	A	0-2	5.94	250.65	73.39	0.59	8.45	2.30	98.60	38.70	100
190	A	2-4	7.19	296.30	75.16	0.65	9.11	2.48	99.40	45.90	100
190	A	4-7	10.26	391.11	81.64	0.26	9.22	1.64	98.90	87.70	100
190	loess	7-11	10.22	383.14	82.38	0.12	9.41	1.56	97.60	93.96	100
190	loess	11-15	10.43	387.53	82.35	0.08	9.39	1.59	97.80	94.96	100
190	loess	15-25	10.55	398.36	81.93	0.04	9.31	1.75	94.60	92.88	100
190	loess	25-35	9.94	378.49	81.90	0.04	9.31	1.73	94.70	93.53	100
190	loess	35-45	8.65	331.48	81.84	0.05	9.59	1.74	98.20	97.14	100
190	loess	45-55	9.44	350.09	81.65	0.04	9.45	1.82	92.50	91.12	100
190	1Bw	56-71	9.16	356.15	80.39	0.05	10.18	2.44	99.00	97.15	100
190	2Bw	71-83	8.32	321.09	76.96	0.09	11.42	4.36	98.90	94.99	100
190	2C	83-110	5.81	233.43	78.85	0.09	9.74	2.92	101.00	96.39	100
190	2C	105-130	6.35	247.66	80.54	0.08	9.14	2.04	99.50	96.10	100
190	2C	144-156	2.91	106.75	77.21	0.13	8.95	2.29	100.00	92.74	100

Table 8-B. Soil elemental oxide percent (fine fraction <2mm) with LOI% removed and renormalized to 100% collected from the excavated soil pit at the distance of 160 m in 2009.

distance (m)	horizon	depth cm	CaO (%)	MgO (%)	Na_2O (%)	K_2O (%)	P_2O_5 (%)	LOI (%)	total (%)	total-LOI (%)	renormalized (%)
160	A	0-2	10.70	1.25	0.99	1.89	0.96	65.60	100.00	34.40	100
160	A	2-4	7.33	0.98	1.19	1.99	0.73	54.10	97.90	43.80	100
160	A	4-7	3.68	0.68	1.59	2.00	0.31	30.20	97.60	67.40	100
160	A	7-9	1.76	0.55	1.80	1.96	0.18	8.29	97.70	89.41	100
160	A	9-12	1.65	0.53	1.95	2.05	0.17	5.03	95.90	90.87	100
160	A-loess	12-17	1.54	0.51	2.02	2.06	0.14	3.30	96.60	93.30	100
160	loess	17-25	1.54	0.48	2.01	1.97	0.12	1.92	99.30	97.38	100
160	loess	25-35	1.59	0.50	2.01	1.97	0.11	1.70	98.50	96.80	100
160	loess	35-44	1.62	0.61	1.94	2.03	0.15	2.30	95.10	92.80	100
160	1Bw	44-54	1.66	0.65	1.95	1.90	0.17	3.04	98.80	95.76	100
160	1Bw	54-64	1.77	0.53	2.14	1.78	0.14	1.73	98.00	96.27	100
160	1C	64-74	1.85	0.60	2.26	1.90	0.16	2.11	97.70	95.59	100
160	1C	74-84	1.84	0.61	2.12	1.80	0.14	2.19	99.90	97.71	100
160	1C	84-94	1.80	0.56	2.13	1.77	0.16	1.82	99.60	97.78	100
160	1C	94-104	1.79	0.61	2.10	1.76	0.14	1.48	97.70	96.22	100
160	1C	104-114	1.80	0.67	2.03	1.76	0.12	2.36	98.00	95.64	100
160	2C	114-126	4.51	2.13	2.03	1.55	0.13	5.75	101.00	95.25	100
160	2C2	126-140	4.84	2.16	2.00	1.56	0.09	6.09	101.00	94.91	100
160	2C2	140-167	3.56	1.83	1.42	1.64	0.13	7.07	100.50	93.43	100

Table 8-B. continued: Soil elemental oxide percent (fine fraction <2mm) with LOI% removed and renormalized to 100% collected from the excavated soil pit at the distance of 160 m in 2009.

distance (m)	horizon	depth (cm)	Hf (ppm)	Zr (ppm)	SiO_2 (%)	MnO (%)	Al_2O_3 (%)	Fe_2O_3 (%)	LOI (%)	total (%)	total-LOI (%)	renormalized (%)
160	A	0-2	6.40	226.74	70.35	1.13	9.51	3.05	65.60	100.00	34.40	100
160	A	2-4	7.99	280.82	72.60	1.51	9.93	2.99	54.10	97.90	43.80	100
160	A	4-7	9.79	379.82	77.45	1.16	9.96	2.40	30.20	97.60	67.40	100
160	A	7-9	10.51	418.30	80.86	0.36	9.86	2.05	8.29	97.70	89.41	100
160	A	9-12	12.22	436.89	80.99	0.30	9.65	1.99	5.03	95.90	90.87	100
160	A-loess	12-17	11.47	451.23	81.56	0.18	9.47	1.85	3.30	96.60	93.30	100
160	loess	17-25	11.09	425.14	81.74	0.07	9.48	1.92	1.92	99.30	97.38	100
160	loess	25-35	11.67	442.15	81.92	0.06	9.48	1.80	1.70	98.50	96.80	100
160	loess	35-44	NSS	NSS	80.28	0.05	10.02	2.66	2.30	95.10	92.80	100
160	1Bw	44-54	9.71	363.41	79.68	0.05	10.55	2.88	3.04	98.80	95.76	100
160	1Bw	54-64	7.48	287.73	81.13	0.05	9.97	2.02	1.73	98.00	96.27	100
160	1C	64-74	8.26	321.16	80.34	0.05	10.06	2.24	2.11	97.70	95.59	100
160	1C	74-84	8.49	331.59	80.14	0.06	10.34	2.47	2.19	99.90	97.71	100
160	1C	84-94	7.98	309.88	81.10	0.06	9.82	2.12	1.82	99.60	97.78	100
160	1C	94-104	10.08	389.73	80.75	0.06	9.96	2.33	1.48	97.70	96.22	100
160	1C	104-114	12.13	451.69	80.30	0.07	10.01	2.75	2.36	98.00	95.64	100
160	2C	114-126	8.61	334.91	75.80	0.13	9.24	3.77	5.75	101.00	95.25	100
160	2C2	126-140	4.53	166.47	77.23	0.14	9.06	2.44	6.09	101.00	94.91	100
160	2C2	140-167	NSS	NSS	79.52	0.16	8.96	2.41	7.07	100.50	93.43	100

Table 8-C. Soil elemental oxide percent (fine fraction <2mm) with LOI% removed and renormalized to 100% collected from the excavated soil pit at the distance of 150 m in 2009.

distance (m)	horizon	depth (cm)	CaO (%)	MgO (%)	Na_2O (%)	K_2O (%)	P_2O_5 (%)	LOI (%)	total (%)	total-LOI (%)	renormalized (%)
150	A	0-2	13.45	1.50	1.09	1.92	1.02	66.90	98.20	31.30	100
150	A	2-4	8.20	1.17	1.29	1.96	0.58	55.30	98.10	42.80	100
150	A	4-6	3.71	0.74	1.58	1.99	0.30	32.60	98.40	65.80	100
150	A	6-8	1.59	0.51	1.88	1.97	0.15	8.66	99.20	90.54	100
150	A	8-11	1.44	0.46	1.95	1.98	0.11	4.30	99.30	95.00	100
150	A-loess	11-17	1.46	0.46	2.05	1.99	0.09	2.33	97.90	95.57	100
150	loess	17-27	1.47	0.43	1.96	1.97	0.08	1.38	98.20	96.82	100
150	loess	27-37	1.60	0.49	2.13	1.95	0.10	1.76	100.50	98.74	100
150	1Bw	37-44	1.64	0.66	1.99	1.93	0.15	3.40	98.30	94.90	100
150	1Bw	44-54	1.73	0.60	2.16	1.88	0.14	2.19	99.20	97.01	100
150	1Bw	54-64	1.69	0.63	2.11	1.87	0.15	2.87	99.00	96.13	100
150	1Bw	64-74	1.74	0.69	2.11	1.87	0.16	3.34	100.00	96.66	100
150	1Bw	74-90	1.67	0.64	2.12	1.77	0.13	2.76	99.90	97.14	100
150	2Bw	90-100	1.70	0.75	2.05	1.85	0.14	2.94	99.50	96.56	100
150	2Bw	100-113	2.69	1.32	2.07	1.80	0.14	4.31	99.70	95.39	100
150	2C	113-130	2.14	1.16	1.67	1.66	0.10	4.33	100.50	96.17	100
150	2C	130-160	4.32	1.64	1.69	1.45	0.08	5.70	98.20	92.50	100

Table 8-C continued: Soil elemental oxide percent (fine fraction <2mm) with LOI% removed and renormalized to 100% collected from the excavated soil pit at the distance of 150 m in 2009.

distance (m)	horizon	depth (cm)	Hf (ppm)	Zr (ppm)	SiO_2 (%)	MnO (%)	Al_2O_3 (%)	Fe_2O_3 (%)	LOI (%)	total (%)	total-LOI (%)	renormalized (%)
150	A	0-2	7.35	271.57	68.69	0.58	8.63	2.43	66.90	98.20	31.30	100
150	A	2-4	8.41	301.40	73.83	0.56	9.25	2.50	55.30	98.10	42.80	100
150	A	4-6	8.97	343.47	78.72	0.47	9.56	2.20	32.60	98.40	65.80	100
150	A	6-8	10.71	461.67	81.51	0.30	9.54	1.89	8.66	99.20	90.54	100
150	A	8-11	11.37	482.11	82.11	0.15	9.39	1.72	4.30	99.30	95.00	100
150	A-loess	11-17	11.09	483.42	82.24	0.07	9.34	1.67	2.33	97.90	95.57	100
150	loess	17-27	10.74	468.91	82.52	0.06	9.14	1.77	1.38	98.20	96.82	100
150	loess	27-37	11.04	478.02	81.73	0.06	9.50	1.85	1.76	100.50	98.74	100
150	1Bw	37-44	9.91	438.36	79.24	0.05	10.75	3.00	3.40	98.30	94.90	100
150	1Bw	44-54	9.59	418.51	80.20	0.05	10.19	2.48	2.19	99.20	97.01	100
150	1Bw	54-64	9.57	417.14	79.89	0.05	10.40	2.72	2.87	99.00	96.13	100
150	1Bw	64-74	9.52	420.03	78.94	0.05	10.76	3.12	3.34	100.00	96.66	100
150	1Bw	74-90	8.13	345.89	80.40	0.05	10.13	2.65	2.76	99.90	97.14	100
150	2Bw	90-100	9.53	414.25	79.23	0.06	10.62	3.02	2.94	99.50	96.56	100
150	2Bw	100-113	8.81	378.45	78.21	0.07	10.19	3.00	4.31	99.70	95.39	100
150	2C	113-130	4.37	177.81	80.90	0.10	9.44	2.42	4.33	100.50	96.17	100
150	2C	130-160	4.65	200.00	80.22	0.13	8.29	1.90	5.70	98.20	92.50	100

Table 8-D. Soil elemental oxide percent (fine fraction <2mm) with LOI% removed and renormalized to 100% collected from the excavated soil pit at the distance of 100 m in 2009.

distance (m)	horizon	depth (cm)	CaO (%)	MgO (%)	Na_2O (%)	K_2O (%)	P_2O_5 (%)	LOI (%)	total (%)	total-LOI (%)	renormalized (%)
100	A	0-2	3.39	0.65	1.76	1.97	0.28	32.40	100.50	68.10	100
100	A	2-4	2.92	0.60	1.80	1.96	0.24	26.40	101.00	74.60	100
100	A	4-6	2.65	0.59	1.78	2.00	0.26	22.00	99.40	77.40	100
100	A	6-9	1.99	0.55	1.85	2.02	0.19	13.20	99.00	85.80	100
100	loess-A	9-14	1.48	0.47	1.99	1.99	0.09	3.33	99.60	96.27	100
100	loess	14-21	1.50	0.48	2.06	1.98	0.10	2.06	99.30	97.24	100
100	loess	21-31	1.56	0.49	2.11	1.96	0.11	1.70	100.50	98.80	100
100	loess	31-41	1.61	0.48	2.15	1.95	0.11	1.35	98.40	97.05	100
100	loess-B	41-53	1.67	0.52	2.19	1.90	0.13	1.75	98.50	96.75	100
100	2Bw1	53-58	1.65	0.64	2.05	1.89	0.17	3.22	99.40	96.18	100
100	2Bw2	58-68	1.71	0.54	2.21	1.84	0.13	2.16	100.00	97.84	100
100	2Bw2	68-77	1.98	0.84	2.70	1.80	0.14	3.11	100.00	96.89	100
100	2Bw2	77-87	1.67	0.81	2.04	1.73	0.12	2.93	99.70	96.77	100
100	2Bw3	87-97	1.51	0.81	1.80	1.70	0.10	3.58	99.80	96.22	100
100	2Bw3	97-107	1.48	0.90	1.68	1.70	0.11	4.75	100.50	95.75	100
100	2Bw3	107-123	1.61	1.00	1.76	1.74	0.13	4.79	100.50	95.71	100
100	2C	123	3.71	2.19	1.51	1.72	0.13	7.55	100.50	92.95	100

Table 8-D continued: Soil elemental oxide percent (fine fraction <2mm) with LOI% removed and renormalized to 100% collected from the excavated soil pit at the distance of 100 m in 2009.

distance (m)	horizon	depth (cm)	Hf (ppm)	Zr (ppm)	SiO_2 (%)	MnO (%)	Al_2O_3 (%)	Fe_2O_3 (%)	LOI (%)	total (%)	total-LOI (%)	renormalized (%)
100	A	0-2	10.43	453.74	79.00	0.70	9.50	2.09	32.40	100.50	68.10	100
100	A	2-4	9.79	427.61	79.49	0.70	9.48	2.08	26.40	101.00	74.60	100
100	A	4-6	10.59	447.03	79.20	0.84	9.72	2.20	22.00	99.40	77.40	100
100	A	6-9	11.07	477.86	80.19	0.71	9.63	2.12	13.20	99.00	85.80	100
100	loess-A	9-14	11.11	472.63	82.06	0.12	9.36	1.77	3.33	99.60	96.27	100
100	loess	14-21	11.31	490.54	81.96	0.08	9.42	1.81	2.06	99.30	97.24	100
100	loess	21-31	11.44	481.78	81.88	0.06	9.38	1.80	1.70	100.50	98.80	100
100	loess	31-41	11.23	496.65	81.81	0.05	9.41	1.83	1.35	98.40	97.05	100
100	loess-B	41-53	9.41	412.40	81.14	0.05	9.72	2.11	1.75	98.50	96.75	100
100	2Bw1	53-58	9.15	398.21	79.43	0.05	10.61	2.97	3.22	99.40	96.18	100
100	2Bw2	58-68	8.99	383.28	81.36	0.06	9.66	2.19	2.16	100.00	97.84	100
100	2Bw2	68-77	7.12	304.47	76.89	0.08	12.02	3.11	3.11	100.00	96.89	100
100	2Bw2	77-87	6.82	300.71	79.36	0.09	10.39	3.27	2.93	99.70	96.77	100
100	2Bw3	87-97	7.59	335.69	79.92	0.14	10.13	3.36	3.58	99.80	96.22	100
100	2Bw3	97-107	5.12	220.37	79.69	0.11	10.55	3.36	4.75	100.50	95.75	100
100	2Bw3	107-123	5.33	228.82	78.78	0.10	10.87	3.40	4.79	100.50	95.71	100
100	2C	123	4.84	204.41	76.60	0.18	10.11	3.36	7.55	100.50	92.95	100

Table 8-E. Soil elemental oxide percent (fine fraction <2mm) with LOI% removed and renormalized to 100% collected from the excavated soil pit at the distance of 50 m in 2009.

distance (m)	horizon	depth (cm)	CaO (%)	MgO (%)	Na_2O (%)	K_2O (%)	P_2O_5 (%)	LOI (%)	total (%)	total-LOI (%)	renormalized (%)
50	A	0-2	2.26	0.60	1.88	1.96	0.20	18.35	98.80	80.45	100
50	A	2-4	1.96	0.48	1.92	1.95	0.19	14.80	98.00	83.20	100
50	A	4-6	1.89	0.55	1.93	1.97	0.17	12.40	99.40	87.00	100
50	A	6-8	1.72	0.52	1.94	1.97	0.14	9.47	99.60	90.13	100
50	A	8-11	1.55	0.50	2.03	2.00	0.11	4.30	98.70	94.40	100
50	loess/A	11-18	1.53	0.47	2.12	1.99	0.11	2.18	99.20	97.02	100
50	loess	18-24	1.55	0.48	2.07	1.98	0.09	1.56	98.20	96.64	100
50	loess	24-34	1.66	0.46	2.23	1.95	0.12	0.78	98.30	97.52	100
50	1Bw	34-43	1.67	0.56	2.20	1.91	0.13	1.57	98.50	96.93	100
50	1Bw	43-53	1.56	0.72	2.00	1.89	0.13	3.23	98.10	94.87	100
50	2Bw	53-63	1.38	0.81	1.74	1.86	0.12	4.54	100.00	95.46	100
50	2Bw	63-73	1.12	1.06	1.31	1.85	0.11	6.64	97.80	91.16	100
50	2Bw	73-83	1.12	1.12	1.23	1.84	0.11	7.37	99.90	92.53	100
50	2Bw	83-93	1.13	1.15	1.16	1.82	0.10	7.66	100.00	92.34	100
50	2Bw	93-103	1.28	1.15	1.28	1.83	0.10	7.14	99.30	92.16	100
50	2Bw	103-113	1.39	1.19	1.25	1.82	0.11	7.09	99.20	92.11	100
50	2Bw	113-123	1.96	1.51	1.28	1.80	0.11	7.23	98.20	90.97	100
50	2Bw	123-133	3.41	2.28	1.27	1.77	0.10	8.81	99.30	90.49	100
50	2Bw	133-150	4.50	2.39	1.05	1.69	0.10	9.76	99.90	90.14	100
50	2C	160-180	5.17	2.72	1.08	1.69	0.11	10.95	100.50	89.55	100

Table 8-E. continued: Soil elemental oxide percent (fine fraction <2mm) with LOI% removed and renormalized to 100% collected from the excavated soil pit at the distance of 50 m in 2009.

distance (m)	horizon	depth (cm)	Hf (ppm)	Zr (ppm)	SiO_2 (%)	Al_2O_3 (%)	Fe_2O_3 (%)	MnO (%)	LOI (%)	total (%)	total-LOI (%)	renormalized (%)
50	A	0-2	1.94	415.16	80.67	9.51	1.94	0.32	18.35	98.80	80.45	100
50	A	2-4	1.89	391.83	81.13	9.63	1.89	0.30	14.80	98.00	83.20	100
50	A	4-6	1.95	428.74	80.92	9.60	1.95	0.41	12.40	99.40	87.00	100
50	A	6-8	1.93	431.60	81.11	9.54	1.93	0.43	9.47	99.60	90.13	100
50	A	8-11	1.84	416.31	81.57	9.49	1.84	0.28	4.30	98.70	94.40	100
50	loess/A	11-18	1.77	411.26	81.94	9.35	1.77	0.09	2.18	99.20	97.02	100
50	loess	18-24	1.76	405.63	82.26	9.20	1.76	0.05	1.56	98.20	96.64	100
50	loess	24-34	1.80	399.92	81.93	9.28	1.80	0.06	0.78	98.30	97.52	100
50	1Bw	34-43	2.30	361.09	80.78	9.82	2.30	0.06	1.57	98.50	96.93	100
50	1Bw	43-53	2.95	290.92	79.58	10.59	2.95	0.08	3.23	98.10	94.87	100
50	2Bw	53-63	3.13	254.56	79.72	10.63	3.13	0.10	4.54	100.00	95.46	100
50	2Bw	63-73	3.92	187.58	78.65	11.30	3.92	0.12	6.64	97.80	91.16	100
50	2Bw	73-83	4.01	165.35	78.46	11.40	4.01	0.14	7.37	99.90	92.53	100
50	2Bw	83-93	4.00	161.36	78.73	11.37	4.00	0.15	7.66	100.00	92.34	100
50	2Bw	93-103	3.85	158.42	78.56	11.23	3.85	0.14	7.14	99.30	92.16	100
50	2Bw	103-113	3.75	162.85	78.82	10.97	3.75	0.15	7.09	99.20	92.11	100
50	2Bw	113-123	3.66	148.40	78.16	10.87	3.66	0.15	7.23	98.20	90.97	100
50	2Bw	123-133	3.44	169.08	76.47	10.56	3.44	0.14	8.81	99.30	90.49	100
50	2Bw	133-150	3.36	158.64	76.21	10.05	3.36	0.17	9.76	99.90	90.14	100
50	2C	160-180	3.53	165.27	74.60	10.36	3.53	0.21	10.95	100.50	89.55	100

Table 8-F. Soil elemental oxide percent (fine fraction <2mm) with LOI% removed and renormalized to 100% collected from the excavated soil pit at the distance of 0 m in 2009.

distance (m)	horizon	depth (cm)	CaO (%)	MgO (%)	Na_2O (%)	K_2O (%)	P_2O_5 (%)	LOI (%)	total (%)	total-LOI (%)	renormalized (%)
0	A	0-2	1.94	0.46	1.54	1.85	0.18	18.35	94.50	76.15	100
0	A	2-4	1.90	0.49	1.53	1.89	0.20	15.85	94.20	78.35	100
0	A	4-6	1.80	0.50	1.78	1.92	0.15	13.95	99.50	85.55	100
0	A	6-8	1.74	0.49	1.81	1.96	0.14	12.55	99.90	87.35	100
0	A	8-10	1.60	0.48	1.84	1.94	0.14	9.84	97.50	87.66	100
0	loess/A	10-18	1.48	0.41	2.21	1.93	0.07	2.40	101.00	98.60	100
0	loess	18-28	1.52	0.41	2.25	1.95	0.08	1.49	101.00	99.51	100
0	loess	28-43	1.54	0.44	2.24	1.97	0.09	1.10	101.00	99.90	100
0	Bw	43-53	1.55	0.61	2.10	1.95	0.11	3.39	99.90	96.51	100
0	Bw	53-63	1.54	0.54	1.99	1.81	0.14	2.58	98.50	95.92	100
0	Bw	63-73	1.61	0.64	2.19	1.88	0.11	2.97	101.00	98.03	100
0	Bw	73-83	1.73	0.69	2.21	1.86	0.13	2.09	97.90	95.81	100
0	Bw	83-94	2.44	1.05	2.26	1.85	0.14	2.83	99.10	96.27	100
0	Bw	94-100	6.02	3.03	2.16	1.72	0.12	7.03	100.00	92.97	100
0	1C	100-107	11.07	2.65	1.21	1.54	0.09	13.40	98.40	85.00	100

Table 8-F. continued: Soil elemental oxide percent (fine fraction <2mm) with LOI% removed and renormalized to 100% collected from the excavated soil pit at the distance of 0 m in 2009.

distance (m)	horizon	depth (cm)	Hf (ppm)	Zr (ppm)	SiO_2 (%)	Al_2O_3 (%)	Fe_2O_3 (%)	MnO (%)	total (%)	total-LOI (%)	renormalized (%)
0	A	0-2	7.35	279.71	82.21	8.69	2.00	0.49	94.50	76.15	100
0	A	2-4	7.53	287.17	81.81	8.97	2.09	0.47	94.20	78.35	100
0	A	4-6	7.95	296.90	81.47	9.26	2.01	0.49	99.50	85.55	100
0	A	6-8	7.33	280.48	81.40	9.31	2.01	0.55	99.90	87.35	100
0	A	8-10	7.30	287.47	81.45	9.30	2.02	0.56	97.50	87.66	100
0	loess/A	10-18	9.53	375.25	82.76	9.05	1.55	0.10	101.00	98.60	100
0	loess	18-28	9.45	365.79	82.81	9.07	1.57	0.05	101.00	99.51	100
0	loess	28-43	9.81	393.39	82.38	9.18	1.71	0.06	101.00	99.90	100
0	Bw	43-53	7.87	321.21	80.30	10.21	2.65	0.04	99.90	96.51	100
0	Bw	53-63	8.44	332.57	81.01	9.89	2.53	0.04	98.50	95.92	100
0	Bw	63-73	7.75	311.13	79.67	10.35	2.81	0.05	101.00	98.03	100
0	Bw	73-83	8.87	353.83	79.43	10.49	2.88	0.05	97.90	95.81	100
0	Bw	83-94	8.62	355.25	79.36	9.93	2.46	0.06	99.10	96.27	100
0	Bw	94-100	8.39	322.68	75.83	8.94	1.94	0.05	100.00	92.97	100
0	1C	100-107	4.35	168.24	70.82	9.21	2.87	0.12	98.40	85.00	100

Table 9-A. Soil elemental oxide percent (fine fraction <2mm) with LOI% included collected from the excavated soil pit at the distance of 190 m in 2009.

distance (m)	depth (cm)	Hf (ppm)	Zr (ppm)	SiO_2 (%)	Al_2O_3 (%)	Fe_2O_3 (%)	CaO (%)	MgO (%)	Na_2O (%)	K_2O (%)	MnO (%)	P_2O_5 (%)	LOI (%)	total (%)
190	0-2	2.3	97	28.4	3.27	0.89	3.68	0.44	0.55	0.73	0.23	0.24	59.9	98.6
190	2-4	3.3	136	34.5	4.18	1.14	3.23	0.45	0.68	0.9	0.3	0.25	53.5	99.4
190	4-7	9	343	71.6	8.09	1.44	1.77	0.45	1.7	1.72	0.23	0.12	11.2	98.9
190	7-11	9.6	360	77.4	8.84	1.47	1.4	0.42	1.87	1.82	0.11	0.11	3.64	97.6
190	11-15	9.9	368	78.2	8.92	1.51	1.41	0.42	1.91	1.84	0.08	0.1	2.84	97.8
190	15-25	9.8	370	76.1	8.65	1.63	1.47	0.44	2.02	1.85	0.04	0.15	1.72	94.6
190	25-35	9.3	354	76.6	8.71	1.62	1.54	0.44	2.08	1.87	0.04	0.11	1.17	94.7
190	35-45	8.4	322	79.5	9.32	1.69	1.64	0.45	2.07	1.82	0.05	0.15	1.06	98.2
190	45-55	8.6	319	74.4	8.61	1.66	1.61	0.45	2.08	1.72	0.04	0.14	1.38	92.5
190	56-71	8.9	346	78.1	9.89	2.37	1.72	0.59	2.03	1.74	0.05	0.15	1.85	99
190	71-83	7.9	305	73.1	10.85	4.14	1.74	0.96	1.81	1.64	0.09	0.18	3.91	98.9
190	83-110	5.6	225	76	9.39	2.81	2.8	1.39	1.72	1.54	0.09	0.12	4.61	101
190	105-130	6.1	238	77.4	8.78	1.96	3	0.95	1.89	1.55	0.08	0.09	3.4	99.5
190	144-156	2.7	99	71.6	8.3	2.12	5.54	1.75	1.53	1.4	0.12	0.08	7.26	100

Table 9-B. Soil elemental oxide percent (fine fraction <2mm) with LOI% included collected from the excavated soil pit at the distance of 160 m in 2009.

distance (m)	depth (cm)	Hf (ppm)	Zr (ppm)	SiO_2 (%)	Al_2O_3 (%)	Fe_2O_3 (%)	CaO (%)	MgO (%)	Na_2O (%)	K_2O (%)	MnO (%)	P_2O_5 (%)	LOI (%)	total (%)
160	0-2	2.2	78	24.2	3.27	1.05	3.68	0.43	0.34	0.65	0.39	0.33	65.6	100
160	2-4	3.5	123	31.8	4.35	1.31	3.21	0.43	0.52	0.87	0.66	0.32	54.1	97.9
160	4-7	6.6	256	52.2	6.71	1.62	2.48	0.46	1.07	1.35	0.78	0.21	30.2	97.6
160	7-9	9.4	374	72.3	8.82	1.83	1.57	0.49	1.61	1.75	0.32	0.16	8.29	97.7
160	9-12	11.1	397	73.6	8.77	1.81	1.5	0.48	1.77	1.86	0.27	0.15	5.03	95.9
160	12-17	10.7	421	76.1	8.84	1.73	1.44	0.48	1.88	1.92	0.17	0.13	3.3	96.6
160	17-25	10.8	414	79.6	9.23	1.87	1.5	0.47	1.96	1.92	0.07	0.12	1.92	99.3
160	25-35	11.3	428	79.3	9.18	1.74	1.54	0.48	1.95	1.91	0.06	0.11	1.7	98.5
160	35-44	NSS	NSS	74.5	9.3	2.47	1.5	0.57	1.8	1.88	0.05	0.14	2.3	95.1
160	44-54	9.3	348	76.3	10.1	2.76	1.59	0.62	1.87	1.82	0.05	0.16	3.04	98.8
160	54-64	7.2	277	78.1	9.6	1.94	1.7	0.51	2.06	1.71	0.05	0.13	1.73	98
160	64-74	7.9	307	76.8	9.62	2.14	1.77	0.57	2.16	1.82	0.05	0.15	2.11	97.7
160	74-84	8.3	324	78.3	10.1	2.41	1.8	0.6	2.07	1.76	0.06	0.14	2.19	99.9
160	84-94	7.8	303	79.3	9.6	2.07	1.76	0.55	2.08	1.73	0.06	0.16	1.82	99.6
160	94-104	9.7	375	77.7	9.58	2.24	1.72	0.59	2.02	1.69	0.06	0.13	1.48	97.7
160	104-114	11.6	432	76.8	9.57	2.63	1.72	0.64	1.94	1.68	0.07	0.11	2.36	98
160	114-126	8.2	319	72.2	8.8	3.59	4.3	2.03	1.93	1.48	0.12	0.12	5.75	101
160	126-140	4.3	158	73.3	8.6	2.32	4.59	2.05	1.9	1.48	0.13	0.09	6.09	101
160	140-167	NSS	NSS	74.3	8.37	2.25	3.33	1.71	1.33	1.53	0.15	0.12	7.07	100.5

Table 9-C. Soil elemental oxide percent (fine fraction <2mm) with LOI% included collected from the excavated soil pit at the distance of 150 m in 2009.

distance (m)	depth (cm)	Hf (ppm)	Zr (ppm)	SiO_2 (%)	Al_2O_3 (%)	Fe_2O_3 (%)	CaO (%)	MgO (%)	Na_2O (%)	K_2O (%)	MnO (%)	P_2O_5 (%)	LOI (%)	total (%)
150	0-2	2.3	85	21.5	2.7	0.76	4.21	0.47	0.34	0.6	0.18	0.32	66.9	98.2
150	2-4	3.6	129	31.6	3.96	1.07	3.51	0.5	0.55	0.84	0.24	0.25	55.3	98.1
150	4-6	5.9	226	51.8	6.29	1.45	2.44	0.49	1.04	1.31	0.31	0.2	32.6	98.4
150	6-8	9.7	418	73.8	8.64	1.71	1.44	0.46	1.7	1.78	0.27	0.14	8.66	99.2
150	8-11	10.8	458	78	8.92	1.63	1.37	0.44	1.85	1.88	0.14	0.1	4.3	99.3
150	11-17	10.6	462	78.6	8.93	1.6	1.4	0.44	1.96	1.9	0.07	0.09	2.33	97.9
150	17-27	10.4	454	79.9	8.85	1.71	1.42	0.42	1.9	1.91	0.06	0.08	1.38	98.2
150	27-37	10.9	472	80.7	9.38	1.83	1.58	0.48	2.1	1.93	0.06	0.1	1.76	100.5
150	37-44	9.4	416	75.2	10.2	2.85	1.56	0.63	1.89	1.83	0.05	0.14	3.4	98.3
150	44-54	9.3	406	77.8	9.89	2.41	1.68	0.58	2.1	1.82	0.05	0.14	2.19	99.2
150	54-64	9.2	401	76.8	10	2.61	1.62	0.61	2.03	1.8	0.05	0.14	2.87	99
150	64-74	9.2	406	76.3	10.4	3.02	1.68	0.67	2.04	1.81	0.05	0.15	3.34	100
150	74-90	7.9	336	78.1	9.84	2.57	1.62	0.62	2.06	1.72	0.05	0.13	2.76	99.9
150	90-100	9.2	400	76.5	10.25	2.92	1.64	0.72	1.98	1.79	0.06	0.14	2.94	99.5
150	100-113	8.4	361	74.6	9.72	2.86	2.57	1.26	1.97	1.72	0.07	0.13	4.31	99.7
150	113-130	4.2	171	77.8	9.08	2.33	2.06	1.12	1.61	1.6	0.1	0.1	4.33	100.5
150	130-160	4.3	185	74.2	7.67	1.76	4	1.52	1.56	1.34	0.12	0.07	5.7	98.2

Table 9-D. Soil elemental oxide percent (fine fraction <2mm) with LOI% included collected from the excavated soil pit at the distance of 100 m in 2009.

distance (m)	depth (cm)	Hf (ppm)	Zr (ppm)	SiO_2 (%)	Al_2O3 (%)	Fe_2O_3 (%)	CaO (%)	MgO (%)	Na_2O (%)	K_2O (%)	MnO (%)	P_2O_5 (%)	LOI (%)	total (%)
100	0-2	7.1	309	53.8	6.47	1.42	2.31	0.44	1.2	1.34	0.48	0.19	32.4	100.5
100	2-4	7.3	319	59.3	7.07	1.55	2.18	0.45	1.34	1.46	0.52	0.18	26.4	101
100	4-6	8.2	346	61.3	7.52	1.7	2.05	0.46	1.38	1.55	0.65	0.2	22	99.4
100	6-9	9.5	410	68.8	8.26	1.82	1.71	0.47	1.59	1.73	0.61	0.16	13.2	99
100	9-14	10.7	455	79	9.01	1.7	1.42	0.45	1.92	1.92	0.12	0.09	3.33	99.6
100	14-21	11	477	79.7	9.16	1.76	1.46	0.47	2	1.93	0.08	0.1	2.06	99.3
100	21-31	11.3	476	80.9	9.27	1.78	1.54	0.48	2.08	1.94	0.06	0.11	1.7	100.5
100	31-41	10.9	482	79.4	9.13	1.78	1.56	0.47	2.09	1.89	0.05	0.11	1.35	98.4
100	41-53	9.1	399	78.5	9.4	2.04	1.62	0.5	2.12	1.84	0.05	0.13	1.75	98.5
100	53-58	8.8	383	76.4	10.2	2.86	1.59	0.62	1.97	1.82	0.05	0.16	3.22	99.4
100	58-68	8.8	375	79.6	9.45	2.14	1.67	0.53	2.16	1.8	0.06	0.13	2.16	100
100	68-77	6.9	295	74.5	11.65	3.01	1.92	0.81	2.62	1.74	0.08	0.14	3.11	100
100	77-87	6.6	291	76.8	10.05	3.16	1.62	0.78	1.97	1.67	0.09	0.12	2.93	99.7
100	87-97	7.3	323	76.9	9.75	3.23	1.45	0.78	1.73	1.64	0.13	0.1	3.58	99.8
100	97-107	4.9	211	76.3	10.1	3.22	1.42	0.86	1.61	1.63	0.11	0.11	4.75	100.5
100	107-123	5.1	219	75.4	10.4	3.25	1.54	0.96	1.68	1.67	0.1	0.12	4.79	100.5
100	123	4.5	190	71.2	9.4	3.12	3.45	2.04	1.4	1.6	0.17	0.12	7.55	100.5

Table 9-E. Soil elemental oxide percent (fine fraction <2mm) with LOI% included collected from the excavated soil pit at the distance of 50 m in 2009.

distance (m)	depth (cm)	Hf (ppm)	Zr (ppm)	SiO_2 (%)	Al_2O_3 (%)	Fe_2O_3 (%)	CaO (%)	MgO (%)	Na_2O (%)	K_2O (%)	MnO (%)	P_2O_5 (%)	LOI (%)	total (%)
50	0-2	1.56	334	64.9	7.65	1.56	1.82	0.48	1.51	1.58	0.26	0.16	18.35	98.8
50	2-4	1.57	326	67.5	8.01	1.57	1.63	0.4	1.6	1.62	0.25	0.16	14.8	98
50	4-6	1.7	373	70.4	8.35	1.7	1.64	0.48	1.68	1.71	0.36	0.15	12.4	99.4
50	6-8	1.74	389	73.1	8.6	1.74	1.55	0.47	1.75	1.78	0.39	0.13	9.47	99.6
50	8-11	1.74	393	77	8.96	1.74	1.46	0.47	1.92	1.89	0.26	0.1	4.3	98.7
50	11-18	1.72	399	79.5	9.07	1.72	1.48	0.46	2.06	1.93	0.09	0.11	2.18	99.2
50	18-24	1.7	392	79.5	8.89	1.7	1.5	0.46	2	1.91	0.05	0.09	1.56	98.2
50	24-34	1.76	390	79.9	9.05	1.76	1.62	0.45	2.17	1.9	0.06	0.12	0.78	98.3
50	34-43	2.23	350	78.3	9.52	2.23	1.62	0.54	2.13	1.85	0.06	0.13	1.57	98.5
50	43-53	2.8	276	75.5	10.05	2.8	1.48	0.68	1.9	1.79	0.08	0.12	3.23	98.1
50	53-63	2.99	243	76.1	10.15	2.99	1.32	0.77	1.66	1.78	0.1	0.11	4.54	100
50	63-73	3.57	171	71.7	10.3	3.57	1.02	0.97	1.19	1.69	0.11	0.1	6.64	97.8
50	73-83	3.71	153	72.6	10.55	3.71	1.04	1.04	1.14	1.7	0.13	0.1	7.37	99.9
50	83-93	3.69	149	72.7	10.5	3.69	1.04	1.06	1.07	1.68	0.14	0.09	7.66	100
50	93-103	3.55	146	72.4	10.35	3.55	1.18	1.06	1.18	1.69	0.13	0.09	7.14	99.3
50	103-113	3.45	150	72.6	10.1	3.45	1.28	1.1	1.15	1.68	0.14	0.1	7.09	99.2
50	113-123	3.33	135	71.1	9.89	3.33	1.78	1.37	1.16	1.64	0.14	0.1	7.23	98.2
50	123-133	3.11	153	69.2	9.56	3.11	3.09	2.06	1.15	1.6	0.13	0.09	8.81	99.3
50	133-150	3.03	143	68.7	9.06	3.03	4.06	2.15	0.95	1.52	0.15	0.09	9.76	99.9
50	160-180	3.16	148	66.8	9.28	3.16	4.63	2.44	0.97	1.51	0.19	0.1	10.95	100.5

Table 9-F. Soil elemental oxide percent (fine fraction <2mm) with LOI% included collected from the excavated soil pit at the distance of 0 m in 2009.

distance (m)	depth (cm)	Hf (ppm)	Zr (ppm)	SiO2 (%)	Al_2O_3 (%)	Fe_2O3 (%)	CaO (%)	MgO (%)	Na_2O (%)	K_2O (%)	MnO (%)	P_2O_5 (%)	LOI (%)	total (%)
0	0-2	5.6	213	62.6	6.62	1.52	1.48	0.35	1.17	1.41	0.37	0.14	18.35	94.5
0	2-4	5.9	225	64.1	7.03	1.64	1.49	0.38	1.2	1.48	0.37	0.16	15.85	94.2
0	4-6	6.8	254	69.7	7.92	1.72	1.54	0.43	1.52	1.64	0.42	0.13	13.95	99.5
0	6-8	6.4	245	71.1	8.13	1.76	1.52	0.43	1.58	1.71	0.48	0.12	12.55	99.9
0	8-10	6.4	252	71.4	8.15	1.77	1.4	0.42	1.61	1.7	0.49	0.12	9.84	97.5
0	10-18	9.4	370	81.6	8.92	1.53	1.46	0.4	2.18	1.9	0.1	0.07	2.4	101
0	18-28	9.4	364	82.4	9.03	1.56	1.51	0.41	2.24	1.94	0.05	0.08	1.49	101
0	28-43	9.8	393	82.3	9.17	1.71	1.54	0.44	2.24	1.97	0.06	0.09	1.1	101
0	43-53	7.6	310	77.5	9.85	2.56	1.5	0.59	2.03	1.88	0.04	0.11	3.39	99.9
0	53-63	8.1	319	77.7	9.49	2.43	1.48	0.52	1.91	1.74	0.04	0.13	2.58	98.5
0	63-73	7.6	305	78.1	10.15	2.75	1.58	0.63	2.15	1.84	0.05	0.11	2.97	101
0	73-83	8.5	339	76.1	10.05	2.76	1.66	0.66	2.12	1.78	0.05	0.12	2.09	97.9
0	83-94	8.3	342	76.4	9.56	2.37	2.35	1.01	2.18	1.78	0.06	0.13	2.83	99.1
0	94-100	7.8	300	70.5	8.31	1.8	5.6	2.82	2.01	1.6	0.05	0.11	7.03	100
0	100-107	3.7	143	60.2	7.83	2.44	9.41	2.25	1.03	1.31	0.1	0.08	13.4	98.4

Table 10-A. Absolute mass losses and gains by depth intervals in A horizons (δ: kg m^{-2}) and A-horizon integrated mass losses and gains (δ: kg m^{-2}) in the soils at the transect distances of 190 and 160 meter. The samples were collected in 2009. The loess cap chemistry was used as a parent material for the A horizon.

distance (m)	depth (cm)	δFe (kg m^{-2})	δSi (kg m^{-2})	δCa (kg m^{-2})	δK (kg m^{-2})	δP (kg m^{-2})	δMg (kg m^{-2})
190	0-2	0.027	0.282	0.200	0.016	0.008	0.007
190	2-4	0.031	0.181	0.162	0.014	0.008	0.006
190	4-7	-0.012	-0.251	0.026	-0.007	0.000	0.001
190	total A horizon δ	0.046	0.211	0.389	0.022	0.015	0.013
160	0-2	0.043	0.383	0.209	0.021	0.012	0.007
160	2-4	0.047	0.347	0.170	0.022	0.011	0.006
160	4-7	0.047	0.236	0.143	0.020	0.008	0.005
160	7-9	0.020	0.104	0.020	0.005	0.003	0.002
160	9-12	0.010	-0.080	0.006	0.006	0.002	0.001
160	12-17	-0.011	-0.339	-0.012	0.001	0.001	0.000
160	total A horizon δ	0.156	0.652	0.537	0.075	0.038	0.022

Table 10-B. Absolute mass losses and gains by depth intervals in A horizons (δ: kg m^{-2}) and A-horizon integrated mass losses and gains (δ: kg m^{-2}) in the soils at the transect distances of 150 and 100 meter. The samples were collected in 2009. The loess cap chemistry was used as a parent material for the A horizon.

distance (m)	depth (cm)	δFe (kg m^{-2})	δSi (kg m^{-2})	δCa (kg m^{-2})	δK (kg m^{-2})	δP (kg m^{-2})	Mg (kg m^{-2})
150	0-2	0.026	0.273	0.242	0.018	0.011	0.008
150	2-4	0.035	0.373	0.190	0.022	0.009	0.008
150	4-6	0.035	0.509	0.105	0.027	0.006	0.006
150	6-8	0.007	0.053	0.005	0.003	0.002	0.001
150	8-11	-0.011	-0.087	-0.010	-0.002	0.001	0.000
150	11-17	-0.030	-0.185	-0.018	-0.003	0.000	-0.001
150	total A horizon δ	0.062	0.936	0.514	0.064	0.029	0.022
100	0-2	0.016	0.067	0.082	0.006	0.005	0.003
100	2-4	0.022	0.221	0.072	0.012	0.004	0.003
100	4-6	0.025	0.117	0.059	0.010	0.005	0.002
100	6-9	0.027	-0.024	0.038	0.007	0.004	0.002
100	total A horizon δ	0.090	0.380	0.251	0.035	0.018	0.010

Table 10-C. Absolute mass losses and gains by depth intervals in A horizons (δ: kg m^{-2}) and A-horizon integrated mass losses and gains (δ: kg m^{-2}) in the soils at the transect distances of 50 and 0 meter. The samples were collected in 2009. The loess cap chemistry was used as a parent material for the A horizon.

distance (m)	depth (cm)	δFe (kg m-2)	δSi (kg m-2)	δCa (kg m-2)	δK (kg m-2)	δP (kg m-2)	Mg (kg m-2)
50	0-2	0.008	-0.153	0.045	-0.004	0.004	0.003
50	2-4	0.012	0.089	0.031	0.004	0.004	0.001
50	4-6	0.005	-0.290	0.016	-0.010	0.003	0.001
50	6-8	0.003	-0.320	0.003	-0.011	0.001	0.001
50	8-11	0.002	-0.215	-0.009	-0.003	-0.001	0.001
50	total A horizon δ	0.030	-0.889	0.087	-0.025	0.011	0.006
0	0-2	0.052	0.920	0.055	0.032	0.005	0.003
0	2-4	0.058	0.856	0.051	0.032	0.006	0.004
0	4-6	0.054	0.814	0.046	0.033	0.004	0.004
0	6-8	0.061	1.007	0.047	0.045	0.004	0.005
0	8-10	0.059	0.936	0.034	0.041	0.004	0.004
0	total A horizon δ	0.283	4.533	0.233	0.183	0.022	0.020

Table 11-A. Exchangeable cation (Ca, K, Mg, Na) concentration (%) for the A horizon soils at transect distances 190, 160, 150, and 100 meter. The samples were collected from the soil pits excavated in 2009.

distance (m)	depth (cm)	K (%)	Ca (%)	Mg (%)	Na (%)
190	0-2	NSS	NSS	NSS	NSS
190	2 - 4	0.05	0.96	0.07	0.003
190	4 - 7	0.01	0.31	0.02	0.001
190	7 - 11	0.01	0.08	0.01	0.001
190	11 - 15	0.01	0.05	0.01	0.000
190	15 - 25	0.01	0.05	0.00	0.001
160	0 - 2	0.06	1.17	0.09	0.003
160	2 - 4	0.05	1.04	0.06	0.004
160	4 - 7	0.03	0.71	0.04	0.003
160	7 - 9	0.02	0.27	0.01	0.001
160	9 - 12	0.01	0.17	0.01	0.001
160	12 - 17	0.01	0.09	0.01	0.001
160	17 - 25	0.01	0.04	0.00	0.000
150	0 - 2	0.06	1.15	0.11	0.003
150	2 - 4	0.06	1.12	0.11	0.003
150	4 - 6	0.04	0.73	0.07	0.003
150	6 - 8	0.01	0.23	0.02	0.002
150	8 -11	0.01	0.12	0.01	0.001
150	11 - 17	0.01	0.08	0.00	0.000
150	17 - 27	0.00	0.06	0.00	0.000
100	0 - 2	0.03	0.73	0.04	0.003
100	2 - 4	0.03	0.68	0.03	0.002
100	4 - 6	0.03	0.55	0.03	0.002
100	6 - 9	0.02	0.45	0.02	0.002
100	9 - 14	0.01	0.12	0.01	0.001
100	14 - 21	0.01	0.08	0.00	0.001

Table 11-B. Soil A horizon exchangeable cation (Ca, K, Mg, Na) concentration (%) for soils collected by excavated soil pits in 2009 at transect distances 50 and 0 meter.

distance (m)	depth (cm)	K (%)	Ca (%)	Mg (%)	Na (%)
50	0 - 2	0.02	0.42	0.04	0.002
50	2 - 4	0.02	0.37	0.03	0.002
50	4 - 6	0.02	0.34	0.03	0.002
50	6 - 8	0.01	0.26	0.02	0.002
50	8 - 11	0.01	0.15	0.01	0.001
50	11 - 18	0.01	0.07	0.01	0.001
50	18 - 24	0.00	0.05	0.00	0.001
0	0 - 2	0.02	0.49	0.03	0.002
0	2 - 4	0.02	0.43	0.03	0.002
0	4 - 6	0.02	0.41	0.02	0.002
0	6 - 8	0.02	0.37	0.02	0.002
0	8 - 10	0.02	0.32	0.02	0.002
0	10 - 18	0.01	0.07	0.01	0.001
0	18 - 28	0.00	0.04	0.01	0.001

Table 12. Exchangeable cation (Ca, K, Mg, Na) concentrations (meq/100g) for the A horizon soils collected in 2006. The soil samples were collected from the soil pits excavated at the transect distances of 190 and 0 meter.

depth (cm)	distance (m)	Exch K (meq/100g)	Exch Ca (meq/100g)	Exch Mg (meq/100g)	Exch Na (meq/100g)	CEC @ pH7 (meq/100g)
0-2.5	0	1.19	20.17	3.18	0.02	35.83
2.5-5	0	1.01	18.59	2.75	0.02	36.81
5-7	0	0.83	13.34	1.88	0.02	30.06
7-10	0	0.54	9.54	1.25	0.02	18.87
10-12	0	0.34	4.79	0.70	0.01	9.72
12-15	0	0.27	3.40	0.53	0.01	5.83
15-17	0	0.25	3.03	0.48	0.01	5.65
17-20	0	0.21	2.34	0.41	0.01	5.26
20-23	0	0.19	1.84	0.34	0.02	3.86
23-30	0	0.15	1.56	0.29	0.02	3.70
30-37	0	0.15	1.41	0.28	0.01	3.03
37-46	0	0.27	3.50	0.92	0.02	7.21
46-60	0	1.04	11.24	3.15	0.04	26.97
60-90	0	1.17	12.46	3.66	0.03	29.50
90-120	0	0.99	11.98	3.59	0.04	29.87
120-150	0	0.28	3.55	1.00	0.06	6.28
225-235	0	0.16	1.78	0.62	0.19	4.73
0-2.5	190	0.75	25.66	3.60	0.03	54.14
2.5-5	190	0.45	6.69	0.86	0.02	11.88
5-7.5	190	0.23	3.32	0.46	0.01	6.28
7.5-10	190	0.17	2.25	0.33	0.01	5.00
10-12.5	190	0.16	2.15	0.35	0.01	4.39
12.5-15	190	0.15	2.10	0.32	0.01	4.09
15-17.5	190	0.15	2.04	0.30	0.01	3.86
17.5-20	190	0.13	1.83	0.28	0.03	-
20-25	190	0.12	1.78	0.30	0.05	-
25-30	190	0.13	1.86	0.44	0.02	-
30-53	190	0.48	10.38	3.87	0.06	29.52
53-77	190	0.54	10.49	4.04	0.09	34.29
77-97	190	0.51	13.97	5.60	0.12	37.70
97-120	190	0.39	15.49	6.22	0.14	40.54

Table 13. The depth profiles of ^{210}Pb activities (Bq/g) for the soils excavated at transect distance 190 and 0 meter in 2006. ^{210}Pb activities were measured with a gamma spectrometer.

distance (m)	depth (cm)	^{210}Pb (Bq/g)	recovery rate
0	0-2.5	0.0646	0.2874
0	2.5-5	0.0512	0.3163
0	5-7	0.0323	0.2804
0	7-10	0.013	0.54
0	10-12	0.00679	0.4344
0	12-15	0.00358	0.6366
0	15-17	0.00376	0.849
0	17-20	0.00294	0.705
0	20-23	0.002	0.776
0	23-30	0.00213	0.764
0	30-37	0.00275	0.5845
0	37-46	0.00366	0.4641
0	46-60	0.004899	0.2955
0	60-90	0.00384	0.4285
0	90-120	0.00212	0.3224
0	120-150	0.00607	0.3895
0	225-235	0.00298	0.783
190	0-2.5	0.15	0.806
190	2.5-5	0.0115	0.8541
190	5-7.5	0.00221	0.5008
190	7.5-10	0.00243	0.8881
190	10-12.5	0.00308	0.9893
190	12.5-15	0.0023	0.8147
190	15-17.5	0.00167	0.876
190	17.5-20	0.00178	0.8999
190	20-25	0.0029	0.7895
190	25-30	0.00359	0.6765
190	30-53	0.00397	0.7978
190	53-77	0.00568	0.6628
190	77-97	0.00975	0.5861
190	97-120	0.007335	0.3078

Table 14. The depth profiles of ^{137}Cs (cpm/g) for the soils excavated at transect distance 190, 160, and 150 meter in 2009. ^{137}Cs activities were measured with a gamma spectrometer well detector.

distance (m)	depth (cm)	energy keV	fwhm	live acquisition	acquisition time (hr)	net peak area @ 661 kev	net peak uncertainty	relative uncertainty	sample weight (g)	137-Cs cpm/g
190	0-2	661.46	1.79	86400	24	4230.00	75.33	0.02	2.7	0.0181
190	2-4	661.42	1.79	86400	24	4580.00	75.52	0.02	2.7	0.0196
190	4-7	661.54	1.85	86400	24	433.00	40	0.09	2.7	0.0019
190	7-11	661.3	NA	86400	24	250	-	-	2.7	0.0011
190	11-15	*	NA	86400	24	-	-	-	2.7	-
160	0-2	661.3	NA	86400	24	2384.00	NA	-	2.7	0.0102
160	2-4	661.3	NA	86400	24	1752.00	NA	-	2.7	0.0075
160	4-7	661.33	1.75	86400	24	1300.00	56.6	0.04	2.7	0.0056
160	7-9	661.49	1.57	86400	24	268.00	35.35	0.13	2.7	0.0011
160	9-12	661.3	NA	86400	24	239	NA	-	2.7	0.0010
160	12-17	661.3	NA	86400	24	255	NA	-	2.7	0.0011
160	17-25	*	NA	86400	-	-	-	-	2.7	-
150	0-2	661.48	1.76	86400	24	3790.00	71.7	0.02	2.7	0.0162
150	2-4	661.53	1.81	86400	24	4970.00	81.23	0.02	2.7	0.0213
150	6-8	661.37	1.58	86400	24	273.00	35.73	0.13	2.7	0.0012
150	8-10	661.39	1.51	86400	24	652.00	42.91	0.07	2.7	0.0028
150	11-17	*	-	-	-	-	-	-	2.7	-
150	17-27	*	-	-	-	-	-	-	2.7	-

*MDA=minimum detectable activity

Table 14. continued: The depth profiles of ^{137}Cs (cpm/g) for the soils excavated at transect distance 100, 50, and 0 meter in 2009. ^{137}Cs activities were measured with a gamma spectrometer well detector.

distance (m)	depth (cm)	energy keV	fwhm	live acquisition	acquisition time (hr)	net peak area @ 661 kev	net peak uncertainty	relative uncertainty	sample weight (g)	137-Cs cpm/g
100	0-2	661.34	1.63	86400	24	2010.00	62.76	0.03	2.7	0.0086
100	2-4	661.3	1.59	86400	24	1.86E+03	61.82	0.03	2.7	0.0080
100	4-6	661.32	1.62	86400	24	1.41E+03	54.46	0.04	2.7	0.0060
100	6-9	661.37	1.74	86400	24	7.14E+02	47.82	0.07	2.7	0.0031
100	9-14	660.4	1.6	86400	24	1.70E+03	54.03	0.03	2.7	0.0073
100	14-21	*	-	-	-	-	-	-	2.7	-
100	21-31	*	-	-	-	-	-	-	2.7	-
50	0-2	661.37	1.69	86400	24	859.00	44.09	0.05	2.7	0.0037
50	2-4	661.32	1.73	86400	24	984.00	49.19	0.05	2.7	0.0042
50	4-6	661.35	1.78	86400	24	862.00	48.25	0.06	2.7	0.0037
50	6-8	661.36	1.87	86400	24	695.00	46.56	0.07	2.7	0.0030
50	8-11	660.27	1.53	86400	24	321.00	40.37	0.13	2.7	0.0014
50	11-18	*	-	-	-	-	-	-	-	-
50	18-24	*	-	-	-	-	-	-	-	-
50	24-34	*	-	-	-	-	-	-	-	-
0	0-2	661.5	1.65	86400	24	925.00	52.72	0.06	2.7	0.0040
0	2-4	661.51	1.74	86400	24	879.00	44.97	0.05	2.7	0.0038
0	4-6	661.63	1.79	86400	24	1050.00	51.05	0.05	2.7	0.0045
0	6-8	661.54	1.61	86400	24	798.00	47.32	0.06	2.7	0.0034
0	8-10	660.49	1.5	86400	24	649.00	43.91	0.07	2.7	0.0028
0	10-18	661.3	NA	86400	24	242	NA		2.7	0.0010
0	18-28	*	-	-	-	-	-	-	2.7	-

Table 15. The depth profiles (0-5cm and 5+ cm) of ^{137}Cs (cpm/g) for the soils excavated with a hammer auger along the B transect in 2011. ^{137}Cs activities were measured with a gamma spectrometer well detector.

plot	distance (m)	depth (cm)	energy keV	fwhm	live acquisition (s)	acquisition time (hr)	net peak area @ 661 keV	net peak uncertainty	relative uncertainty	sample weight (g)	137-Cs cpm/g
B1	0	0-5	661.29	1.64	86400	24	8.41E+02	46.27	0.06	2.7	0.00361
B2	20	0-5	660.26	1.53	86400	24	8.42E+02			2.7	0.00361
B3	30	0-5	660.22	1.64	86400	24	9.27E+02	48.25	0.05	2.7	0.00397
B4	40	0-5	660.4	1.6	86400	24	7.22E+02	44.42	0.06	2.7	0.00309
B5	50	0-5	660.15	1.63	86400	24	9.09E+02	46.06	0.05	2.7	0.00390
B6	60	0-5	661.4	1.74	86400	24	8.37E+02	43.09	0.05	2.7	0.00359
B7	70	0-5	661.39	1.57	86400	24	9.79E+02	42.8	0.04	2.7	0.00420
B8	80	0-5	661.41	1.59	86400	24	1.02E+03	49.44	0.05	2.7	0.00437
B9	90	0-5	661.38	1.62	86400	24	1.62E+03	56.87	0.04	2.7	0.00694
B10	100	0-5	661.39	1.68	86400	24	1.20E+03	49.72	0.04	2.7	0.00514
B12	120	0-5	661.33	1.59	86400	24	9.52E+02	53.61	0.06	2.7	0.00408
B13	130	0-5	660.07	1.54	86400	24	4.02E+02	42.55		2.7	0.00172
B14	140	0-6	661.42	1.7	86400	24	1.19E+03	53.51	0.04	2.7	0.00510
B15	150	0-5	661.43	1.81	86400	24	1.53E+03	58.57	0.04	2.7	0.00656
B16	160	0-5	661.42	1.74	86400	24	1.60E+03	56.43	0.04	2.7	0.00686
B17	170	0-5	661.76	1.58	86400	24	2.64E+03	59.94	0.02	2.7	0.01132
B18	180	0-6	660.16	1.56	86400	24	1.98E+03	57.8	0.03	2.7	0.00849

Table 16. Estimated optically stimulated luminescence (OSL) ages of quartz grains (kyr) for the soils excavated at transect distances 190 and 0 meter in 2009. OSL measurements were made with a Risø TL/OSL DA-15.

distance (m)	depth (cm)	OSL BIN File	analysis type	disc-grain	paleodose (sec)	±	recycling ratio	est. kyr
190	8	Worm3_80cm_SG-5d.BIN	SG	1-27	256.54	110.3	0.81	9.2
190	8	Worm3_80cm_SG-5d.BIN	SG	1-30	55.93	29.48	1.06	2.0
190	8	Worm3_80cm_SG-5d.BIN	SG	1-31	0		0.8	0.0
190	8	Worm3_80cm_SG-5d.BIN	SG	1-36	263.78	53.99	1.59	9.4
190	8	Worm3_80cm_SG-5d.BIN	SG	1-37	231.73	215.7	1.78	8.3
190	8	Worm3_80cm_SG-5d.BIN	SG	1-39	195.89	91.14	0.92	7.0
190	8	Worm3_80cm_SG-5d.BIN	SG	1-46	180.85	43.69	1.14	6.5
190	8	Worm3_80cm_SG-5d.BIN	SG	1-55	131.53	12.96	0.94	4.7
190	8	Worm3_80cm_SG-5d.BIN	SG	1-56	88.94	7.66	1.36	3.2
190	8	Worm3_80cm_SG-5d.BIN	SG	1-60	341.63	451.9	0.74	12.2
190	8	Worm3_80cm_SG-5d.BIN	SG	4-34	186.3	72.44	1	6.7
190	8	Worm3_80cm_SG-5d.BIN	SG	4-42	15	20.01	0.62	0.5
190	8	Worm3_80cm_SG-5d.BIN	SG	4-44	1.84	8.35	0.82	0.1
190	8	Worm3_80cm_SG-5d.BIN	SG	4-54	67.98	7.31	1.36	2.4
190	8	Worm3_80cm_SG-5d.BIN	SG	4-56	193.32	93.77	0.72	6.9
190	8	Worm3_80cm_SG-5d.BIN	SG	4-82	213.84	47.57	0.74	7.6
190	8	Worm3_80cm_SG-5d.BIN	SG	4-84	37.01	9.18	0.6	1.3

Table 16. continued: Estimated optically stimulated luminescence (OSL) ages of quartz grains (kyr) for the soils excavated at transect distances 190 and 0 meter in 2009. OSL measurements were made with a Risø TL/OSL DA-15.

distance (m)	depth (cm)	OSL BIN File	analysis type	disc-grain	paleodose (sec)	±	recycling ratio	est. kyr
190	8	Worm3_30cm_SG-5d.BIN	single grain	4-10	79.68	27.67	0.62	2.9
190	8	Worm3_30cm_SG-5d.BIN	single grain	4-30	260.07	62.86	1.18	9.3
190	8	Worm3_30cm_SG-5d.BIN	single grain	4-39	255.98	15.18	0.96	9.2
190	8	Worm3_30cm_SG-5d.BIN	single grain	4-44	110.92	49.02	0.73	4.0
190	8	Worm3_30cm_SG-5d.BIN	single grain	4-45	149.34	55.31	1.03	5.3
190	8	Worm3_30cm_SG-5d.BIN	single grain	4-50	89.06	68.37	0.62	3.2
190	8	Worm3_30cm_SG-5d.BIN	single grain	4-59	91.75	40.79	1.32	3.3
190	8	Worm3_30cm_SG-5d.BIN	single grain	4-66	178.7	27.51	0.76	6.4
190	8	Worm3_30cm_SG-5d.BIN	single grain	4-68	113.97	85.44	1.31	4.1
190	8	Worm3_30cm_SG-5d.BIN	single grain	4-79	228.78	46.57	0.65	8.2
190	8	Worm3_30cm_SG-5d.BIN	single grain	4-85	118.51	87.17	1.75	4.2
190	8	Worm3_30cm_SG-5d.BIN	single grain	4-89	121.88	63.3	1.02	4.4
190	8	Worm3_30cm_SG-5d.BIN	single grain	4-90	0	11.44	1.08	0.0
190	8	Worm3_30cm_SG-5d.BIN	single grain	7-4	250.48	57.77	0.78	9.0
190	8	Worm3_30cm_SG-5d.BIN	single grain	7-24	164.55	28.37	0.81	5.9
190	8	Worm3_30cm_SG-5d.BIN	single grain	7-41	506.77	195	1.48	18.1
190	8	Worm3_30cm_SG-5d.BIN	single grain	7-45	63.7	24.59	1.09	2.3
190	8	Worm3_30cm_SG-5d.BIN	single grain	7-58	88.86	72.29	0.96	3.2
190	8	Worm3_30cm_SG-5d.BIN	single grain	7-61	361.67	34.87	0.89	12.9
190	8	Worm3_30cm_SG-5d.BIN	single grain	7-78	198.01	146.1	1.58	7.1
190	8	Worm3_30cm_SG-5d.BIN	single grain	7-81	315.63	57.11	1.33	11.3
190	8	Worm3_30cm_SG-5d.BIN	single grain	7-91	84.91	13.17	0.86	3.0
190	8	Worm3_30cm_SG-5d.BIN	single grain	7-98	197.25	29.49	0.91	7.1

Table 16. continued: Estimated optically stimulated luminescence (OSL) ages of quartz grains (kyr) for the soils excavated at transect distances 190 and 0 meter in 2009. OSL measurements were made with a Risø TL/OSL DA-15.

distance (m)	depth (cm)	OSL BIN File	analysis type	disc-grain	paleodose (sec)	±	recycling ratio	est. kyr
190	8	Worm3_30cm_SG-5d.BIN	single grain	13-31	540.48	358	1.41	19.3
190	8	Worm3_30cm_SG-5d.BIN	single grain	13-34	252.76	41.6	0.89	9.0
190	8	Worm3_30cm_SG-5d.BIN	single grain	13-46	189.86	52.83	0.67	6.8
190	8	Worm3_30cm_SG-5d.BIN	single grain	13-55	181.31	54.39	0.84	6.5
190	8	Worm3_30cm_SG-5d.BIN	single grain	13-66	371.29	185.6	1.32	13.3
0	50	Worm8_50cm_SG-5d_II_III_combined.BIN	single grain	1-1	139.76	26.17	1.25	4.8
0	50	Worm8_50cm_SG-5d_II_III_combined.BIN	single grain	1-6	689.14	433.7	0.97	23.7
0	50	Worm8_50cm_SG-5d_II_III_combined.BIN	single grain	1-27	288.07	229	1.37	9.9
0	50	Worm8_50cm_SG-5d_II_III_combined.BIN	single grain	1-46	531.14	162.8	0.81	18.3
0	50	Worm8_50cm_SG-5d_II_III_combined.BIN	single grain	1-60	185.99	49.31	0.82	6.4
0	50	Worm8_50cm_SG-5d_II_III_combined.BIN	single grain	1-85	143.86	32.32	0.84	5.0
0	50	Worm8_50cm_SG-5d_II_III_combined.BIN	single grain	1-99	234.52	31.93	1	8.1
0	50	Worm8_50cm_SG-5d_II_III_combined.BIN	single grain	4-43	311.96	141.4	0.94	10.7
0	50	Worm8_50cm_SG-5d_II_III_combined.BIN	single grain	4-54	185.25	52.42	0.86	6.4
0	50	Worm8_50cm_SG-5d_II_III_combined.BIN	single grain	4-67	448.95	328.1	0.83	15.4
0	50	Worm8_50cm_SG.BIN	single grain	7-45	418.79	209.6	0.6	14.4
0	50	Worm8_50cm_SG.BIN	single grain	7-47	0	71.79	0.63	0.0
0	50	Worm8_50cm_SG.BIN	single grain	7-54	169.38	66.42	1.37	5.8
0	50	Worm8_50cm_SG.BIN	single grain	19-5	0	11.12	0.54	0.0
0	50	Worm8_50cm_SG.BIN	single grain	19-11	-5.08	6.96	1.47	-0.2
0	50	Worm8_50cm_SG.BIN	single grain	'19-12	14.66	7.35	1.27	0.5
0	50	Worm8_50cm_SG.BIN	single grain	19-15	48.51	9.46	0.77	1.7

Table 16. continued: Estimated optically stimulated luminescence (OSL) ages of quartz grains (kyr) for the soils excavated at transect distances 190 and 0 meter in 2009. OSL measurements were made with a Risø TL/OSL DA-15.

distance (m)	depth (cm)	OSL BIN File	analysis type	disc-grain	paleodose (sec)	±	recycling ratio	est. kyr
0	50	Worm8_50cm_SG.BIN	single grain	19-16	58.71	19.9	1.29	2.0
0	50	Worm8_50cm_SG.BIN	single grain	19-24	11.96	8.24	0.63	0.4
0	50	Worm8_50cm_SG.BIN	single grain	19-27	67.52	24.93	0.94	2.3
0	50	Worm8_50cm_SG.BIN	single grain	19-28	52.14	24.77	0.91	1.8
0	50	Worm8_50cm_SG.BIN	single grain	19-30	57.09	30.7	0.64	2.0
0	50	Worm8_50cm_SG.BIN	single grain	19-34	79.28	30.66	0.84	2.7
0	50	Worm8_50cm_SG.BIN	single grain	19-38	397.79	294.8	0.71	13.7
0	50	Worm8_50cm_SG.BIN	single grain	19-42	68.18	72.42	0.87	2.3
0	50	Worm8_50cm_SG.BIN	single grain	19-54	0	34.3	1.27	0.0
0	50	Worm8_50cm_SG.BIN	single grain	19-68	51.61	26.73	0.89	1.8
0	50	Worm8_50cm_SG.BIN	single grain	19-73	0	15.65	0.85	0.0
0	50	Worm8_50cm_SG.BIN	single grain	19-75	24.92	8.69	0.99	0.9
0	50	Worm8_50cm_SG.BIN	single grain	19-76	71.71	20.02	1.34	2.5
0	50	Worm8_50cm_SG.BIN	single grain	19-86	0	8.31	1.01	0.0
0	50	Worm8_50cm_SG.BIN	single grain	19-87	19.79	3.56	1.13	0.7
0	50	Worm8_50cm_SG.BIN	single grain	19-90	45.64	24.18	1.37	1.6
0	50	Worm8_50cm_SG.BIN	single grain	19-92	-1.24	20.5	0.8	0.0
0	50	Worm8_50cm_SG.BIN	single grain	19-95	167.34	7.44	0.84	5.8
0	50	Worm8_50cm_SG.BIN	single grain	19-97	75.45	14.57	0.92	2.6
0	50	Worm8_50cm_SG.BIN	single grain	19-98	129.47	91.53	1.25	4.5
0	50	Worm8_50cm_SG_IV.BIN	single grain	1-7	267.64	86.77	1.14	9.2
0	50	Worm8_50cm_SG_IV.BIN	single grain	1-50	314.22	92.85	0.76	10.8
0	50	Worm8_50cm_SG_IV.BIN	single grain	1-85	553.49	258.7	0.65	19.0
0	50	Worm8_50cm_SG_IV.BIN	single grain	1-99	0	20.51	1.48	0.0

Table 16. continued: Estimated optically stimulated luminescence (OSL) ages of quartz grains (kyr) for the soils excavated at transect distances 190 and 0 meter in 2009. OSL measurements were made with a Risø TL/OSL DA-15.

distance (m)	depth (cm)	OSL BIN File	analysis type	disc-grain	paleodose (sec)	±	recycling ratio	est. kyr
0	97	Worm8_97cm_SG-4d.BIN	single grain	10-35	212.91	7.2	0.98	8.5
0	97	Worm8_97cm_SG-4d.BIN	single grain	10-93	7.19	5.36	1.29	0.3
0	97	Worm8_97cm_SG-4d.BIN	single grain	13-34	256	112.9	1.06	10.2
0	97	Worm8_97cm_SG-4d.BIN	single grain	13-77	108.41	63.65	1.1	4.3
0	97	Worm8_97cm_SG-4d.BIN	single grain	13-85	0	33.84	0.9	0.0
0	97	Worm8_97cm_SG-4d.BIN	single grain	16-3	13.59	14.54	1.16	0.5
0	97	Worm8_97cm_SG-4d.BIN	single grain	16-13	-12.68	7.57	1.13	-0.5
0	97	Worm8_97cm_SG-4d.BIN	single grain	16-14	171.94	66.58	1.14	6.9
0	97	Worm8_97cm_SG-4d.BIN	single grain	16-84	125.68	209.3	1.05	5.0
0	97	Worm8_97cm_SG-6d.BIN	single grain	4-24	288.34	94.23	0.88	11.5
0	97	Worm8_97cm_SG-6d.BIN	single grain	4-32	129.06	153.8	0.96	5.1
0	97	Worm8_97cm_SG-6d.BIN	single grain	4-36	242.92	51.09	0.69	9.7
0	97	Worm8_97cm_SG-6d.BIN	single grain	4-37	395.08	516.9	1.14	15.8
0	97	Worm8_97cm_SG-6d.BIN	single grain	4-40	219.7	58.1	1.14	8.8
0	97	Worm8_97cm_SG-6d.BIN	single grain	4-49	316.76	85.04	0.58	12.6
0	97	Worm8_97cm_SG-6d.BIN	single grain	4-58	203.6	43.45	0.84	8.1
0	97	Worm8_97cm_SG-6d.BIN	single grain	4-84	147.43	29.36	0.73	5.9
0	97	Worm8_97cm_SG-6d.BIN	single grain	4-85	268.81	76	0.84	10.7
0	97	Worm8_97cm_SG-6d.BIN	single grain	4-95	190.55	44.08	0.77	7.6

Table 16. continued: Estimated optically stimulated luminescence (OSL) ages of quartz grains (kyr) for the soils excavated at transect distances 190 and 0 meter in 2009. OSL measurements were made with a Risø TL/OSL DA-15.

distance (m)	depth (cm)	OSL BIN File	analysis type	disc-grain	paleodose (sec)	±	recycling ratio	est. kyr
0	97	Worm8_97cm_SG-6d.BIN	single grain	7-29	299.91	198.6	1.13	12.0
0	97	Worm8_97cm_SG-6d.BIN	single grain	7-37	163.04	52.56	0.64	6.5
0	97	Worm8_97cm_SG-6d.BIN	single grain	7-52	228.01	125.5	0.92	9.1
0	97	Worm8_97cm_SG-6d.BIN	single grain	7-58	192.81	80.27	0.61	7.7
0	97	Worm8_97cm_SG-6d.BIN	single grain	7-69	185.52	56.32	1.15	7.4
0	97	Worm8_97cm_SG-6d.BIN	single grain	7-73	188.19	21.02	1.37	7.5
0	97	Worm8_97cm_SG-6d.BIN	single grain	7-80	273.98	210.9	0.77	10.9
0	97	Worm8_97cm_SG-6d.BIN	single grain	7-81	204.29	105.2	0.69	8.1
0	97	Worm8_97cm_SG-6d.BIN	single grain	10-10	306.02	91	0.88	12.2
0	97	Worm8_97cm_SG-6d.BIN	single grain	10-11	250.36	87.84	1.02	10.0
0	97	Worm8_97cm_SG-6d.BIN	single grain	10-17	219.24	23.01	1.13	8.7
0	97	Worm8_97cm_SG-6d.BIN	single grain	10-19	147.64	29.43	0.75	5.9
0	97	Worm8_97cm_SG-6d.BIN	single grain	10-36	114.92	69.7	0.61	4.6
0	97	Worm8_97cm_SG-6d.BIN	single grain	10-42	227.69	23.24	1.17	9.1
0	97	Worm8_97cm_SG-6d.BIN	single grain	10-63	211.61	11.73	1.03	8.4
0	97	Worm8_97cm_SG-6d.BIN	single grain	10-74	551.47	274.6	1.19	22.0
0	97	Worm8_97cm_SG-6d.BIN	single grain	10-75	229.07	98.41	1.01	9.1
0	97	Worm8_97cm_SG-6d.BIN	single grain	10-88	139.05	46.68	0.63	5.5
0	97	Worm8_97cm_SG-6d.BIN	single grain	13-28	0	6.09	0.89	0.0
0	97	Worm8_97cm_SG-6d.BIN	single grain	13-66	62.59	26.69	0.81	2.5
0	97	Worm8_97cm_SG-6d.BIN	single grain	13-80	0	110.2	0.45	0.0

Table 16. continued: Estimated optically stimulated luminescence (OSL) ages of quartz grains (kyr) for the soils excavated at transect distances 190 and 0 meter in 2009. OSL measurements were made with a Risø TL/OSL DA-15.

distance (m)	depth (cm)	OSL BIN File	analysis type	disc-grain	paleodose (sec)	±	recycling ratio	est. kyr
0	97	Worm8_97cm_SG-6d.BIN	single grain	16-35	205.28	63.63	0.97	8.2
0	97	Worm8_97cm_SG-6d.BIN	single grain	16-68	274.41	285.6	0.64	10.9
0	97	Worm8_97cm_SG-6d.BIN	single grain	16-99	-23.15	2.06	1.21	-0.9
0	105	Worm8_105cm_SG-7d.BIN	single grain	1-23	246.21	70.6	0.81	10.8
0	105	Worm8_105cm_SG-7d.BIN	single grain	1-34	221.36	48.88	0.84	9.7
0	105	Worm8_105cm_SG-7d.BIN	single grain	1-55	101.89	48.99	1.3	4.5
0	105	Worm8_105cm_SG-7d.BIN	single grain	4-66	144.63	100.1	0.81	6.4
0	105	Worm8_105cm_SG-7d.BIN	single grain	4-77	380.85	32.45	1.14	16.7
0	105	Worm8_105cm_SG-7d.BIN	single grain	7-54	51.26	41.14	1.23	2.3
0	105	Worm8_105cm_SG-7d.BIN	single grain	10-3	0	27.66	1.15	0.0
0	105	Worm8_105cm_SG-7d.BIN	single grain	10-9	646.28	155.1	0.83	28.4
0	105	Worm8_105cm_SG-7d.BIN	single grain	10-30	940.82	211.4	0.95	41.3
0	105	Worm8_105cm_SG-7d.BIN	single grain	10-36	386.77	220.9	1.02	17.0
0	105	Worm8_105cm_SG-7d.BIN	single grain	10-65	468.73	227.2	0.77	20.6
0	105	Worm8_105cm_SG-7d.BIN	single grain	10-74	331.75	96.46	1.36	14.6
0	105	Worm8_105cm_SG-7d.BIN	single grain	16-17	0	36.18	1.77	0.0
0	105	Worm8_105cm_SG-7d.BIN	single grain	19-10	603.14	262.4	1.26	26.5
0	105	Worm8_105cm_SG-7d.BIN	single grain	19-19	190.97	324.6	0.71	8.4
0	105	Worm8_105cm_SG-7d.BIN	single grain	19-50	353.45	121.2	0.67	15.5

Lab Procedures

OSL sample measurements

OSL measurements were made at depths 8 and 100 cm for the pit at transect distance 190 m, and 20, 50, 97 and 105 cm depths for the pit at transect distance 0 m.. Estimated OSL ages were used to determine the ages of different soil horizons and their parent materials.

OSL sample outline:

Transect distance 190m, 8cm depth: timing of aeolian deposit
Transect distance 190m, 100cm depth: timing of glacial deposit
Transect distance 0m, 20cm depth: timing of aeolian deposit
Transect distance 0m, 50cm depth: aeolian or glacial derivation
Transect distance 0m, 97cm depth: timing of glacial deposit
Transect distance 0m, 105cm depth: timing of glacial deposit

Single grain soil ages were estimated with optically stimulated luminescence (OSL) measurements using the SG (single grain) and SAR (single aliquot regeneration) protocol at the Physical Laboratory in Ahmedabad, India, in Dr. Ashok Singhvi's lab. All samples outlined above were processed under red light conditions. The ends of each OSL sample tube were removed, and the inner portion of the tube was treated with 1 N HCl to remove carbonates. After the samples no longer reacted with HCl, the soil was washed with deionized water and treated with H_2O_2 to remove organic matter. The samples were washed, dried, and hand-sieved to for the 150-210 µm size fraction. The samples were magnetically separated, and the quartz fraction was etched using a 40% hydrofluoric acid for 70 minutes to remove feldspars. The etched quartz grains were dusted onto single grain discs (~100 grains/disc) and tested for feldspar contamination by exposure to infra-red light. A Risø TL/OSL DA-15 reader fitted with a blue diode array was used for OSL measurements. Measurement results were processed with using Risø Luminescence Analyst software (v. 3.22b).

Cs-137 measurements

To investigate soil mixing, ^{137}Cs radioactivity was determined across the earthworm invasion transect from the least invaded soils at 190, 160, and 150 to the most invaded soils at distances 100, 50, and 0 meter. Dried soils were sieved into the coarse (>2mm) and fine fraction (<2mm). The fine fraction was homogenized and 2.7 grams were sampled into a 4 dram vial. One sample was counted per day in a Canberra well-type Ge gamma spectrometer and multichannel analyzer for 24 hours to minimize counting error. The well detector energy calibration was performed according to the Canberra Genie 2000 Tutorials Manual. Net peak area was obtained by performing a peak locate and peak area analysis using Genie 2000 software. Counts per minute (cpm) were calculated by dividing peak area for the 137-Cs peak (661.3 keV) by the sample live acquisition time (86400 s) and sample weight (2.7 g).

Fine fraction soils (<2mm) from 2009 were run from all pits down to depths of 30 centimeters (Table 14). In 2011 soil auger corers were used to collect cores every ten meters along the transect adjacent to earthworm sampling plots. The cores were split into an upper A (0-5cm), a lower A (5- ~10cm), and loess parent materials (~10+ cm). Soils were air dried and sieved into fine and coarse fragments. 2.7 grams of the fine fraction were run for 127-Cs using the same procedure and instrument as the 2009 samples (Table 15). The loess parent material samples were collected and run, but did not have 137-Cs activity above the MDA (minimum detectable activity).

Iron oxide extractions procedure
Used by Resner in 2010
Author: Junling Ji, University of Delaware, 2008

Sodium Pyrophosphate Extraction

Extraction of Al and Fe

1. Weigh 0.5g (record exact weight m1) <2-mm or fin-grind, oven-dry soil and place in a marked 50-mL centrifuge tube.

2. Add 30-mL of 0.1M $Na_4P_2O_7$, pH 10.0 solutions to centrifuge tube.

3. Cap tube and shake briefly by hand to dislodge soil from tube bottom. Place tube in rack.

4. Place tubes in shaker and shake overnight (12 to 16h) at 200 oscillations min^{-1} at room temperature (20 ºC±2 ºC).

5. Remove tubes from shaker and manually shake tubes to dislodge any soil from cap. Allow samples to sit overnight.

6. Next day centrifuge sample at 4000rpm for 15min.

7. Measure the volume of suspension V by graduated flaks and transfer the sample into sample bottle from centrifuge tube.

8. The Fe and Al are determined from the clear solution. Filter if necessary.

Dilution of Sample Extracts and Standards for ICP-AES analysis

1. Dilute extracts (1:10) with RODI water. Add 1 part sample extract with 9 parts dilution solution. Pipet 0.7 mL of extract and 6.3 mL RODI water into test tube.

2. Send the samples with matrix to Roger at the University of Minnesota Research Analytical Lab

Reagents:
$Na_4P_2O_7$, Sodium pyrophosphate solution, 0.1 M. Dissolve 44.6g$Na_4P_2O_7 \cdot 10H_2O$ in 1L of RODI water.

Equipment:
Balance, 22 test tubes, dispenser (30mL), dropping tube, shaker, centrifuge,

Calculation:

Convert analyte concentrations (mg/L) to percent in soil as follows:
Soil Fe, Al (%) =(A×B×C×R×100)/(E×1000)

Where:
A = Sample extract reading (mg/L)
B = Extract Volume (L)
C =Dilution, required (I used 10 here)
R =Air-dry/oven-dry ratio (procedure 3D1 from SSL)
E =Sample weight (g)
100 =Conversion factor to 100-g basis
1000=mg/g

Dithionite Citrate Extraction (SSL 4G1)

Procedures:
Measurement of R air-dry/oven-dry ratio (SSL 3D1)

1. Mark crucible, weigh and record *m*.

2. Weigh 10~20g (record the exact weight *m1*) of <2-mm or fine-grand, air-dry soil sample and place in the marked crucible, cover the crucible with the lid and heat in the oven at 110ºC for 12 hours.

3. Weigh again (with crucible) within 30minutes, record the exact weight *m2*.

4. Calculate the air-dry/oven-dry ratio R as m1/(m2-m)

Note: R value is needed in calculation of three extraction methods.

Extraction of Al and Fe (SSL 4G1)

1. Weight 0.75g air dry soil and put into marked 50-mL centrifuge tube.

2. Add 0.4g of sodium dithionite with scoop and 24mL of sodium citrate solution with dispenser.

3. Cap tubes and shake briefly by hand to dislodge soil from tube bottom. Place tubes in rack.

4. Place tubes in shaker and shake overnight (12 to 16h) at 200 oscillations min-1 at room temperature (20ºC±2ºC).

5. Remove tubes from shaker and manually shake tubes to dislodge any soil form cap. Allow samples to sit overnight.

6. The following day, centrifuge at 4000rpm for 15min.

7. Measure the volume of suspension V by graduated flaks and transfer the sample into sample bottle from centrifuge tube.

Dilution of Sample Extracts

1. For 1:50 dilution of samples for Fe analysis, use the H_3PO_4 dilution solution. Dilute 1 part CD sample extract with 49 parts of H_3PO_4 diluting solution (1:50 dilution).

2. A 1:5 dilution in RODI water is used for Al. Dilute 1 part CD sample extract with 4 parts RODI water into test tubes.

3. Dilute extracts (1:10) with RODI water. Add 1 part sample extract with 9 parts dilution solution. Pipet 0.7 mL of extract and 6.3 mL RODI water into test tube.

4. Mix the extract.

5. Send the samples with matrix to Roger at the University of Minnesota Research and Analytical Lab

Reagents:

$Na_2S_2O_4$, Sodium dithionite, 0.4*22=8.8g

$Na_3C_6H_5O_7$, Sodium citrate dehydrate, 0.57M, 25ml*22=550mL.Dissolve 168g sodium citrate in 1L RODI water

Equipment:

22 crucible, 22 test tube, Balance (0.75g), calibrated scoop (0.4g), dispenser (25mL), pipet and pipet pump for 1mL, 25mL, shaker, centrifuge tube (22), 1 graduated flask (25ml)

Calculation:

Convert analyte concentrations (mg/L) to percent in soil as follows:

Soil Fe, Al (%) $=(A\times B\times C\times R\times 100)/(E\times 1000)$

Where:

A = Sample extract reading (mg/L)

B = Extract Volume (L)

C =Dilution, required (I used 10 here)

R =Air-dry/oven-dry ration (procedure 3D1 from SSL)

E =Sample weight (g)

100 =Conversion factor to 100-g basis

1000=mg/g

Safety:
Wear protective clothing (lab coat and gloves), eye protection (goggles) and a breathing filter when handling dry sodium dithionite. Sodium dithionite may spontaneously ignite if allowed to become moist, even by atmospheric moisture. Keep dithionite in a fume hood.

Ammonium Oxalate Extraction (SSL 4G2)

Procedures:
Extraction of Al and Fe (SSL 4G2)

8. Weight 0.50g air dry soil and put into marked 50-mL centrifuge tube.

9. Add 50mL 0.275M pH3.25 Ammonium oxalate buffer solution with dispenser, prepare matrix solution as well.

10. Cap tubes and shake briefly by hand to dislodge soil from tube bottom. Place tubes in rack; cover the tubes with black plastic bag.

11. Place tubes in shaker and shake overnight (12 to 16h) at 200 oscillations min-1 at room temperature (20ºC±2ºC) (make sure to cover the samples with black bag).

12. Remove tubes from shaker and manually shake tubes to dislodge any soil form cap. Allow samples to sit overnight.

13. The following day, centrifuge at 4000rpm for 15min.

14. Measure the volume of suspension V by graduated flaks and transfer the sample into sample bottle from centrifuge tube.

15. If the samples cannot be analyzed immediately it should to stored in the dark to prevent photoinduced decomposition of oxalate, which could result in precipitation of Fe .

Dilution of Sample Extracts for ICP-AES analysis

6. Dilute extracts (1:10) with RODI water. Add 1 part sample extract with 9 parts dilution solution. Pipet 1.4 mL of extract and 12.6 mL RODI water into test tube.

7. Mix the extract.

8. Send the samples with matrix to Roger at the University of Minnesta, Research Analytical Lab

Reagents:
Ammonium oxalate buffer solution, 0.275 M, pH 3.25.

Solution A (base): Dissolve 34.66g $(NH_4)_2C_2O_4 \cdot H_2O$ in 1L of DDI water and transfer the solution in 2 L flask.

Solution B (acid): Dissolve 40.425g $H_2C_2O_4 \cdot 2H_2O$ in 1L DDI water and transfer the solution in 1 L flask.

Adjust ammonium oxalate solution A pH by adding solution B, until pH3.25. (about 700mL of oxalic acid solution needed for pH adjustion; if the pH drops below 3.25, add NH_4OH to raise the pH to 3.25)

Invert the flask slowly ten times to mix thoroughly.

Store the solution and label.

Equipment:
22 test tube, Balance (0.5g), dispenser (50mL), pipet and pipet pump for 2mL, 25mL, shaker, centrifuge tube (22), 1 graduated flask (25ml), pH meter

Calculation:
Convert analyte concentrations (mg/L) to percent in soil as follows:
Soil Fe, Al (%) $=(A \times B \times C \times R \times 100)/(E \times 1000)$
Where:
A = Sample extract reading (mg/L)
B = Extract Volume (L)
C =Dilution, required (I used 10 here)
R =Air-dry/oven-dry ration (procedure 3D1 from SSL)
E =Sample weight (g)
100 =Conversion factor to 100-g basis
1000=mg/g

Safety:
Wear protective clothing (lab coat and gloves), eye protection (goggles).

Interferences:
The ammonium oxalate buffer extraction is sensitive to light, especially UV light. The exclusion of light reduces the dissolution effect of crystalline oxides and clay minerals. The procedure must be performed in the dark to prevent photoreduction and retard rate of dissolution of crystalline iron oxides.

If the sample contains large amounts of amorphous material (>2% Al), an alternate method should be used, i.e., shaking with 0.275 M ammonium oxalate, pH 3.25, 1:100 soil extractant.

Appendix III

Earthworm biomass data were compiled with Amy Lyttle (see Lyttle 2013)

Table 17-A. Earthworm species' biomass collected from transect B in 2009.

distance (m)	*Apporectodea spp.*	*Dendrobaena spp.*	*Octolasion spp.*	*L.* juvenille	*L. rubellus*	*L. terrestris*
190	0.000	0.473	0.000	0.146	0.000	0.000
180	0.000	0.000	0.000	0.000	0.000	0.000
170	0.000	0.286	0.000	0.150	0.000	0.000
160	0.000	0.000	0.000	0.000	0.000	0.000
150	0.000	0.624	0.000	0.572	0.244	0.000
140	0.000	0.081	0.000	1.288	0.000	0.000
130	0.072	0.303	0.000	1.372	0.000	0.000
120	0.028	0.662	0.000	1.486	1.785	0.000
110	0.090	0.384	0.000	0.000	0.000	0.000
100	1.406	1.168	0.000	1.364	0.345	0.000
90	0.413	0.206	0.000	0.265	0.000	0.000
80	0.421	0.171	0.000	0.692	0.000	0.000
70	1.615	0.629	0.000	0.340	0.000	0.000
60	1.216	0.651	0.000	1.098	0.000	2.342
50	0.663	0.479	0.000	0.732	0.276	4.538
40	2.567	0.226	0.000	0.767	0.000	9.567
30	0.000	0.039	0.000	0.665	0.309	0.000
20	0.216	0.352	0.209	0.837	0.000	4.376
0	0.297	0.736	0.000	0.639	0.000	0.000

Table 17-B. Earthworm species' biomass collected in 2010.

distance (m)	*Aporrectodea spp.*	SE n=3	*Dendrobaena spp.*	SE n=3	*Octolasion spp.*	SE n=3	*L.* juvenille	SE n=3	*L. rubellus*	SE n=3	*L. terrestris*	SE n=3
190	0.000	0.00	0.378	0.18	0.000	0.00	0.279	0.16	0.282	0.28	0.000	0.00
180	0.003	0.00	0.396	0.21	0.000	0.00	0.101	0.06	0.000	0.00	0.000	0.00
170	0.000	0.00	0.160	0.08	0.000	0.00	0.000	0.00	0.000	0.00	0.000	0.00
160	0.291	0.16	0.657	0.16	0.000	0.00	0.313	0.16	0.221	0.22	0.000	0.00
150	2.359	0.80	1.103	0.36	0.000	0.00	1.459	0.53	0.346	0.17	1.296	1.30
140	0.459	0.35	0.732	0.28	0.000	0.00	0.887	0.12	0.081	0.08	0.000	0.00
130	1.144	0.50	0.882	0.29	0.000	0.00	1.925	0.27	0.341	0.34	1.459	1.46
120	1.035	0.73	0.653	0.07	0.000	0.00	1.135	0.48	0.506	0.29	1.400	1.01
110	0.926	0.09	0.625	0.08	0.000	0.00	1.636	1.09	0.000	0.00	0.000	0.00
100	2.262	1.17	0.442	0.13	0.000	0.00	2.057	0.51	0.984	0.98	0.000	0.00
90	2.019	1.13	0.647	0.11	0.000	0.00	3.378	0.81	0.463	0.31	0.714	0.71
80	0.947	0.07	0.785	0.40	0.000	0.00	2.176	0.48	0.637	0.33	0.000	0.00
70	3.961	1.67	0.673	0.05	0.000	0.00	1.169	0.28	0.492	0.49	0.000	0.00
60	3.497	1.76	0.527	0.23	0.259	0.26	1.812	0.92	0.291	0.29	5.164	2.69
50	1.644	1.40	0.148	0.08	0.520	0.52	3.027	0.63	1.010	0.84	1.532	1.53
40	0.288	0.07	0.129	0.13	0.552	0.45	1.956	0.59	0.280	0.15	1.658	1.66
30	1.303	0.67	0.182	0.06	0.281	0.28	2.098	1.09	0.642	0.32	1.296	1.30
20	0.275	0.17*	0.119	0.10*	0.029	0.03*	1.727	1.53*	0.221	0.22*	0.000	0.00*
0	1.952	0.70	0.379	0.08	0.252	0.15	2.098	0.82	0.811	0.68	3.901	2.08

SE = Standard Error
*Standard error n=2

Table 17-C. Earthworm species' biomass collected in 2011.

distance (m)	*Aporrectodea spp.*	SE n=3	*Dendrobaena spp.*	SE n=3	*Octolasion spp.*	SE n=3	*L.* juvenille	SE n=3	*L. rubellus*	SE n=3	*L. terrestris*	SE n=3
190	0.000	0.00	0.451	0.16	0.000	0.00	0.088	0.09	0.311	0.31	0.000	0.00
180	0.005	0.01	1.352	0.20	0.000	0.00	0.250	0.13	0.367	0.37	0.000	0.00
170	0.069	0.07	0.343	0.17	0.000	0.00	0.609	0.25	0.560	0.34	0.000	0.00
160	0.457	0.35	1.062	0.33	0.000	0.00	1.031	0.42	0.333	0.17	0.000	0.00
150	0.298	0.09	0.587	0.25	0.027	0.03	0.803	0.36	0.511	0.51	0.000	0.00
140	1.537	1.20	0.428	0.11	0.000	0.00	1.230	0.34	0.516	0.01	0.000	0.00
130	0.719	0.33	0.370	0.12	0.000	0.00	2.177	0.26	0.193	0.19	0.981	0.98
120	0.636	0.25	0.454	0.15	0.000	0.00	1.584	0.47	0.645	0.37	2.148	1.42
110	0.775	0.27	0.560	0.24	0.000	0.00	1.341	0.53	0.452	0.25	0.000	0.00
100	1.172	0.30	0.224	0.05	0.000	0.00	1.617	0.68	0.370	0.22	0.000	0.00
90	0.554	0.11	0.433	0.18	0.000	0.00	2.947	0.61	0.416	0.22	0.000	0.00
80	0.564	0.14	0.379	0.13	0.000	0.00	2.270	0.14	0.299	0.30	0.000	0.00
70	0.745	0.27	0.394	0.09	0.009	0.01	1.543	0.85	0.000	0.00	1.186	1.19
60	0.872	0.16	0.125	0.10	0.077	0.08	1.666	0.53	0.000	0.00	0.000	0.00
50	1.036	0.16	0.187	0.19	0.135	0.12	2.008	0.70	0.000	0.00	0.981	0.98
40	0.961	0.19	0.031	0.02	0.447	0.44	0.671	0.33	0.000	0.00	1.963	1.96
30	0.000	0.00*	0.023	0.02*	0.004	0.00*	0.664	0.10*	0.000	0.00*	3.251	3.25*
20	0.349	0.22*	0.052	0.05*	0.557	0.14*	1.054	0.04*	0.000	0.00*	3.416	3.24*
0	0.609	0.29	0.068	0.04	0.126	0.07	2.383	0.37	0.000	0.00	2.277	1.45

SE = Standard Error
*Standard error n=2

Table 18. Total earthworm biomass (AFD g m-2) for 2009, 2010, and 2011.

Distance (m)	Total Earthworm Biomass (AFD g m^{-2}) 2009	Total Earthworm Biomass (AFD g m^{-2}) 2010	Total Earthworm Biomass (AFD g m^{-2}) 2011
190	0.62	1.88	0.85
180	0	0.53	1.975
170	0.437	0.16	1.581
160	0	2.942	2.884
150	1.441	18.208	2.226
140	1.369	3.522	3.711
130	1.747	8.701	4.439
120	3.962	9.342	5.467
110	0.474	4.86	3.128
100	4.283	9.41	3.384
90	0.885	11.05	4.35
80	1.285	7.551	3.512
70	2.584	14.144	3.878
60	5.307	24.924	2.74
50	6.688	8.522	4.347
40	13.127	5.836	4.072
30	1.013	12.132	3.942
20	5.99	2.501	6.899
0	1.672	25.024	5.464

Table 19. Earthworm species and their associated ecological group

Species	Ecological group
L. rubellus (adults)	epi-endogeic
Dendrobaena octaedra	epigeic
Aporrectodea spp. (*A. caliginosa*, *A. rosea*)	endogeic
L. terrestris (adults)	anecic
Octolasion tyrtaeum	endogeic
L. juveniles	epi-endogeic/anecic